NTNU – Trondheim
Norwegian University of
Science and Technology

Modeling of a Hydrogen Refueling Station

Nina Helene Omdahl

Chemical Engineering and Biotechnology
Submission date: June 2014
Supervisor: Heinz A. Preisig, IKP
Co-supervisor: Federico Zenith, Stiftelsen SINTEF

Norwegian University of Science and Technology
Department of Chemical Engineering

Abstract

Gaseous hydrogen is one of several alternatives to fossil-based vehicle fuels. In order to establish hydrogen as a good alternative, it is necessary to implement hydrogen refueling stations that can compete with conventional refueling stations. That is, the hydrogen refueling stations must be able to meet the customer's demands and expectations. The Society of Automotive Engineers has therefore developed a protocol that provides performance requirements for gaseous hydrogen refueling stations. These requirements include average pressure ramp rates (APRR) which describe the desired pressure rise in the vehicle tank along with precooling temperatures of the hydrogen prior to entering the vehicle. The precooling is necessary due to two phenomena occurring during refueling: 1) reverse Joule-Thomson effect, and 2) heat of compression.

In this thesis, a simple dynamic model of a hydrogen refueling station with a direct compression design has been developed and implemented in MATLAB. The direct compression design consists of two parallel process lines where one contains a reduction valve and the other a compressor. The pressure difference between the station and the vehicle decides which process line is utilized during the refueling. In order to comply with the precooling temperature set by the protocol, a heat exchanger has to be included after the compressor and reduction valve but prior to the nozzle connected to the vehicle. A production section where hydrogen is produced from electrolysis of water has also been included in the model. Two pressure controllers have been implemented; one for each process line. These controllers are of the PI type and control the pressure rise in the vehicle tank.

Various conditions such as different initial vehicle tank pressures, ambient temperatures and APRRs have been tested. These conditions were all handled well by the model. Additionally, the implemented controllers were able to track the APRR tightly under all the various conditions. The waste heat generated in different components at the station was quantified to see whether an absorption refrigeration process can be utilized for cooling the hydrogen prior to the vehicle tank. In total, four different cases for making the absorption refrigeration process workable were considered. However, the process is only achievable in one of the cases for an ambient temperature of 15°C and presumably below.

Sammendrag

Hydrogengass er ett av flere alternativer til fossilbaserte drivstoff. For å kunne etablere hydrogen som et bra alternativ er det nødvendig å implementere hydrogenfyllestasjoner som kan konkurrere med konvensjonelle bensinstasjoner. Det vil si, fyllestasjonene må kunne oppfylle kundens behov og forventninger. "Society of Automotive Engineers" har derfor utviklet en protokoll som inneholder ytelseskrav for hydrogenfyllestasjoner. Kravene inkluderer blant annet ønsket trykkøkning i biltanken og temperatur på hydrogengassen før den fylles på biltanken. Dette temperaturkravet er nødvendig på grunn av to fenomener som forekommer under en fylleprosess: 1) invers Joule-Thomson-effekt, og 2) kompresjonsvarme.

I denne avhandlingen har det blitt utviklet og implementert en en enkel, dynamisk modell av en hydrogenfyllestasjon med et direkte-kompresjonsdesign i MATLAB. Designet består av to parallelle prosesslinjer hvor den ene inneholder en reduksjonsventil og den andre en kompressor. Trykkforskjellen mellom fyllestasjonen og bilen avgjør hvilken av prosesslinjene som blir brukt i løpet av fylleprosessen. For å overholde temperaturkravet satt av protokollen må en varmeveksler inkluderes etter reduksjonsventilen og kompressoren men før munnstykket som bilen kobler seg til. En produksjonsdel hvor hydrogen blir produsert fra elektrolyse av vann har også blitt inkludert i modellen. I tillegg har to trykkregulatorer blitt implementert; en for hver prosesslinje. Disse regulatorene er av typen PI-regulator og regulerer trykkstigningen i biltanken.

Forskjellige forhold som ulike starttrykk i biltanken, omgivelsestemperaturer og trykkøkninger har blitt testet. Alle disse forholdene ble håndtert bra av modellen. I tillegg var regulatorene i stand til å regulere trykkøkingen i henhold til det som er gitt i protokollen. Varmen som blir generert av de ulike komponentene på stasjonen ble kvantifisert for å se om en absorpsjonskjøleprosess kan benyttes for kjøling av hydrogenet før biltanken. Fire forskjellige tilfeller som kan føre til at absorpsjonskjøleprosessen blir gjennomførbar ble vurdert. Prosessen er kun gjennomførbar for ett av tilfellene, og da ved en omgivelsestemperatur på 15°C og formodentlig lavere.

Preface

This master thesis constitutes the final part of the 5 year integrated master program in Chemical Engineering and Biotechnology at the Norwegian University of Science and Technology (NTNU). The thesis was completed during spring semester in 2014.

There are several persons associated to this thesis whom I would like to thank. First, I would like to thank Federico Zenith, my supervisor at SINTEF, who proposed this thesis and who has provided me with excellent support and guidance whenever needed. Second, I would like to thank my supervisor at the department, Professor Heinz Preisig, for providing valuable assistance and help in the modeling process. I would also like to thank the whole process systems engineering group. The threshold for asking questions to any of the group members is very low, whether they are professors or master students. This is something I have really appreciated and exploited during my time in the group.

Finally, I would like to thank my class mates through five years who have made these years unforgettable, and especially those in K4-230. It has been a pleasure sharing many coffee breaks, frustrations and even more laughs with you.

Declaration of Compliance

I hereby declare that this is an independent work according to the exam regulations of the Norwegian University of Science and Technology (NTNU).

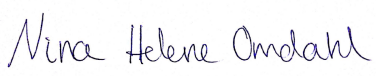

Nina Helene Omdahl
Trondheim, June 23, 2014

Table of Contents

List of Tables

List of Figures

Nomenclature

Symbols

Symbol	Unit	Description
A	m^2	Cross-sectional pipe area
c	%	Compressor cylinder clearance
c_p	kJ/kg K	Specific constant pressure heat capacity
c_v	kJ/kg K	Specific constant volume heat capacity
C_p	kJ/K	Constant pressure heat capacity
C_v	m^2	Valve coefficient
D	m	Pipe diameter (inner)
e	MPa	Control error from set point
E	kJ	Energy
f	-	Darcy friction factor
$\mathbf{F}$	-	Incidence matrix
h	kJ/kg	Specific enthalpy
H	kJ	Enthalpy
H_m	kJ/mol	Molar enthalpy
k	-	Sampling instant
k'	MPa/m^2 s, MPa	Integrating process gain
K_c	m^2/MPa, 1/MPa s	Controller gain
L	m	Pipe length
m	kg	Mass
$\dot{m}$	kg/s	Mass flow
N	1/s	Compressor speed
N_{Re}	-	Reynolds number

Continued on next page

Symbol	Unit	Description
p	MPa	Pressure
$\dot{P}$	kW	Power input to electrolyzer
$\dot{Q}$	kW	Heat transfer rate
r	-	Compression ratio
R	J/K mol	Gas constant
s	kJ/K kg	Specific entropy
S	kJ/K	Entropy
t	s	Time
T	K, °C	Temperature
u	m^2, 1/s	Controller output
$\mathbf{u}$	m^2, 1/s	Vector of controller outputs
U	kJ	Internal energy
v	m/s	Flow velocity
$\mathbf{v}$	kg/s	Vector of transport quantities
V	m^3	Volume
$\dot{V}$	m^3/s	Volumetric flow rate
$\dot{W}$	kW	Work rate
$\mathbf{x}$	kJ, kg	Vector of primary states
$\mathbf{y}$	-	Vector of secondary states
Z	-	Compressibility factor
α	-	Reduced helmholtz free energy
γ	-	Specific heat capacity ratio
ϵ	m	Roughness of pipe
η	-	Efficiency
θ	s	Process time delay
μ	Pa s	Dynamic viscosity
ρ	kg/m^3	Density
τ_c	s	Desired closed-loop time constant
τ_I	s	Integral time constant

Subscript/superscript

Symbol	Description
o	Initial, standard
A	Absorber
act	Actual
amb	Ambient
c	Critical
C	Condenser
cw	Cooling water
cyl	Compressor cylinder
E	Evaporator
f	Formation
G	Generator
ig	Ideal gas
hw	Hot water
in	Inlet
is	Isentropic
k	Kinetic
liq	Liquid
out	Outlet
p	Potential
P	Pump
r	Residual
ref	Reference
refill	Refilling storage tank
req	Required
rx	Reaction
s	Shaft work, steam
switch	Switching from valve flow to compressor flow
sys	System
v	Volumetric
vap	Vaporization

Abbrevations

Symbol	Description
APRR	Average pressure ramp rate
C	Compressor
COP	Coefficient of performance
DAE	Differential algebraic equation
EL	Electrolyzer
EOS	Equation of state
HX	Heat exchanger
HXEL	Internal heat exchanger in electrolyzer
IC	Intercooler
NWP	Nominal working pressure
ODE	Ordinary differential equation
PI	Proportional integral
PEM	Proton exchange membrane/polymer electrolyte membrane
RV	Reduction valve
SAE	Society of Automotive Engineers
SIMC	Skogestad/Simple Internal Model Control
SOC	State of charge
SOEC	Solid oxide electrolysis
ST	Storage tank
TIR	Technical information report
VT	Vehicle tank

1 | Introduction

Gaseous hydrogen (H_2) is one of several alternatives to fossil-based vehicle fuels such as gasoline and diesel. Hydrogen is an energy carrier which in reaction with oxygen generates water and energy. This reaction is exploited in a fuel cell where its chemical energy is converted into electrical energy. The produced electrical energy can be used to, for instance, power a vehicle. There are several reasons why hydrogen is considered as an alternative to fossil-based fuels. First, hydrogen is one of the most abundant elements on earth and occurs naturally in chemical compounds such as hydrocarbons and water. Second, the reaction between hydrogen and oxygen produces water as the only by-product. This will eliminate local vehicle-caused air pollution which is an increasing problem in densely populated areas [1]. Third, if the hydrogen is produced by using renewable energy resources, the carbon dioxide emission related to production of fuel can be significantly reduced.

Essentially, gaseous hydrogen is more environmentally friendly as a fuel than the fossil-based ones. To establish hydrogen as a fuel, a hydrogen infrastructure and accordingly, hydrogen refueling stations must be implemented. For hydrogen to be established as a *superior* fuel, it is essential that these hydrogen refueling stations can compete with conventional refueling stations. That is, the hydrogen refueling stations must be able to meet the customer's demands and expectations. This includes supplying a full tank of hydrogen within an acceptable time frame without violating any of the safety limits. Additionally to fulfilling the customer's demands, the refueling stations face some challenges regarding both storing and refueling gaseous hydrogen. One challenge is that the density of hydrogen gas is very low. At atmospheric pressure and 25°C, the density of hydrogen is 0.082 kg/m^3 [2]. One kilogram of hydrogen gas at these conditions will take up a volume of approximately 12 m^3. Therefore, the hydrogen gas must be compressed to high pressures in order to make it compact enough for storage and mobile applications [3].

To achieve an acceptable driving range, the hydrogen should be stored at a pressure between 35 - 70 MPa in the vehicle tank. This, of course, imposes high requirements to the equipment at the station and in the vehicle. Another challenge is during refueling, the gas temperature will increase due to two physical phenomena:

1) reverse Joule-Thomson effect during isenthalpic expansion through valves, and 2) heat of compression occurring in compressors and during tank filling. As the temperature in the tank will increase more with a faster refueling due to the heat of compression, it is necessary to cool the hydrogen before it enters the vehicle tank. This will enable a fast refueling without running the risk of overheating the tank.

The customer's demand and the safety limits are often competing. As discussed above, a fast refueling which is a customer expectation may result in overheating of the vehicle tank. On the other hand, a slow refueling which easily will comply the safety limits may result in no customers. In order to ensure safe and "customer-acceptable" hydrogen refueling stations, the Society of Automotive Engineers (SAE) has developed a protocol that establishes safety limits and performance requirements for gaseous hydrogen refueling stations [4]. This protocol is denoted SAE TIR J2601 and will be referred to as such or solely as J2601. The safety limits include lower and upper temperature bounds for the station and the vehicle tank. The performance requirements contain refueling targets and proposed pressure ramp rates that will define the appropriate refueling time. The pressure ramp rate defines how much the pressure should increase per unit of time at the nozzle which the vehicle is connected to. An appropriate refueling time in this case is between 2-5 minutes. In order to achieve a customer-acceptable and safe refueling, the J2601 protocol provides look-up tables that suggest: 1) the target pressure at which the refueling is complete, and 2) the average pressure ramp rate which ensures that the maximum temperature limit is not exceeded. However, the protocol does not mention anything about how to achieve a full vehicle tank.

There are in principle two methods for refueling a tank with hydrogen gas. One of the methods is denoted *tank-to-tank refueling* and is when the hydrogen gas is compressed to high pressures and stored in one or several stationary tank(s) at the station [5]. The refueling is then forced by the pressure difference between the station tank(s) and the vehicle tank. The advantage with tank-to-tank refueling is that the refueling can occur at high mass flows. However, since the hydrogen first is compressed and then expanded during the refueling due to the pressure difference, some of the compressor work performed during the compression is wasted. This will, to a large extent, be avoided in the second method in which the hydrogen is stored at low pressures and compressed directly into the vehicle. Hence the name *direct compression refueling*. Since the hydrogen gas is compressed to the actual pressure in the vehicle tank, no compressor work will go to waste. The challenge with direct compression is that large compressors are required to complete the refueling in the time frame set by the SAE TIR J2601.

Common for both approaches is that cooling of the hydrogen is required prior to the vehicle tank. As mentioned above, the cooling is necessary because of the reverse Joule-Thomson effect and heat of compression occurring during the refueling. Typically, the hydrogen is cooled down to -40°C before entering the tank [4]. Hence, the refrigeration process requires a lot of energy. As several other

units at the station generate waste heat (e.g. compressor, electrolyzer), an *absorption refrigeration process* could be utilized instead of a conventional *compression refrigeration process*. An absorption refrigeration process uses waste heat to separate a refrigerant and an absorbent at high pressures. The refrigerant is then condensed at high pressures and evaporated under low pressure, thereby cooling the surroundings. Thermal energy is driving this process, and the only electrical energy required is for pumping the refrigerant/absorbent solution from low to high pressure. As this electrical energy only corresponds to 5% of the total required energy, a significant amount of energy can be saved compared to a conventional compression refrigeration process.

The goal with this thesis is to develop a simple dynamic model of a hydrogen refueling station with a direct compression refueling design. The hydrogen refueling station will include a production section where hydrogen is produced from electrolysis of water. The model will be implemented in MATLAB, and an external thermodynamic property database named CoolProp will be used for obtaining the thermodynamic properties of the hydrogen. In addition, the cooling demand of the hydrogen before entering the vehicle tank along with the waste heat generated in the different process components will be estimated. The heat needed to drive the absorption refrigeration process will be calculated based on coefficient of performance considerations. The generated waste heat and the required heat input will be compared to see whether it is possible to utilize an absorption refrigeration process at the station.

The report starts with an introduction to the hydrogen refueling protocol developed by the Society of Automotive Engineers. Then, a brief presentation of the tank-to-tank refueling approaches together with a thoroughly description of the refueling station modeled in this thesis are given. Thereafter, the working principle and requirements for the absorption refrigeration process will be introduced along with a description of the absorption refrigeration process at the hydrogen refueling station. Furthermore, the model development for each component at the station follows. This chapter also includes the control configuration of the station. The next chapter contains a brief description of the implementation of the model and the applied thermodynamic property database, CoolProp. Then, a results and discussion chapter on the model behavior follows. This behavior involves pressure, temperature and mass flow evolution as well as cooling demands and compressor works at the station. The next chapter includes results and discussion from the estimation on whether the absorption refrigeration process is achievable in a hydrogen refueling station. Finally, the conclusion and suggestions for further work wrap up the thesis.

2 | Refueling protocol and procedure

The Society of Automotive Engineers (SAE) has developed a technical information report (TIR) for hydrogen refueling stations. The report is named SAE TIR J2601 and its scope is to establish safety limits and performance requirements for gaseous hydrogen fuel dispensers [4]. These safety limits and performance requirements are described in this chapter. The J2601 provides refueling guidelines for both hydrogen vehicles with and without the possibility to communicate with the station, here called "communication" and "non-communication" vehicles. "Communication" means that the vehicle and the station are able to communicate through a data interface and thereby exchange useful information. However, only non-communication vehicles are considered in this report.

2.1 Refueling station ratings

The J2601 protocol applies for hydrogen vehicles with nominal working pressures (NWP) at 35 MPa and 70 MPa. The nominal working pressure corresponds to the pressure at which the vehicle tank is full at a temperature of 15°C. During refueling, the temperature of the hydrogen gas will increase due to heat of compression and the reverse Joule-Thomson effect. Therefore, the fuel is precooled right before entering the vehicle tank in order to ensure that the maximum temperature limit is not exceeded within the tank. A hydrogen refueling station is rated based on its precooling temperature as well as the station's highest possible refueling pressure. In addition to the two pressure ratings (35 and 70 MPa), there are four different temperature ratings, each assigned a letter (A, B, C or D). For instance, an A70 station will precool the hydrogen down to -40°C and can deliver the fuel at 70 MPa. The ratings are presented in Table 2.1. Note that the vehicles with NWP of 70 MPa are further split into two types depending on the mass capacity of the vehicle tank. C70 and D70 ratings are not included as these are not recommended.

Table 2.1: *The different ratings of a hydrogen refueling station based on precooling temperature and highest possible refueling pressure.*

Type	Pressure [MPa]	Precooling temperature [°C]	Mass capacity [kg]
A70	70	-40	1-7
A70	70	-40	7-10
A35	35	-40	1-7.5
B70	70	-20	1-7
B70	70	-20	7-10
B35	35	-20	1-7.5
C35	35	0	1-7.5
D35	35	No precooling	1-7.5

2.2 General requirements

At the two different NWPs, the gas densities in the vehicle tanks are 24.0 kg/m^3 (35 MPa) and 40.2 kg/m^3 (70 MPa). These densities correspond to a filling level, or state of charge (SOC), of 100% for the two different NWP vehicles. The SOC is defined as the ratio between the actual density and the target density (at a temperature of 15°C) [4]. The ratio can be expressed as

$$\mathrm{SOC} = \frac{\rho(p,T))}{\rho(\mathrm{NWP}, 15^{\circ}\mathrm{C})} \times 100\% \tag{2.1}$$

where ρ is the gas density, p the pressure and T the temperature in the tank. The goal of the refueling is to achieve an SOC of 100% without violating the safety limits. However, neither the hydrogen density nor the temperature in the vehicle tank can be measured by the station. Therefore, appropriate target pressures based on the desired target density and ambient temperatures are given in J2601. Since the refueling is aborted when the specified target pressure is reached, and since this target pressure is set based on ambient temperature, the SOC is not necessarily 100% when the refueling is finished. This is because the initial temperature in the vehicle tank is not necessarily equal to the ambient temperature. A lower initial tank temperature may lead to overfilling as the final actual temperature is lower than the expected temperature, thus resulting in a higher density which may result in a SOC $>$ 100%. If the initial tank temperature is higher than the ambient temperature, which may occur if the vehicle has been parked in the sun, the vehicle tank may be overheated during the refueling.

2.2.1 Refueling process limits

As mentioned above, the goal of the refueling is to reach a SOC of 100%. However, the SOC must never exceed 100%. In addition, the temperature must be

maintained between -40°C and 85°C. This is to avoid thermal stress damage to the tanks [5]. The maximum allowed pressure is 125%×NWP. That is 87.5 MPa for a 70 MPa NWP vehicle and 43.75 MPa for a 35 MPa NWP vehicle. Below follows a list that summarizes some of the refueling process limits set by the J2601:

- The state of charge (SOC) must never exceed 100%.
- The maximum gas temperature in the vehicle tank is 85°C.
- The minimum gas temperature in the vehicle tank is -40°C.
- The maximum allowed pressure in the vehicle tank is 125%×NWP.
- The maximum allowed fuel flow rate at the dispenser nozzle is 0.06 kg/s.

These limits constitute an operating range for the fueling process. The operating range for a 70 MPa NWP fuel system is presented in Figure 2.1 [6].

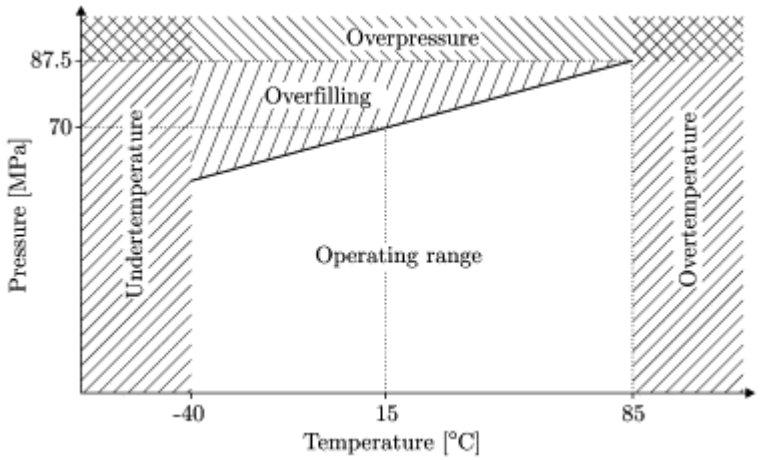

Figure 2.1: *The operating range for a 70 MPa NWP vehicle [6].*

2.2.2 Refueling control

The refueling is controlled by an average pressure ramp rate (APRR). That is, the pressure rise over time is constant. The APRR is set at the dispenser nozzle and is designed such that the gas temperature inside the vehicle tank will not exceed 85°C during a complete fill as long as the cooling demand is met. The refueling can also be controlled by limiting the mass flow upwards; a so-called peak-flow-rate control [6]. However, tanks with smaller volumes will be filled much faster than larger tanks, and will thus run the risk of getting overheated. This problem is overcome by refueling with a constant pressure rise since tanks with different sizes will be refueled equally fast, thereby preventing the risk of overheating smaller tanks. The J2601 provides look-up tables containing the APRR and target pressure for different initial conditions. The purpose of these tables is to optimize the performance of

refueling stations without violating the safety constraints. The ramp rates were found by running simulations to determine the fastest possible ramp rate that could fill the tank from 2 MPa to 100% SOC without surpassing the maximum temperature limit (85°C) and the maximum flow rate limit (0.06 kg/s).

2.3 Procedure for compressed hydrogen refueling

When a vehicle connects to the refueling station, the station measures the initial pressure in the vehicle tank. Then the station uses a pressure pulse along with flow measurements to determine the tank volume and hence the mass capacity of the tank. Which look-up table to use is decided by the mass capacity of the tank along with the station's refueling rating which is given in Table 2.1. Within the look-up table, the initial tank pressure and the ambient temperature are used to find the correct APRR and target pressure. When the APRR is set, the refueling starts. Due to the possibility of overheating or overfilling as discussed in Section 2.2, the actual pressure ramp rate cannot vary from the average pressure ramp rate by more than 10%. When the target pressure is reached, the refueling is aborted. An overview of the procedure is presented in Figure 2.2. Note that this procedure applies only for "non-communication" vehicles.

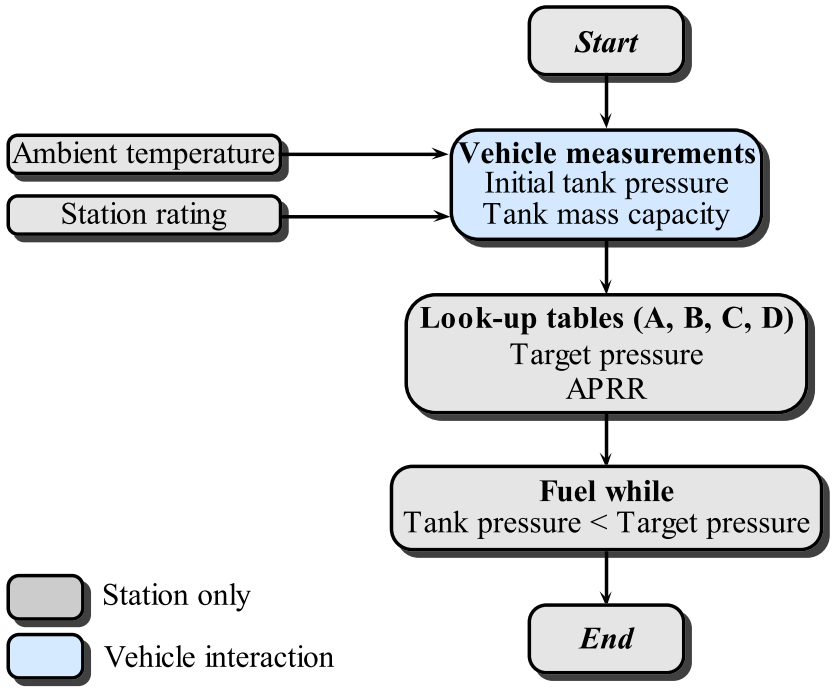

Figure 2.2: *The refueling procedure for compressed gaseous hydrogen.*

3 | Hydrogen refueling station designs

This chapter provides a description of the process designs presented in the introduction. The tank-to-tank refueling will be described briefly while a more thoroughly description will be given for the direct compression design. The production section of the station will be explained only in the direct compression part. The station being described is an A70 station. That is, the station precools the hydrogen to -40°C and is able to refuel a vehicle tank to 70 MPa.

3.1 Tank-to-tank refueling

The simplest tank-to-tank refueling design provides only one stationary hydrogen storage tank at the station [5]. This design is shown in Figure 3.1 and will be referred to as a single-tank storage system.

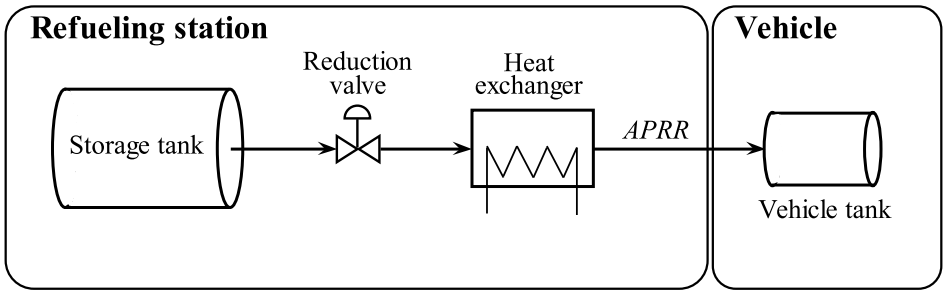

Figure 3.1: *Tank-to-tank refueling with only one hydrogen storage tank at the station.*

In the single-tank storage system, the hydrogen gas is stored at a pressure around 90 MPa in the storage tank. The hydrogen vehicle connects to the station through a dispenser nozzle. After the connection has been established, the target pressure and the APRR are obtained as explained in Section 2.3. Thereafter, the station opens for the storage tank, and a mass flow of hydrogen is forced from the storage tank to the vehicle tank due to the pressure difference. The reduction valve controls

the pressure rise at the dispenser nozzle so that it corresponds to the given APRR. This is achieved by altering the mass flow through the reduction valve. When the hydrogen gas is expanded through this valve, the gas temperature increases due to the reverse Joule-Thomson effect. In addition, the temperature in the vehicle tank will increase as more mass enters. This is due to the heat of compression occurring when the hydrogen already in the tank is compressed by the hydrogen entering the tank. Because of these two phenomena, a heat exchanger must be included in order to comply the maximum temperature limit (85°C) set by the J2601 [4]. This heat exchanger will cool the hydrogen to one of the precooling temperatures presented in Table 2.1. At this station, to -40°C. After each refueling, the high-pressure tank at the station has to be refilled from a low-pressure storage tank by a compressor. This is, however, not included in Figure 3.1.

The single-tank storage design is simple and provides easy control of the pressure rise. One of the disadvantages with this design, however, is that some of the compressor work used for obtaining the high pressure in the storage tank is going to waste. This occurs when the gaseous hydrogen is expanded through the reduction valve during refueling. Typically in a single-tank storage system, the pressure difference across the valve is considerably greater than necessary to comply the APRR in the majority of the refueling period. Hence, the entropy generation is large. In addition, a larger pressure difference across the reduction valve causes a larger temperature increase, thus resulting in a higher cooling demand. Furthermore, storing the hydrogen at a high pressure in only one tank requires a large high-pressure storage tank. These high-pressure hydrogen storage tanks are expensive. An improvement of the single-tank storage system is the cascade-tank storage system This design is most commonly used by the industry and is presented in Figure 3.2 [5].

The cascade-tank storage system consists of one high-, one medium- and one low-pressure tank at pressures around 90-100, 60-70 and 40-50 MPa, respectively. The rest of the process design is similar to the single-tank storage design. When a vehicle connects to the station, the station starts refueling from the low-pressure tank. The refueling continues until the pressure in the low-pressure tank becomes insufficient to maintain the APRR. At this point, the station switches to the medium-pressure tank and the refueling proceeds. When the pressure in the medium-pressure tank is not sufficient to comply the APRR either, the station starts refueling from the high-pressure tank. Hence, the high-pressure tank is used for refueling in a shorter time period compared to the single-tank storage design. The size of the expensive high-pressure tank can thus be reduced. The work of the compressor refilling the tanks will also be less since not all of the hydrogen must be compressed to 90 MPa.

Using several tanks with different pressures results in a lower pressure difference across the reduction valve. This means that the entropy generation is reduced compared to the single-tank storage design. In other words, less of the compressor work used to achieve the high pressures in the tanks is going to waste. Additionally,

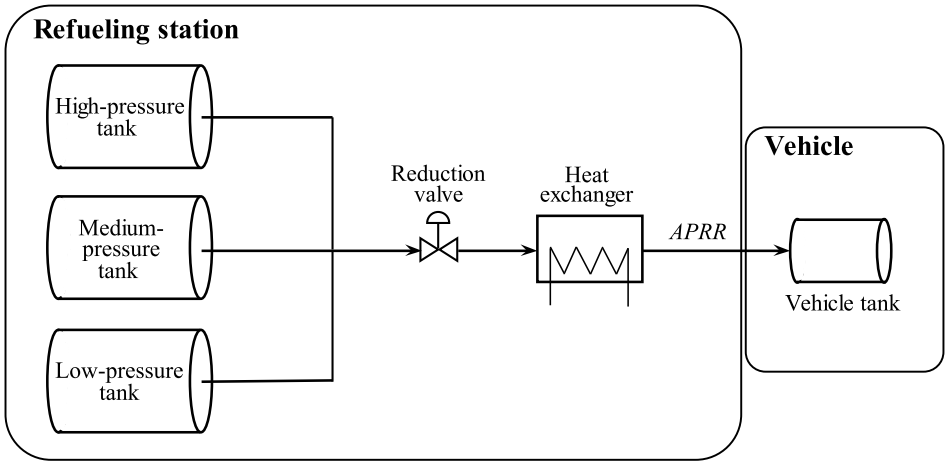

Figure 3.2: *Tank-to-tank refueling with three storage tanks each having different pressures.*

a lower pressure difference across the valve results in a lower temperature increase. This implies a smaller cooling demand in heat exchanger 3. Although the cascade-tank design improves the performance of the tank-to-tank refueling design, some compressor work is still lost since a pressure difference across the valve is required for the refueling to take place. Furthermore, in a tank-to-tank refueling design, the storage tanks must be refilled with hydrogen from a low-pressure storage after each refueling. This implies that the station requires some time to recover before a new refueling. Thus, customer may have to wait for the storage tanks to be refilled before he or she can refuel. This does not comply with the goal of being "customer-acceptable". By compressing the hydrogen directly into the vehicle, these issues will be eliminated.

3.2 Direct compression

The direct compression refueling process along with the production section is presented in Figure 3.3.

3.2.1 Production section

The hydrogen gas is produced from electrolysis of water. Typical electrolyzers used for this are alkaline electrolyzers, proton exchange membrane (PEM) electrolyzers[1] and solid oxide electrolyzer (SOEC) [7]. The alkaline electrolyzer is the most extended technology at a commercial level and has an efficiency range of 47%-82% [8].

1. The technology is also referred to as polymer electrolyte membrane electrolyzer, also with the same acronym PEM [7].

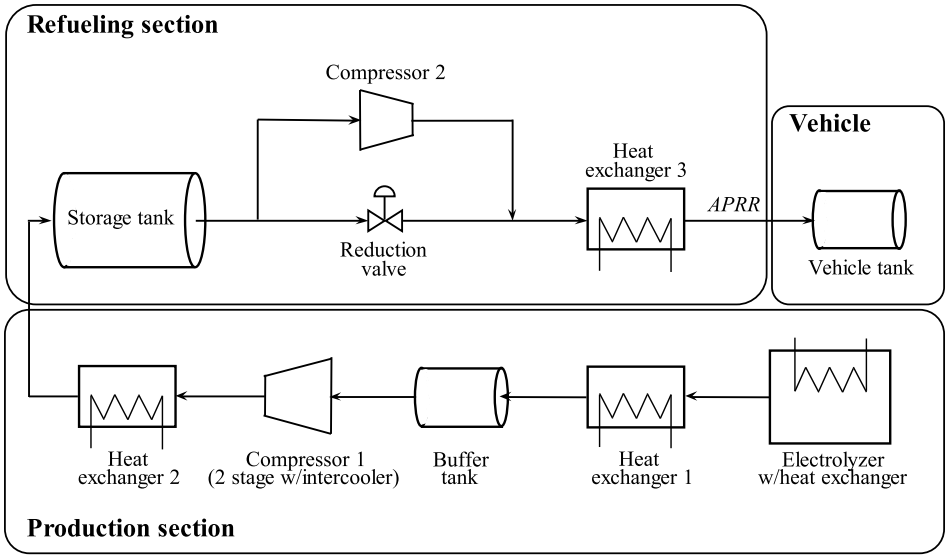

Figure 3.3: *The flow sheet for the direct compression design along with the production section.*

PEM electrolyzers are not that extended commercially due to their limited production capacity and short lifetime compared to their high investment cost. Their efficiencies are in the range 48%-65%. The SOECs, on the other hand, are still on the research and development stage. Therefore, the electrolyzer at this station is of the alkaline electrolyzer type. The operating temperature and pressure of an alkaline electrolyzer lie in the intervals 70-100°C and 0.1-3 MPa, respectively [9]. The electrolyzer in this refueling station will produce at a pressure of 1.2 MPa and a temperature of 90°C. Typically, the simplest electrolyzers produce hydrogen at a fixed power input until the pressure reaches a certain maximum limit (e.g. 1.2 MPa). Then the electrolyzer stops producing until the pressure drops below a specified minimum value. There exist also more complicated electrolyzers which can produce at varying power input. The electrolyzer in this model will be of the latter type and will start producing hydrogen when a vehicle initiate a refueling. After the refueling is complete, the electrolyzer will continue the production of hydrogen until the storage tank reaches its nominal pressure.

A large amount of waste heat is produced during the electrolysis, mainly due to electrical inefficiencies [9]. It is assumed that all of this waste heat is removed by an internal heat exchanger in the electrolyzer unit. That is, the operating temperature of the electrolyzer is fixed during operation. Because of the elevated operating temperature, a heat exchanger (heat exchanger 1) has been included after the electrolyzer in order to cool the hydrogen to the ambient temperature. This is to ensure that the inlet temperature of the compressor is low in order to avoid a very

high outlet temperature. The buffer tank following the heat exchanger is included to provide stable operating conditions for the compressor. That is, ensuring that hydrogen is always available when the compressor starts working. This is, however, a design issue and the buffer tank will not be included in the model as it will be assumed as a steady-state operation.

Several compressor types are applied for compression of hydrogen. The most common compressor type is the positive displacement type which includes reciprocating, membrane and ionic liquid compressors [10]. These all work by sucking in hydrogen gas, decreasing the enclosed volume the gas is trapped in (i.e. compressing the gas) before releasing the newly compressed gas. The reciprocating compressor, for instance, achieve this by piston displacement in a cylinder [11]. The two compressors at the station will be considered as the reciprocating type. The compressor in the production section (compressor 1) compresses in two stages due to the high compression ratio (from 1.2 MPa to 30 MPa in the storage tank). An intercooler is included between the two stages, cooling the hydrogen to the ambient temperature. Because of the heat of compression occurring both during compression but also in the storage tank, a heat exchanger is included after the compressor as well. The heat exchanger is referred to as heat exchanger 2 and ensures that the hydrogen is cooled to ambient temperature before entering the storage system.

3.2.2 Refueling section

As can be seen in Figure 3.3, the direct compression design consists of two "process lines" in the refueling section. One line contains a reduction valve, the other a compressor. The compressor is referred to as compressor 2. The produced hydrogen gas is stored at a pressure of 30 MPa in the storage tank [12]. When a vehicle connects to the station, the same procedure for obtaining the target pressure and APRR as for the two previously discussed designs is performed. As long as the pressure in the vehicle tank is lower than the pressure in the storage tank, the process line with the reduction valve is utilized for refueling. The reduction valve sets the APRR at the dispenser nozzle similar as in the tank-to-tank refueling approach. However, when the pressure difference across the reduction valve reaches a certain limit, the station switches to the compressor line. The hydrogen gas is now directly compressed into the vehicle tank. Consequently, the APRR is controlled by manipulating the compressor speed which will affect the mass flow. For both process lines, the hydrogen must pass through a heat exchanger for the same reasons discussed in the tank-to-tank refueling designs: 1) the reverse Joule Thomson effect, and 2) heat of compression. This heat exchanger is referred to as heat exchanger 3. Note that the cooling demand will be higher when the compressor line is utilized. The heat of compression is more significant than the heat generated by the reverse Joule-Thomson effect [13]. In addition, the cooling demand will vary as the mass flow is changed during operation in order to maintain the APRR. Heat exchanger 3 must therefore be capable of working at variable load.

The advantage of direct compression is that, when the compressor is utilized, the hydrogen will be compressed to the current pressure in the vehicle tank. Hence, none of the applied compressor work is going to waste, neither in the production section nor in the refueling section. This will be the case when the reduction valve line is utilized. However, both the time period for utilizing the valve and the pressure difference across the reduction valve will be less compared to the tank-to-tank refueling designs. The direct compression design also removes the need for storing hydrogen at high pressures which is a safety concern in itself for not mentioning the need for expensive high-pressure storage tanks. Furthermore, the station does not require recovery time after a refueling. Even though the storage tank is not completely filled due to a recent refueling, it can still refuel a new vehicle because of the direct compression. This will be an important factor if hydrogen vehicles shall be utilized in the future as the customers do not have to wait for the station to recharge. However, direct compression requires large compressors, and additionally, the control of the compressors may pose a challenge.

4 | Absorption refrigeration

According to the SAE TIR J2601, the hydrogen gas cannot exceed a temperature of 85°C inside the vehicle tank [4]. For a 70 MPa vehicle it is recommended that the hydrogen is cooled down to the lowest of the specified precooling temperatures, -40°C, before entering the vehicle tank. This cooling is performed in heat exchanger 3. Because of the low precooling temperature and the elevated inlet temperature caused either by expansion or compression in the process lines, a large amount of heat needs to be removed from the hydrogen in order to reach the precooling temperature. This requires a considerable amount of work in a conventional compressor refrigeration cycle. However, the electrolyzer and compressor 1 also generate heat that must be disposed of. Instead of rejecting this heat to the surroundings as waste, it can instead be utilized in an absorption refrigeration process. This will reduce the energy input to the refrigeration process required in heat exchanger 3 for achieving the precooling temperature.

4.1 Working principle

In an absorption refrigeration process, the working fluid is a binary solution consisting of an absorbent and a refrigerant. The most common working fluids are water/ammonia (NH_3) and LiBr/water [14]. In the case of a water/NH_3 solution, water is the absorbent and NH_3 is the refrigerant. Conversely, for a LiBr/water solution, LiBr is the absorbent and water is the refrigerant. Using water as a refrigerant limits the cooling process to above water's freezing point at 0°C. NH_3, on the other hand, has a freezing point of -77°C. Therefore, the water/NH_3 solution is utilized as the working fluid in this process. Figure 4.1 shows the single-effect absorption refrigeration system which is the simplest and most commonly used design [14]. Single-effect refers to systems in which only one generator is utilized and will be the design considered in this thesis. An absorption refrigeration cycle consists of a high-pressure and a low-pressure part. In brief, the refrigerant is liquefied in the condenser under high pressure and evaporated in the evaporator under low pressure [15]. Heat transferred from the refrigerated space (i.e. hydrogen in this case) ($\dot{Q}_E$) causes vaporization of the liquid refrigerant passing through the evaporator [16]. In other words, it is the evaporator unit that facilitates the refrigeration.

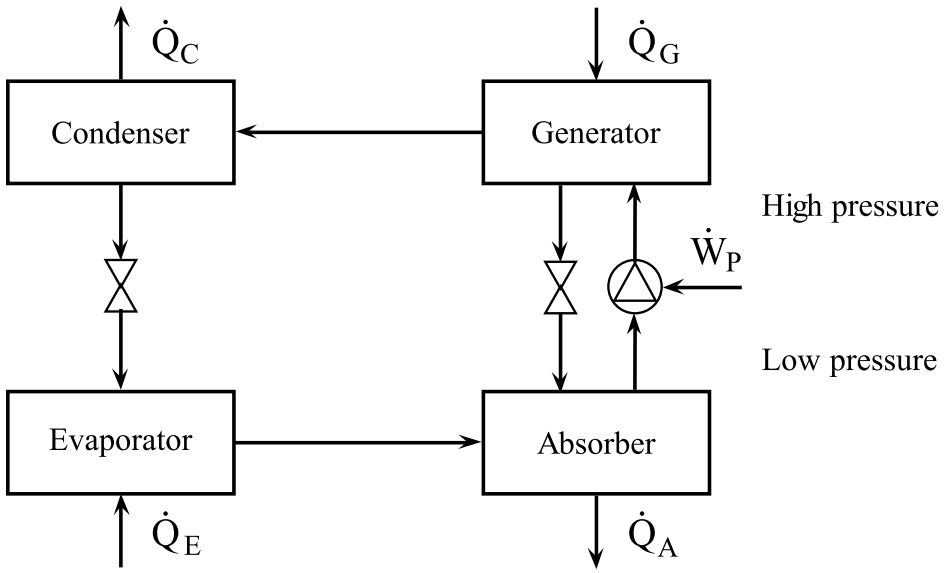

Figure 4.1: *A water/NH_3 absorption refrigeration cycle. $\dot{Q}_A$ and $\dot{Q}_C$ are heat rejected in the absorber and condenser, respectively. $\dot{Q}_E$ and $\dot{Q}_G$ are heat absorbed in the evaporator and the generator, respectively. $\dot{W}_P$ is the electrical energy input to the pump.*

The refrigerant vapor leaving the evaporator is then absorbed by the weak solution in the absorber. Weak solution refers to a solution which has a low concentration of refrigerant and mainly consists of the absorbent. This absorption process is exothermic. Since the amount of NH_3 that can be dissolved in water increases as the solution temperature decreases, it is desired to keep the temperature in the absorber as low as possible. Typically, cooling water is circulated around the absorber to remove the generated heat during the absorption ($\dot{Q}_A$).

The solution leaving the absorber has a high concentration of refrigerant, hence the label strong solution. This solution must be pumped to the generator as the generator is working at a higher pressure than the absorber. The only electrical energy required in an absorption refrigeration process is the energy necessary to run the pump. This corresponds to 5% of the total energy required by the cycle [15]. The rest of the energy is added as thermal energy to the generator ($\dot{Q}_G$). The thermal energy, or heat, drives refrigerant vapor out of the strong solution, leaving a weak refrigerant-absorbent solution. This solution is returned to the absorber through a valve while the refrigerant vapor is passed to the condenser. In the condenser, the refrigerant is liquefied by rejecting heat ($\dot{Q}_C$) to cooling water circulating the unit. The liquid refrigerant is then returned to the evaporator through a throttling valve and the cycle is complete.

In practice, this simple design is not utilized when the working fluid is water/NH_3. Because of the volatility of water, it is necessary to include a rectifier after the generator to strip away water evaporating along with NH_3 [14]. Without a rectifier, there is a risk that water will form ice in the evaporator and the expansion valve, thereby reducing the overall performance [16]. In addition, a heat exchanger can be included between the absorber and the generator. The strong solution coming from the absorber can thus be preheated by the hot weak solution returning from the generator. This has a dual effect: 1) decreasing the required heat input to the generator ($\dot{Q}_g$), as well as 2) causing that less heat must be rejected in the absorber. Hence, the size of the absorber can be reduced. An additional design feature not shown in Figure 4.1 is that the refrigerant can be stored in a fluid reservoir between the condenser and the evaporator [17]. The refrigerant is then stored as a liquid at the pressure of the high-pressure side. That is, the reservoir will be prior to the valve providing the pressure drop.

4.2 Requirements of generator heat input

The heat added in the generator ($\dot{Q}_G$) is the energy that drives the absorption refrigeration process. This heat may come from a direct-fired burner but also from other heat sources such as industrial waste heat. Regardless of the source, there are some requirements to the heat. In order to achieve a certain temperature in the evaporator, there is a minimum temperature requirement for the waste heat. This minimum temperature is dependent on two factors: 1) the desired evaporator temperature, and 2) the temperature of the cooling water used for heat removal in the absorber and condenser. An indicative relationship provided by Colibri b.v. which is an engineering office with specialization within absorption technology is summarized in Table 4.1 [15]. In order to be able to cool the hydrogen down to the precooling temperature, the evaporator temperature is set to -45°C.

Table 4.1: *The relationship between the required temperature of the waste heat, evaporator temperature and cooling water temperatures in an absorption refrigeration process [15]. The evaporator temperature is -45° C.*

Evaporator temperature [°C]	Cooling water temperature [°C]	Required temperature [°C]
-45	15	150
	20	160
	25	175
	30	186

It is assumed that the heat transferred to the generator is from saturated steam at the required temperature given in Table 4.1.

4.3 Coefficient of performance

The coefficient of performance (COP) is used to express the efficiency of an absorption refrigeration process and is defined as the ratio of the heat absorbed in the evaporator ($\dot{Q}_E$) to the total energy supplied to the system. The total energy is the sum of the heat input to the generator ($\dot{Q}_G$) and the work performed by the pump ($\dot{W}_P$). The coefficient of performance can be expressed as:

$$\text{COP} = \frac{\dot{Q}_E}{\dot{Q}_G + \dot{W}_P} \tag{4.1}$$

However, the work input to the pump is negligible compared to the heat input to the generator and will therefore be neglected. The expression can be simplified to

$$\text{COP} = \frac{\dot{Q}_E}{\dot{Q}_G} \tag{4.2}$$

and the heat input required in the generator can then be found from:

$$\dot{Q}_G = \frac{\dot{Q}_E}{\text{COP}} \tag{4.3}$$

As for the driving temperature requirements, the COP is dependent on the evaporator temperature and the temperature of the cooling water. A low cooling water temperature and a high evaporator temperature result in a higher COP. The relations between the COP, the evaporator temperature and different cooling water temperatures are summarized in Table 4.2. The values are only indicative and are obtained from [15].

Table 4.2: *The relation between the COP and evaporator temperature for different cooling water temperatures in an absorption refrigeration process [15]. The evaporator temperature is -45° C.*

Evaporator temperature [°C]	Cooling water temperature [°C]	COP
-45	10 - 20	0.45
	20 - 30	0.40
	30 - 40	0.30

4.4 Available waste heat sources at the station

As mentioned earlier, heat will be generated in the electrolyzer and the two compressors. The generated heat is removed in one of the several heat exchangers at the station. These heat exchangers, excluding heat exchanger 3 where the absorption refrigeration will take place, are available heat sources for the absorption refrigeration process. That is, the removed heat can be used to drive the refrigeration cycle.

These heat exchangers include:

- The internal heat exchanger in the electrolyzer.
- The heat exchanger following the electrolyzer (i.e. heat exchanger 1).
- The intercooler in compressor 1.
- The heat exchanger following the first compressor (i.e. heat exchanger 2).

Water is applied as cooling medium in these heat exchangers.

4.4.1 Fulfilling the requirements

As the operating temperature in the electrolyzer is 90°C, the temperatures of the heat removed by its internal heat exchanger and in heat exchanger 1 are not sufficient according to Table 4.1. Hence, the waste heat from heat exchanger 1 and the internal heat exchanger in the electrolyzer cannot be used directly in an absorption refrigeration process. If the temperatures of the heat removed by heat exchanger 2 and the intercooler are not sufficient either, it is not possible to utilize an absorption refrigeration process at the station at all. However, if the temperatures are high enough, but the amount of heat is not sufficient to drive the process alone, it may still be possible to utilize an absorption refrigeration process. The four cases that will be considered in this thesis are listed below:

I. Use the heat from only one heat source.

II. Increase the temperature of the low-temperature waste heat from the electrolyzer heat exchanger with high-temperature waste heat from heat exchanger 2 and intercooler.

III. Include a heat exchanger after the compressor in the refueling section (i.e. compressor 2) [12].

IV. A combination of II and III.

Case I is the optimal situation as it implies that one of the heat sources is sufficient to drive the absorption refrigeration process alone. However, if this is not the case, the remaining alternatives may still facilitate the utilization of the refrigeration process. For instance, in Case II, although the temperature of the heat rejected in the electrolyzer is not high enough, the amount of generated heat will likely be sufficient as an electrolysis process produces a significant amount of heat. Therefore, the assumed high-temperature heat coming from heat exchanger 2 and the intercooler can be used to increase the temperature of the heat generated in electrolyzer.

In Case III, an additional heat exchanger is included at the station. As the heat of compression is more significant than the reverse Joule-Thomson effect, the cooling demand in heat exchanger 3 will be substantially larger when the compressor is utilized in the refueling compared to when the reduction valve is used [13]. Including

a heat exchanger after compressor 2 but prior to heat exchanger 3 will therefore reduce the cooling demand considerably, and thereby decrease the required heat input to the generator. Typically, this heat exchanger will cool the hydrogen down to ambient conditions. By reducing the required heat input to the generator, the generated waste heat which is available at the station may be sufficient to drive the absorption refrigeration process[1]. Figure 4.2 shows the refueling section with the heat exchanger included. The heat exchanger is referred to as heat exchanger 4. Note that this heat exchanger only removes heat when compressor 2 is utilized, and it will therefore not be considered as a possible heat source for the absorption refrigeration process.

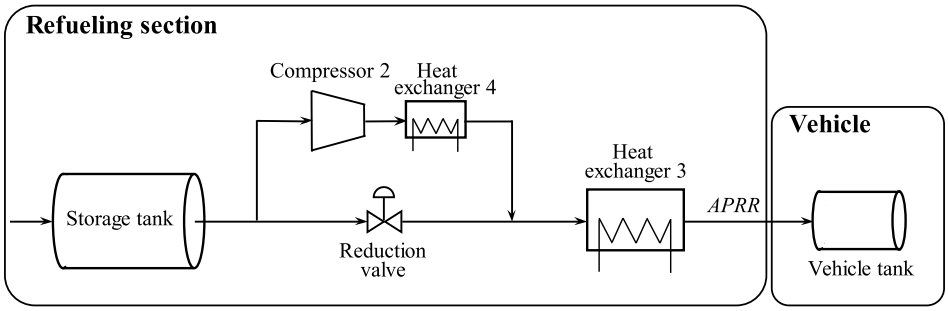

Figure 4.2: *The direct compression refueling design with a heat exchanger following the compressor in the refueling section. The heat exchanger is referred to as heat exchanger 4.*

If still neither of the heat sources are able to drive the process alone, a combination of Case II and III is applied in Case IV.

1. Assuming the temperatures of the heat are high enough.

5 | Model development

This chapter is twofold. The first part introduces the model equations for the different components in the direct compression refueling station including on-site hydrogen production. In addition, a section describing the pressure control configuration is included in this part. The second part explains the four cases for enabling the absorption refrigeration process at the station. A simplified topology on which the modeling of the station is based on is presented in Figure 5.1. More complex topologies for each component will be given in the text where the component's model is developed.

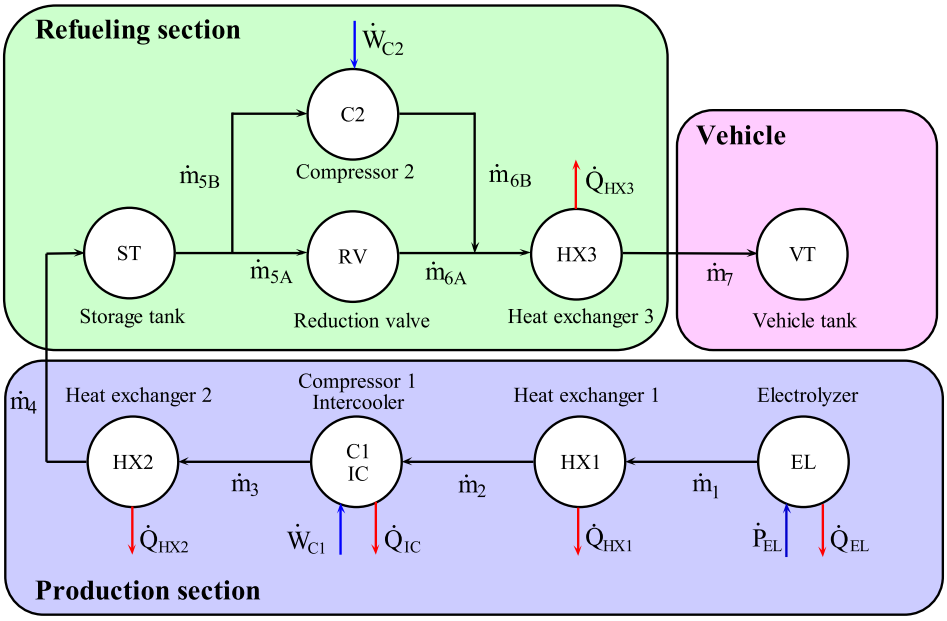

Figure 5.1: *The model topology for the hydrogen refueling station with direct compression refueling design and on-site production. The black, blue and red lines correspond to mass, work and heat flows, respectively.*

Note that the buffer tank is not included in the topology as it is assumed to be at steady state and thereby have no influence on the rest of the process. Generally

in the model development, the label $R_{station}$ refers to the rest of the station as a reservoir and the label R_W refers to the reservoir in which energy for work is obtained.

5.1 General model assumptions

Some of the more general assumptions made during the modeling are listed below:

- Pressure losses in pipelines and across heat exchangers are neglected.
- Heat exchange in pipelines is neglected.
- There is no height difference between the components of the station. Therefore, the gravitational potential energy is neglected.
- The velocities are small so the kinetic energy is also neglected.
- The hydrogen is well stirred within the tanks so that the distribution of hydrogen is uniform. The tanks are thus modeled as lumped capacities.
- At the start of each refueling, the mass in the storage tank at the station and the vehicle tank holds ambient temperature.

5.2 Generalized mass and energy balances

For a non-reacting open control volume with one component, the total mass balance is

$$\frac{dm}{dt} = \dot{m}_{in} - \dot{m}_{out} \tag{5.1}$$

where dm/dt is the rate of accumulation of mass in the control volume, and $\dot{m}_{in}$ and $\dot{m}_{out}$ are mass flows flowing in and out of the control volume, respectively. At steady state, the accumulation term is equal to zero and the mass balance is reduced to

$$\dot{m}_{in} - \dot{m}_{out} = 0 \tag{5.2}$$

$$\dot{m}_{in} = \dot{m}_{out} \hat{=} \dot{m} \tag{5.3}$$

where $\dot{m}$ is the steady-state mass flow.

The total energy balance for a non-reactive open control volume can be written as

$$\frac{dU_{sys}}{dt} = \dot{Q} - \dot{W}_s + (\dot{m}h)_{in} - (\dot{m}h)_{out} \tag{5.4}$$

where dU_{sys}/dt is the rate of accumulation of internal energy in the control volume, $\dot{Q}$ is the rate of heat flow into the control volume, $\dot{W}_s$ is the rate of shaft work

performed by the control volume and h_{in} and h_{out} are the enthalpies of the in- and outflow, respectively. Note that potential, kinetic and other energies have been neglected. At steady state, the accumulation term will be zero. By substituting the zero accumulation term and the steady-state mass balance (5.3) into Equation 5.4, the steady-state energy balance is found:

$$\dot{m}(h_{in} - h_{out}) = \dot{W}_s - \dot{Q} \tag{5.5}$$

A complete derivation of the energy balance from the first law of thermodynamics is presented in Appendix A.

5.3 Electrolyzer

The total reaction for decomposition of water is:

$$\mathrm{H_2O(l)} \rightarrow \mathrm{H_2(g)} + \frac{1}{2}\mathrm{O_2(g)} \tag{5.6}$$

At standard conditions (25°C and 0.1 MPa) this reaction is non-spontaneous. However, by passing a direct current between two electrodes separated by an electrolyte, the decomposition will occur [9]. These two electrodes are called a cathode and anode, and hydrogen gas will be produced at the former while oxygen gas will be produced at the latter. The electrolyte in an alkaline electrolyzer is typically potassium hydroxide (KOH). The reactions occurring at each electrode are as follows:

$$\begin{aligned} \text{Cathode}: \quad & 2\mathrm{H_2O(l)} + 2\mathrm{e^-} \rightarrow \mathrm{H_2(g)} + 2\mathrm{OH^-(aq)} \\ \text{Anode}: \quad & 2\mathrm{OH^-(aq)} \rightarrow \frac{1}{2}\mathrm{O_2(g)} + \mathrm{H_2O(l)} + 2\mathrm{e^-} \end{aligned}$$

It is assumed that the operating pressure and temperature of the electrolyzer remain fixed, also during off-time.

5.3.1 Electrolyzer model

The topology of the electrolyzer is presented in Figure 5.2. Note that the supply of water and removal of oxygen gas are not included in the topology. HXEL refers to the internal heat exchanger in the electrolyzer, $\dot{m}_{EL,cw}$ to the cooling water entering the heat exchanger and $\dot{m}_{EL,hw}$ to the hot water leaving after the heat exchange has occurred. $\mathrm{R_{cw}}$ and $\mathrm{R_{hw}}$ refer to the corresponding cold and hot water reservoirs.

The energy required to split one mole of water into hydrogen and oxygen is equal to the change in enthalpy, ΔH, of the reaction, in other words the reaction enthalpy [18]. This corresponds to the total amount of energy needed in a water electrolysis process. However, due to electrical inefficiencies, heat is generated during an electrolysis process [9]. The energy efficiency, η_{el}, describes how much of the electrical

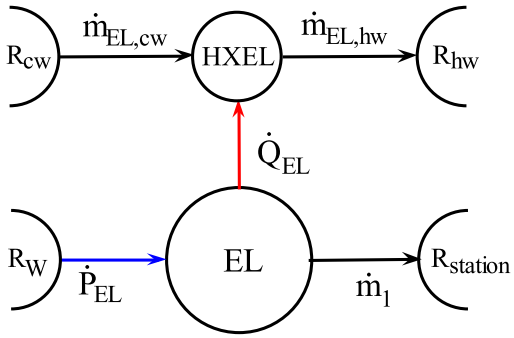

Figure 5.2: *Electrolyzer topology. $\dot{P}_{EL}$ and $\dot{Q}_{EL}$ are the electrical energy input and the heat removal rate in the electrolyzer, respectively. $\dot{m}_1$ is the mass flow of produced hydrogen. HXEL refers to the internal heat exchanger in the electrolyzer, $\dot{m}_{EL,cw}$ and $\dot{m}_{EL,hw}$ refer to the cold water entering the heat exchanger and the hot water leaving it, and R_{cw} and R_{hw} to their corresponding reservoirs.*

power input ($\dot{P}_{EL}$) is used for producing hydrogen. The required electrical power achieve a certain production rate of hydrogen ($\dot{m}_{EL}$) and can thus be expressed as

$$\dot{P}_{EL} = \frac{\dot{m}_{EL}\Delta_{rx}H_m}{\eta_{EL}} \tag{5.7}$$

where $\Delta_{rx}H_m$ is the reaction enthalpy [18]. The subscript m implies that the enthalpy is on molar form. The reaction enthalpy is found from

$$\Delta_{rx}H_m(T,p) = \Delta H_{m,H_2}(T,p) + \frac{1}{2}\Delta H_{m,O_2}(T,p) - \Delta H_{m,H_2O}(T,p) \tag{5.8}$$

where $\Delta H_{m,i}(T, p)$ is the molar enthalpy at the specified temperature and pressure for component i. The total differential of enthalpy can be used to find the enthalpy of components at other temperatures and pressures than the tabulated standard values. The differential as a function of temperature and pressure can be written as

$$dH(T,p) = C_p dT + \left[V - T\left(\frac{\partial V}{\partial T}\right)_p\right] dp \tag{5.9}$$

where C_p is the constant pressure heat capacity [J/K] and V is the fluid volume. The derivation of the temperature and pressure dependent differential is presented in Appendix A. At the operating pressure (1.2 MPa) and temperature (90°C) of the electrolyzer, the hydrogen and oxygen gas can be approximated as ideal gases[1]. By substituting the ideal gas law in Equation 5.9 it can be seen that the enthalpy of an ideal gas is independent of pressure. Refer to Appendix A for the substitution. Equation 5.9 can then be simplified. It is also assumed that the water remains in

1. Their compressibility factors are 1.0062 and 0.9982, respectively [2].

liquid phase during the electrolysis. Liquid water is assumed to be incompressible, hence the dependence of pressure is negligible. This implies that the enthalpies of both the gases and the liquid are independent of the pressure. Thus, the enthalpy calculations can be simplified:

$$dH(T,p) = C_p \mathrm{d}T \tag{5.10}$$

Integration of this equation yields (on molar form):

$$\Delta H_{m,i}(T) = \Delta_f H^o_{m,i}(T_{ref}) + \int_{T_{ref}}^{T} C_{p,m}(T)\,\mathrm{d}T \tag{5.11}$$

where $\Delta_f \mathrm{H}^o_{m,i}$ is the molar formation enthalpy at a reference condition for component i and T_{ref} is the reference temperature. The heat capacity is assumed to be independent of the temperature in the given temperature range. Thus, equation 5.11 can be simplified to:

$$\Delta H_{m,i}(T) = \Delta_f H^o_{m,i}(T_{ref}) + C_{p,m}(T - T_{ref}) \tag{5.12}$$

The heat generation in the electrolysis process ($\dot{Q}_{EL}$) can be expressed as:

$$\dot{Q}_{EL} = (1 - \eta_{EL})\dot{P}_{EL} \tag{5.13}$$

5.4 Heat exchangers

There are three independent heat exchangers at the refueling station (excluding the internal heat exchanger in the electrolyzer and the intercooler in compressor 1), and they are all modeled in the same manner. Heat exchanger 1 and 2 both cool down to the ambient temperature while heat exchanger 3 cools the hydrogen to -40°C.

5.4.1 Heat exchanger model

The physical topologies of the heat exchangers are shown in Figures 5.3a, 5.3b and 5.3c. The model development is only given for heat exchanger 1, but is similar for the other two. It is assumed that the heat exchangers are at steady state and that there is no pressure drop across them. The amount of heat that needs to be removed is calculated based on a specified outlet temperature of the hydrogen gas. The heat removal rate can be obtained from the steady-state energy balance (5.5) with the assumption that no work is performed ($\dot{W}_s = 0$):

$$\dot{Q}_{HX1} = \dot{m}(h_2 - h_1) \tag{5.14}$$

$\dot{m}_2 = \dot{m}_1 \triangleq \dot{m}$ because of the steady-state assumption. The outlet enthalpy will be calculated from the specified outlet temperature and the outlet pressure by using the equation of state. Due to no pressure drop, the outlet pressure is equal to the inlet pressure. It will be assumed that the heat exchanger is capable of removing the necessary amount of heat in order to reach the specified outlet temperature.

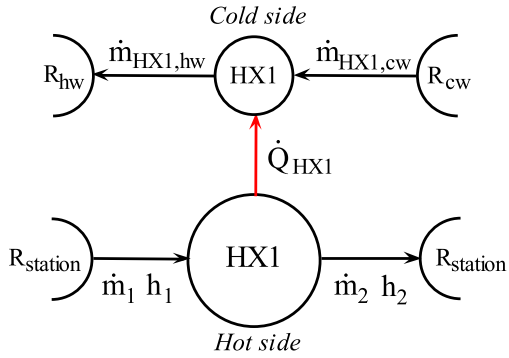

(a) *The topology of heat exchanger 1. $\dot{m}_{HX1,cw}$ refers to the mass flow of cold water entering the heat exchanger on the cold side, while $\dot{m}_{HX1,hw}$ refers to the hot water flow leaving. R_{cw} and R_{hw} refer to the cold and hot water reservoirs, respectively.*

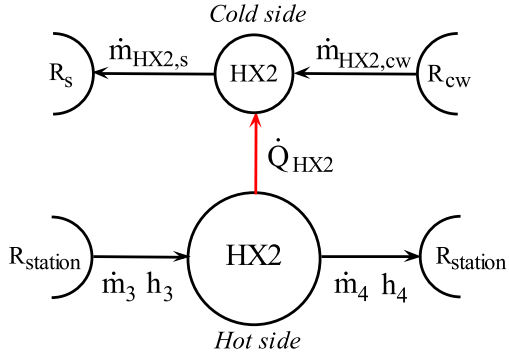

(b) *The topology of heat exchanger 2. $\dot{m}_{HX2,cw}$ refers to the mass flow of cold water entering the heat exchanger on the cold side, while $\dot{m}_{HX2,s}$ refers to the steam flow leaving. R_{cw} and R_{s} refer to the cold water and steam reservoirs, respectively.*

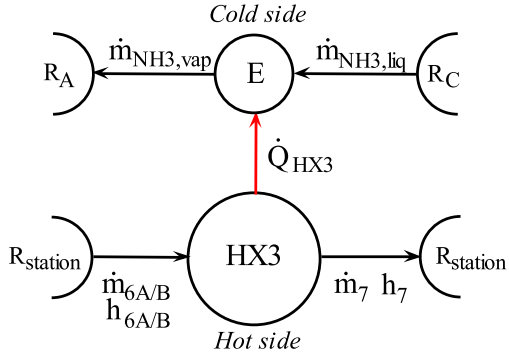

(c) *The topology of heat exchanger 3. $\dot{m}_{NH3,liq}$ refers to the mass flow of liquid NH_3 entering the evaporator (E), while $\dot{m}_{NH3,vap}$ refers to the vaporized NH_3 flow leaving. R_{C} and R_{A} refer to the condenser and absorber reservoirs, respectively.*

Figure 5.3: *The topologies of heat exchanger 1, 2 and 3. $\dot{m}$ refers to the inlet and outlet flows, h refers to the specific enthalpy of the corresponding flow and $\dot{Q}$ refers to the heat removal rate.*

5.5 Compressors

There are two compressors in the direct compression design and both will be defined as reciprocating compressors. The first compressor (compressor 1) is compressing the hydrogen in two stages because of the high compression ratio (1.2 MPa to 30 MPa). The first stage will have a fixed compression ratio (i.e. p_{out}/p_{in}) of 5 while the compression ratio of the second stage will vary depending on the pressure in the storage tank. Between the two compression stages, there will be an intercooler which refrigerates the hydrogen to the ambient temperature. Further, the mass flow through the compressor will be constant. The reciprocating compressors are modeled as continuous processes, however, in reality they are discontinuous. It is assumed that the compressors have many pistons in each phase, thus resulting in an almost continuous mass flow.

5.5.1 Compressor model

The physical topologies for compressor 1 and compressor 2 are presented in Figure 5.4 and Figure 5.5, respectively.

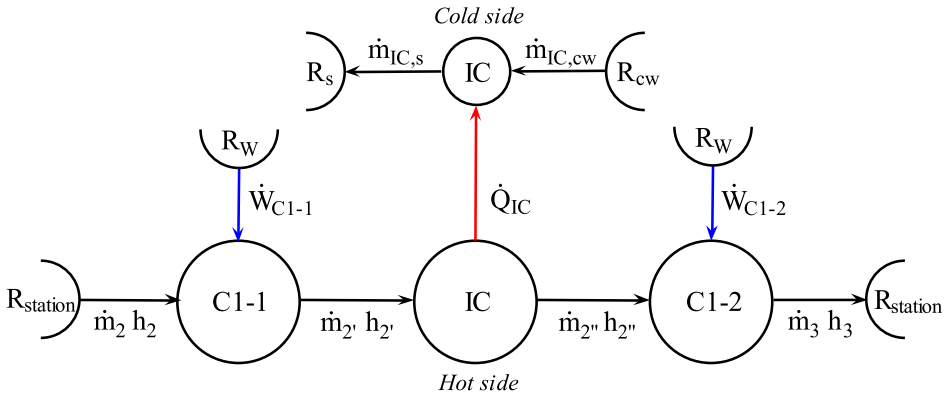

Figure 5.4: *Topology of compressor 1 with the two compressor stages and the intercooler. $\dot{W}_{C1-1}$ and $\dot{W}_{C1-2}$ are the work input in compression stage 1 and 2, respectively, while $\dot{Q}_{IC}$ is the heat removal rate in the intercooler. $\dot{m}_2$ and $\dot{m}_3$ are the inlet and outlet flow of the compressor while $\dot{m}_{2'}$ and $\dot{m}_{2''}$ are intermediate flows before and after intercooling. h refers to the specific enthalpy of the flows. On the cold side, $\dot{m}_{IC,cw}$ refers to the cold water entering the intercooler and $\dot{m}_{IC,s}$ refers to the steam flow leaving. R_{cw} and R_s refers to the cold water and steam reservoirs, respectively.*

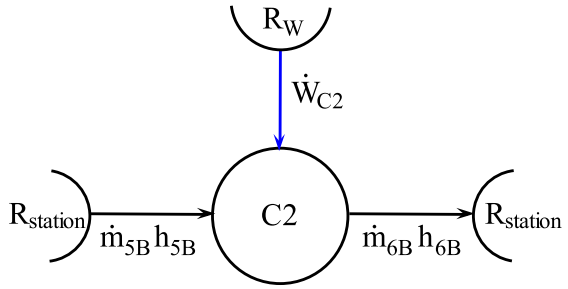

Figure 5.5: *Topology of compressor 2 where $\dot{W}_{C2}$ is the work input rate. $\dot{m}_{5B}$ and $\dot{m}_{6B}$ are the inlet and outlet flows, and h_{5B} and h_{5B} are the specific enthalpies of the inlet and outlet flow, respectively.*

The following equations are presented for compressor 2, however, all equations apply to compressor 1 as well. The difference is that the equations are applied twice for compressor 1; once per stage. The intercooler is modeled by using the same equation for a heat exchanger (Equation 5.14).

$$\dot{Q}_{IC} = \dot{m}(h_{2''} - h_{2'}) \tag{5.15}$$

The compression process is assumed to be adiabatic ($\dot{Q} = 0$) and at steady state. The steady-state energy balance (5.5) is therefore reduced to the following

$$\dot{W}_{C2} = \dot{m}(h_{5B} - h_{6B}) \tag{5.16}$$

where $\dot{m}$ is the mass flow through the compressor, $\dot{W}_{C2}$ is the added shaft work and h_{5B} and h_{6B} are the enthalpy of the in- and outflow, respectively. The required work for the compression can thus be found from Equation 5.16. For compressor 1, the performed work will be the sum of the work each compression stage carries out.

$$\dot{W}_{C1} = \dot{W}_{C1-1} + \dot{W}_{C1-2} \tag{5.17}$$

Since the compression is adiabatic, the specific entropy (s) remains constant during the compression. That is

$$\mathrm{d}s = 0 \text{ and } s_{6B} = s_{5B} \tag{5.18}$$

The outlet pressure (p_{6B}) is known, and hence, the outlet enthalpy can be found from the outlet entropy and pressure by using an equation of state. However, the obtained enthalpy ($h_{6B,is}$) is based on the assumption that the compression is adiabatic. The real enthalpy of the outlet flow (h_{6B}) can be found by using the isentropic efficiency (η_{is}) in the following relationship [11]:

$$h_{6B} - h_{5B} = \frac{h_{6B,is} - h_{5B}}{\eta_{is}} \tag{5.19}$$

The isentropic efficiency is given by

$$\eta_{is} = 0.1091(\ln r)^3 - 0.5247(\ln r)^2 + 0.8577 \ln r + 0.3727 \tag{5.20}$$

where r is the pressure ratio between the outlet and the inlet of the compressor (p_{6B}/p_{5B}) [19]. This equation is valid for $1.1 < r < 5$. When the real enthalpy is obtained, the required compressor work can be calculated from Equation 5.16, and the real outlet temperature (T_{6B}) can be found by using the equation of state.

The capacity of the compressor, the mass flow $\dot{m}_{5B}$, is calculated from

$$\dot{m}_{5B} = \rho_{5B}\eta_v N_2 V_{cyl,2} \tag{5.21}$$

where ρ_{5B} is the density of the inlet flow, η_v the volumetric efficiency, N_2 is the compressor speed (piston strokes per second) and $V_{cyl,2}$ is the volume of the compressor cylinder. The volumes of the compressor cylinders are calculated in Appendix B. In reality, the piston does not travel all the way to the end of the cylinder; the gas volume drawn into the cylinder is less than the given cylinder volume [11]. This is because a clearance volume occurs between the piston and the cylinder head. The cylinder clearance is defined as the ratio of the clearance volume to the cylinder volume and will vary between 4% - 16% for standard cylinders [20]. The effect this clearance has on compressor capacity is described by the volumetric efficiency. The volumetric efficiency [%] decreases as the pressure ratio (r) increases and can be expressed as

$$\eta_v = 100 - r - c\Big[\frac{Z_{5B}^2}{Z_{6B}^2} r^{\frac{1}{\gamma}} - 1\Big] \tag{5.22}$$

where c denotes the cylinder clearance, γ the ratio of specific heats of the inlet flow ($c_{p,5B}/c_{v,6B}$) and Z the compressibility factor of the hydrogen gas [21].

5.6 Tanks

Only the storage and vehicle tanks are considered in the modeling phase as the buffer tank is assumed to be at steady state. Both tanks are modeled as lumped capacities. This means that the states are uniform in the control volume (e.g. the temperature is similar throughout the whole tank).

5.6.1 Storage tank model

The topology of the storage tank can be seen in Figure 5.6.

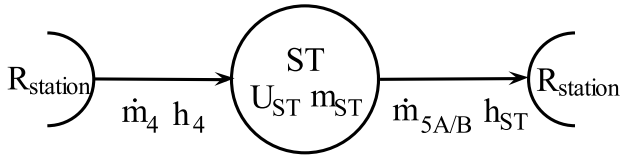

Figure 5.6: *The topology of the storage tank where U_{ST} is the conserved internal energy and m_{ST} is the conserved mass in the control volume. $\dot{m}_4$ and $\dot{m}_{5A/B}$ are the inlet and outlet flows, respectively, and h_4 and h_{ST} their corresponding specific enthalpies.*

For simplicity, the outlet flow will be referred to as $\dot{m}_5$. The storage tank undergoes charging and discharging at the same time, thus the mass balance remains the same as in Equation 5.1.

$$\frac{dm_{ST}}{dt} = \dot{m}_4 - \dot{m}_5 \tag{5.23}$$

The tank volume is constant ($dV/dt = 0$) and no shaft work is performed ($\dot{W}_s = 0$). In addition, it is assumed that the storage tank is large such that the temperature in the tank is close to the ambient temperature. Therefore, it is assumed that there is no or negligible little heat exchange between the tank and the environment, hence $\dot{Q} = 0$. The energy balance (5.4) is then reduced to:

$$\frac{dU_{ST}}{dt} = (\dot{m}h)_4 - (\dot{m}h)_5 \tag{5.24}$$

The inlet enthalpy, h_4, is the enthalpy of the inlet flow and is independent of the state in the tank. Conversely, the enthalpy of the outlet flow, h_5, is generally not constant since the state inside the system changes continuously [22]. However, it is assumed that the state in the control volume is uniform, hence the specific enthalpy at the boundary, h_5, is equal to the enthalpy in the tank, h_{ST}:

$$\frac{dU_{ST}}{dt} = \dot{m}_4 h_4 - \dot{m}_5 h_{ST} \tag{5.25}$$

5.6.2 Vehicle tank model

The vehicle tank topology is presented in Figure 5.7.

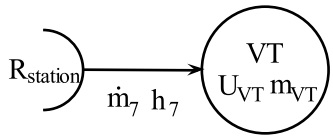

Figure 5.7: *The vehicle tank topology where U_{VT} is the conserved internal energy and m_{VT} is the conserved mass in the control volume. $\dot{m}_7$ and h_7 are the inlet mass flow and specific enthalpy of that flow, respectively.*

The inside of the tank walls is chosen as the boundary for the system. Since the vehicle tank is only considered during filling, there is no outflow of the tank. Hence $\dot{m}_{out} = 0$, and the mass balance can be written as:

$$\frac{dm}{dt} = \dot{m}_7 \tag{5.26}$$

It is assumed that the filling is fast and hence adiabatic, that is, $\dot{Q} = 0$. In addition, similar to the storage tank the volume of the tank is constant, $dV/dt = 0$ and no shaft work crosses the boundary, $\dot{W}_s = 0$. This reduces the energy balance (5.4) to:

$$\frac{dU_{sys}}{dt} = (\dot{m}h)_7 \tag{5.27}$$

Similar to the storage tank, the inlet enthalpy is the enthalpy of the inlet flow, $\dot{m}_7$.

5.7 Reduction valve

The reduction valve topology can be seen in Figure 5.8.

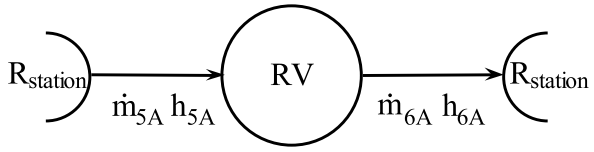

Figure 5.8: *The reduction valve topology. $\dot{m}_{5A}$ and $\dot{m}_{6A}$ are the inlet and outlet mass flows, and h_{5A} and h_{6A} are the corresponding specific enthalpies of the flows. $h_{5A} = h_{6A}$ since the expansion is isenthalpic.*

It is assumed that the expansion through the valve is irreversible and adiabatic ($\dot{Q} = 0$). There is no shaft work during the expansion: $\dot{W}_s = 0$. The energy balance for a steady-state process (5.5) can then be reduced to

$$\dot{W}_s = \dot{m}(h_{5A} - h_{6A}) = 0 \tag{5.28}$$

$$h_{5A} = h_{6A} \tag{5.29}$$

where $\dot{m}_{6A} = \dot{m}_{5A} \triangleq \dot{m}$ because of the steady-state operation. As can be seen from the equation, the enthalpy is fixed during the expansion. Hence, the expansion is isenthalpic and the outlet enthalpy is known. Since the outlet enthalpy and pressure are known, the outlet temperature can easily be calculated.

The mass flow, $\dot{m}_{5A}$, through the reduction valve is given by

$$\dot{m}_{5A} = \rho_{5A} C_v \sqrt{\frac{p_{6A} - p_{5A}}{\rho_{5A}}} \tag{5.30}$$

where ρ_{5A} is the density of the hydrogen gas, C_v is the valve coefficient and p_{6A} and p_{5A} are the outlet and inlet pressures, respectively. Since pressure losses in pipelines and heat exchangers are neglected, the outlet pressure of the reduction valve is equal to the pressure in the vehicle tank. That is, $p_{6A} = p_{VT}$. The inlet density is equal to the density in the storage tank: $\rho_{5A} = \rho_{ST}$.

5.8 Control strategy

The refueling is controlled by the average pressure ramp rate set by the SAE TIR J2601. Thus, a controller adjusting the pressure rise in the vehicle tank (i.e. the pressure rise at the nozzle) is required. Since both a reduction valve and a compressor are utilized during a refueling, two controllers are necessary. The control configuration is shown in Figure 5.9.

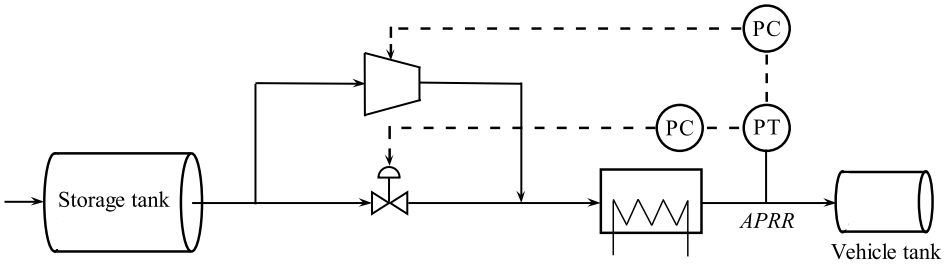

Figure 5.9: *The pressure control configuration in the refueling section. The APRR is set at the dispenser nozzle, however, this corresponds to the pressure in the vehicle tank due to the assumption of no pressure loss in the system.*

The pressure rise is controlled by changing the mass flows through either the valve or the compressor depending on which process line being utilized. The reduction valve controller changes the mass flow by manipulating the valve coefficient (C_v) directly. This correlates to the opening percentage of the valve. Note that saturation limits have not been considered for the valve. The compressor controller alters the mass flow by manipulating the compressor speed (N_2).

The pressure rise during the refueling of the vehicle tank is an integrating process. According to the Simple[2] Internal Model Control (SIMC) tuning rules, the controllers should be proportional-integral (PI) controllers[3] [23]. The general equation for a digital PI controller in time domain is given as [24]

$$u_k = \bar{u} + K_c\Big[e_k + \frac{\Delta t}{\tau_I}\sum_{j=1}^{k-1} e_j\Big] \tag{5.31}$$

where

u_k is the controller output at the kth sampling instant for k = 1,2...

$\bar{u}$ is the bias value of the controller output.

e_k is the error (offset from set point) at the kth sampling instant.

Δt is the sampling period.

K_c is the controller gain.

τ_I is the integral time constant.

2. Simple or Skogestad.
3. These controllers are included to make the model comply the APRR. In reality, a more advanced control system is required for the compressor.

Accordingly, the control equations for the reduction valve and compressor controllers are as follows:

$$C_{v,k} = C_v^o + K_{c,RV}\Big[e_k + \frac{\Delta t}{\tau_{I,RV}} \sum_{j=1}^{k-1} e_j\Big] \tag{5.32}$$

$$N_{2,k} = N_2^o + K_{c,C2}\Big[e_k + \frac{\Delta t}{\tau_{I,C2}} \sum_{j=1}^{k-1} e_j\Big] \tag{5.33}$$

The error is defined as

$$e_k = p_{SP,k} - p_k \tag{5.34}$$

where $p_{SP,k}$ is the set point and p_k the measured pressure in the vehicle tank at the kth sampling instant. The controller bias for the reduction valve controller (C_v^o) is predefined for each refueling. The bias for the compressor controller is calculated based on the mass flow through the valve at the time of the switch from valve flow to compressor flow.

5.8.1 Controller tuning

The SIMC tuning rules are used for tuning the controllers. Both processes are approximated with integrating models

$$G(s) = \frac{k' e^{-\theta s}}{s} \tag{5.35}$$

where k' is the process gain (or slope of integrating response) and θ is the process time delay. The SIMC tuning rules for an integrating process are as follows

$$K_c = \frac{1}{k'} \frac{1}{\tau_c} \tag{5.36}$$

$$\tau_I = 4(\tau_c + \theta) \tag{5.37}$$

where K_c is the controller gain, τ_c the desired closed-loop time constant and τ_I the integral time constant. The desired closed-loop time constant can be chosen freely. However, the optimal value is determined by a trade-off between output performance and robustness [25]. The former is denoted tight control and corresponds to a fast response and good disturbance rejection. Tight control is favored by a small τ_c, and the "tightness" of the controller can be quantified by the magnitude of the error (e). The latter refers to smooth control, results in good robustness and is favored by a large τ_c. As the set point of the pressure will change continuously (i.e. a ramp) during a refueling, a fast controller is preferable; thus having a small value of τ_c.

5.9 Absorption refrigeration at the station

Section 4.4 presented the possible heat sources for the absorption refrigeration process. These include the internal heat exchanger in the electrolyzer ($\dot{Q}_{EL}$), heat exchanger 1 ($\dot{Q}_{HX1}$), the intercooler in compressor 1 ($\dot{Q}_{IC}$) and heat exchanger 2 ($\dot{Q}_{HX2}$). Heat exchanger 1, however, is not considered as neither the heat amount nor the temperature of the heat will be sufficient. Additionally, Section 4.4 presented four cases that will be considered in this thesis. The modeling and calculation of these are given below.

5.9.1 Assumptions

The following assumptions were made in the modeling:

- The inlet temperature of the cooling water is equal to the ambient temperature.
- The outlet temperature of the cooling water is equal to the inlet temperature of the flow being cooled (countercurrent heat exchange)[4].
- The steam used for heat transfer to the generator is saturated at the driving temperature.
- The coefficient of performance remains constant also during partial load operation[5].
- The pressure is the same through the cooling system and corresponds to the pressure that provides saturated steam at the required driving temperature of the generator.
- Resistance to heat transfer is neglected.

5.9.2 Case I

The heat removed by the considered heat exchangers are found in Section 5.4 and Section 5.5.

5.9.3 Case II

Figure 5.10 illustrates how the waste heat from the intercooler and heat exchanger 2 can be utilized to increase the temperature of the waste heat generated in the electrolyzer unit to the required temperature (T_{req}). The black, purple and blue lines correspond to steam, hot water and cold water flows, respectively, while the red lines correspond to heat flows. T^{o}_{cw} refers to the temperature of the inlet cooling water and is always similar to the ambient temperature. The cooling water flows

4. This assumption does not apply for heat exchanger 3 as a pinch temperature of 5°C is assumed.
5. According to [15], a partial load operation down to 20% of the maximum load is possible with nearly constant coefficient of performance.

entering the intercooler and heat exchanger 2 ($\dot{m}_{IC}$ and $\dot{m}_{HX2}$) are vaporized during the heat exchange with the hot hydrogen gas. The steam flows leaving these heat exchangers are mixed, forming a new flow ($\dot{m}_{HX}$). This flow, having a temperature of T_{HX}, is used to increase the temperature of some of the hot water ($\dot{m}_{req}$) coming from the internal heat exchanger in the electrolyzer. The hot water, holding a temperature of T_{EL}, is heated up to and vaporized at the required temperature, T_{req}. The flow, now saturated steam, then transfers heat to the generator ($\dot{Q}_G$), denoted G in the figure.

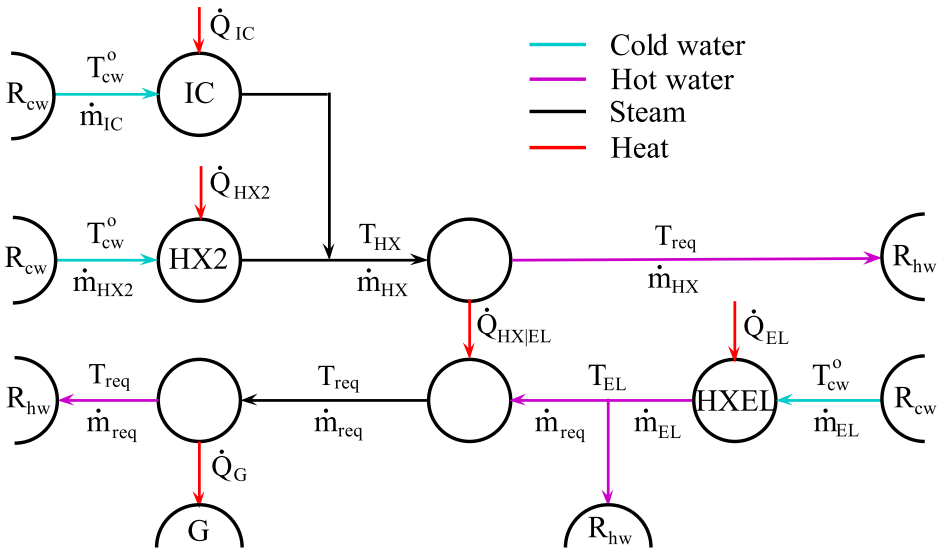

Figure 5.10: *Illustration of how to increase the temperature of the low-temperature heat coming from the electrolyzer ($\dot{Q}_{EL}$) with the high-temperature heat removed in the intercooler ($\dot{Q}_{IC}$) and heat exchanger 2 ($\dot{Q}_{HX2}$). $\dot{m}_{HX}$ is the mass flow of the combined flows of the intercooler and heat exchanger 2 ($\dot{m}_{IC}$ and $\dot{m}_{HX2}$), $\dot{m}_{EL}$ is the available mass flow of hot water in the electrolyzer and $\dot{m}_{req}$ is the required mass flow of hot water to be heated up to the required temperature (T_{req}). T^o_{cw} refers to the inlet temperature of the cooling water, T_{EL} to the temperature of the hot water exiting the electrolyzer and T_{HX} to the temperature of the mixed steam flows. The black, purple and blue lines correspond to steam, hot water and cold water flows while the red lines correspond to heat flows.*

It is assumed that all heat exchange operations are at steady state. The energy balance for a heat exchanger has been applied in the calculations:

$$\dot{Q} = \dot{m}(h_{out} - h_{in}) \tag{5.38}$$

$\dot{Q}$ is the rate of heat transferred, $\dot{m}$ is the mass flow of either steam or water, h_{out} and h_{in} are the outlet and inlet enthalpy, respectively. The data for saturated steam is given in Appendix C.

Generator

The required heat input to the generator is calculated from

$$\dot{Q}_G = \frac{\dot{Q}_E}{\text{COP}} = \frac{\dot{Q}_{HX3}}{\text{COP}} \tag{5.39}$$

where $\dot{Q}_{HX3}$ is the cooling demand in heat exchanger 3. The mass flow of saturated steam ($\dot{m}_{req}$) necessary to deliver this amount of heat can then be calculated from Equation 5.38. The COP is found from Table 4.2 based on the temperature of the cooling water.

Electrolyzer

First, the flow of cooling water passing through the internal heat exchanger in the electrolyzer ($\dot{m}_{EL}$) is calculated in order to see whether the flow is sufficient compared to the required flow ($\dot{m}_{req}$). This is found by using the heat removed from the electrolyzer ($\dot{Q}_{EL}$) with Equation 5.38. Then, the heat ($\dot{Q}_{HX|EL}$) required to heat up and vaporize the hot water at the required temperature (T_{req}) is found using the same equation.

Heat exchanger 2 and intercooler

The cooling water enters both heat exchangers holding ambient temperature, but exits as steam. By using the heat removal rates of the heat exchangers ($\dot{Q}_{IC}$ and $\dot{Q}_{HX2}$), the available mass flows of the steam can be calculated ($\dot{m}_{IC}$ and $\dot{m}_{HX2}$). These outlet flows are mixed, forming a new flow, $\dot{m}_{HX,act}$. The subscript **act** refers to the actual mass flow. The new mass flow is found from:

$$\dot{m}_{HX,act} = \dot{m}_{IC} + \dot{m}_{HX2} \tag{5.40}$$

The properties of the new flow can be found from the steady-state energy balance given in Equation 5.5. No shaft work or heat transfer occur during the mixing, and the equation is therefore reduced to

$$h_{HX} = h_{HX2} + h_{IC} \tag{5.41}$$

where h_{HX}, h_{HX2} and h_{IC} are the specific enthalpies of the mixed flow, the outlet flow from heat exchanger 2 and the outlet flow of the intercooler, respectively. The heat required to generate the necessary amount of steam ($\dot{Q}_{HX|EL}$) is used to calculate the required mass flow of the mixed flow ($\dot{m}_{HX,req}$). This flow is then compared to the actual flow ($\dot{m}_{HX,act}$) to see whether the actual flow is sufficient to produce the necessary amount of saturated steam at the required temperature.

5.9.4 Case III

The topology of the compressor process line when heat exchanger 4 is included is shown in Figure 5.11. A new intermedate flow, $\dot{m}_{5B'}$, is introduced.

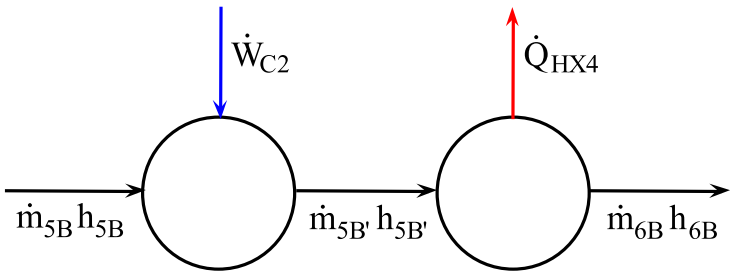

Figure 5.11: *The topology of the compressor line when heat exchanger 4 is included. $\dot{W}_{C2}$ is the work input to the compressor and $\dot{Q}_{HX4}$ is the heat removal rate. $\dot{m}_{5B}$ is the inlet flow to compressor 2, $\dot{m}_{5B'}$ is the intermediate flow between the two components and $\dot{m}_{6B}$ is the outlet flow of heat exchanger 4. h refers to the specific enthalpies of the flows.*

The rate of the heat removal ($\dot{Q}_{HX4}$) is calculated from Equation 5.38 as the mass flow $\dot{m}_{5B}$ is known.

5.9.5 Case IV

The approaches presented for Case II and Case III are applied together in Case IV.

6 | Model implementation

The previous chapter introduced the model equations for each component at the refueling station. The system of model equations consists of both ordinary differential equations (ODEs) and algebraic equations and constitutes therefore a differential algebraic equation (DAE) system. The DAE system is of the form

$$\frac{d\boldsymbol{x}}{dt} = \boldsymbol{f}(\boldsymbol{v}) \tag{6.1}$$

$$\boldsymbol{v} = \boldsymbol{g}(\boldsymbol{y}, \boldsymbol{u}) \tag{6.2}$$

$$\boldsymbol{y} = \boldsymbol{h}(\boldsymbol{x}) \tag{6.3}$$

$$\boldsymbol{u} = \boldsymbol{j}(\boldsymbol{y}) \tag{6.4}$$

where $\mathbf{x}$ is the vector of conserved quantities (i.e. primary states), $\mathbf{v}$ is the vector of transport quantities (i.e. mass flows), $\mathbf{y}$ is the vector of secondary states and $\mathbf{u}$ is the vector of controller output (i.e. manipulated variables). The primary states consist of internal energy and mass, while the secondary states include pressure, temperature, density and specific enthalpy. Figure 6.1 presents a block diagram of the computation scheme. A description of each block follows below. The MATLAB script is presented in Appendix G.

6.1 Initiation

Initiation is performed once per simulation. The variables that can be specified before a refueling simulation are summarized in Table 6.1. These correspond to variables that typically will vary between refuelings.

Table 6.1: *Variables that can be specified before a refueling.*

Variable	Unit	Description
p_{VT}	MPa	Pressure in vehicle tank
T_{amb}	K	Ambient temperature

These variables belong to the secondary states. The remaining secondary states and the initial primary states are calculated from the specified variables and other predefined parameters by using the equation of state.

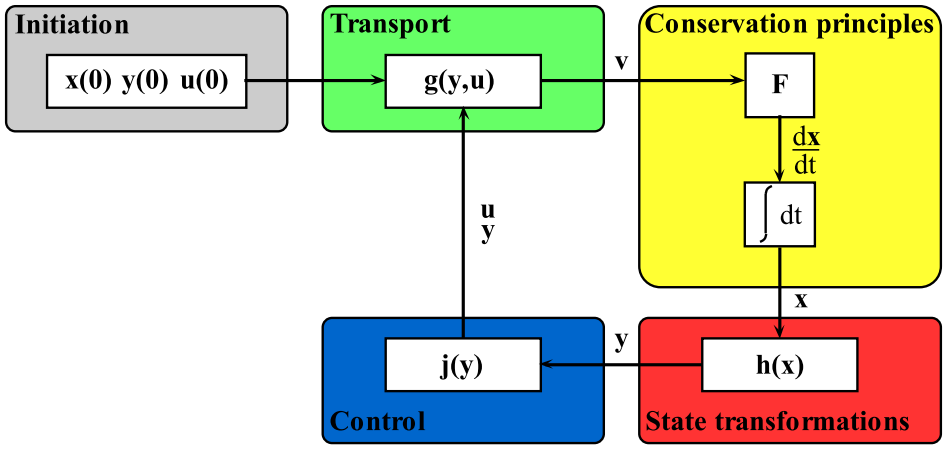

Figure 6.1: *The computation scheme presented as a block diagram.* $\boldsymbol{x}$ *is the vector of conserved quantities (primary states),* $\boldsymbol{v}$ *is the vector of transport quantities,* $\boldsymbol{y}$ *is the vector of secondary states and* $\boldsymbol{u}$ *is the vector of controller output.*

6.2 Transport

The mass flows in the station are induced either by the pressure difference across the reduction valve or by the work input to the compressors. The mass flow in the production section is set by compressor 1 ($\dot{m}_2$). The two heat exchangers (1 and 2) and compressor 1 are at steady state, implying:

$$\dot{m}_1 = \dot{m}_2 \text{ and } \dot{m}_4 = \dot{m}_3 = \dot{m}_2$$

For the refueling section, there are two options for mass transport: 1) the reduction valve ($\dot{m}_{5A}$), and 2) compressor 2 ($\dot{m}_{5B}$). Since both the compressor, reduction valve and heat exchanger 3 are operating at steady state, the remaining mass flows are given automatically by one of the two transport equations presented in Section 5.5 and Section 5.7.

$$\dot{m}_{6A} = \dot{m}_{5A} \text{ and } \dot{m}_{6B} = \dot{m}_{5B} \tag{6.5}$$

The governing transport equation for in the refueling section depends on the pressure difference between the two tanks. At first, the mass flow is induced by the pressure difference across reduction valve, however, when the pressure difference reaches a certain minimum limit, Δp_{switch}, the station switches to the compressor.

$$\dot{m}_7 = \begin{cases} \dot{m}_{5A}, & p_{vt} < p_{st} - \Delta p_{switch} \\ \dot{m}_{6A}, & p_{vt} > p_{st} - \Delta p_{switch} \end{cases} \tag{6.6}$$

The transport vector for the station can be expressed as

$$\boldsymbol{v} = \begin{bmatrix} \dot{m}_4 \\ \dot{m}_7 \end{bmatrix} \tag{6.7}$$

$$\tag{6.8}$$

or

$$\boldsymbol{v} = \boldsymbol{g}(\boldsymbol{y}, \boldsymbol{u}) \tag{6.9}$$

since the mass flows are dependent on the secondary states ($\mathbf{y}$) and the manipulated variables ($\mathbf{u}$).

The required compressor work ($\dot{W}$) for the two compressors, the power input ($\dot{P}_{EL}$) in the electrolyzer and the heat removal ($\dot{Q}$) in the electrolyzer and the heat exchangers will also be calculated in this block. Since the refueling station switches from the reduction valve to the compressor when the pressure drop across the reduction valve has reached a certain limit, the outlet pressure of the compressor will at first be lower than the inlet pressure. Because the pressure drop limit is low (0.5 - 1 MPa), the outlet pressure has been set equal to the inlet pressure in order to avoid negative work in the compressor model. This, however, occurs over a very short time frame as the defined pressure rise per second is approximately 0.5 MPa/s.

6.3 Conservation principles

The dynamic equations derived in Section 5.6 imply that the internal energy (U) and the mass (m) are the primary states of the system. The system of ODEs can be expressed as:

$$\begin{bmatrix} \frac{dm_{ST}}{dt} \\ \frac{dU_{VT}}{dt} \\ \frac{dm_{VT}}{dt} \\ \frac{dU_{VT}}{dt} \end{bmatrix} = \begin{bmatrix} \dot{m}_4 - \dot{m}_7 \\ \dot{m}_4 h_4 - \dot{m}_7 h_{ST} \\ \dot{m}_7 \\ \dot{m}_7 h_7 \end{bmatrix} = \begin{bmatrix} 1 & -1 \\ h_4 & -h_{ST} \\ 0 & 1 \\ 0 & h_7 \end{bmatrix} \begin{bmatrix} \dot{m}_4 \\ \dot{m}_7 \end{bmatrix} \tag{6.10}$$

Generally, this can be written as

$$\frac{d\boldsymbol{x}}{dt} = \boldsymbol{f}(\boldsymbol{v}) = \boldsymbol{F}\boldsymbol{v} \tag{6.11}$$

where $\mathbf{F}$ is the incidence matrix providing the flow directions and $\mathbf{v}$ the vector of transport quantities.

6.3.1 Integrator

An explicit Euler integrator has been implemented to solve the energy and mass balances of the storage and vehicle tanks. The explicit Euler method for the multivariable ordinary differential equation

$$\frac{d\boldsymbol{x}}{dt} = \boldsymbol{f}(\boldsymbol{v}) \tag{6.12}$$

is given in equation 6.13,

$$\boldsymbol{x}(k+1) = \boldsymbol{x}(k) + \Delta t \boldsymbol{f}(\boldsymbol{v}(k)) \tag{6.13}$$

where k represents the kth discrete time step of the integration and Δt is the integration step size [26].

6.4 State transformations

The secondary states are a result of the "new variables" being introduced by the transport relations presented in Section 6.2 [27]. It is therefore necessary to provide links from the secondary states and back to the primary states. These so-called links are denoted state transformations and can be described as:

$$\boldsymbol{y} = \boldsymbol{h}(\boldsymbol{x}) \tag{6.14}$$

State transformations in this system are provided through the relationship between mass, density and volume as well as an equation of state. The mass, density and volume relationship (at constant volume) is given as

$$\rho = \frac{m}{V} \tag{6.15}$$

where ρ is the density, m is the mass in the tank and V is the tank volume. The equation of state is explained more in detail below.

6.4.1 Equation of state

At low pressures, hydrogen gas can be considered as an ideal gas. However, at the high pressures reached at the refueling station, the compressibility factor (Z) of hydrogen implies that a real gas equation is required to determine the thermodynamic properties. For instance, at a pressure of 70 MPa and a temperature of 25°C, the compressibility factor is approximately 1.45 [2]. The thermodynamic properties of the hydrogen gas are therefore found using a free, open-source property database named CoolProp [2].

The equation of state applied for molecular hydrogen can be found in [28]. The EOS is explicit in the reduced Helmholtz free energy (α)

$$\alpha(\tau, \delta) = \frac{a(T, \rho)}{RT} \tag{6.16}$$

where a is the specific Helmholtz free energy, R the gas constant, τ the reciprocal reduced temperature and δ the reduced density. The last two are given as

$$\tau = \frac{T_c}{T} \tag{6.17}$$

$$\delta = \frac{\rho}{\rho_c} \tag{6.18}$$

where the subscript c refers to a critical-point property. The reduced Helmholtz free energy can be expressed as a sum of two parts: 1) the residual contribution (α^r), and 2) the ideal-gas contribution (α^{ig}):

$$\alpha = \alpha^r + \alpha^{ig} \tag{6.19}$$

The ideal-gas contribution is found from nonlinear regression of calculated ideal-gas heat capacity data from the literature while the residual contribution is found from nonlinear regression of experimental thermodynamic data. This is thoroughly explained in [2] and [28]. When the value of the reduced Helmholtz free energy is calculated, other thermodynamic properties can be obtained through analytical derivatives of the α^r and α^{ig} terms [2].

The desired thermodynamic property is obtained using the `Props` command. An example where the density ('D') of molecular hydrogen ('H2') at a temperature ('T') of 25°C (298 K) and a pressure ('P') of 0.1 MPa (100 kPa) is obtained is shown below.

```
1    D   =   Props('D', 'T', 298, 'P', 100, 'H2')
```

Table 6.2 shows the valid sets of input values for the `Props` command. D refers to density and H and S correspond to the specific enthalpy and entropy, respectively.

Table 6.2: *The sets of input values which are valid for the* `Props` *command. D refers to density and H and S correspond to the specific enthalpy and entropy, respectively.*

Input 1	Input 2
T	P
T	D
P	D
H	P
S	H
T	S

In each time step, the model calculates the new primary states of the system. As the primary states are internal energy and mass (which is converted to density by the relationship given in Equation 6.15), the available set of inputs, U and D, is

not valid according to Table 6.2. The `Props` command can therefore not be used directly. However, this can be solved with MATLAB's fsolve-function by iterating on the difference between the known internal energy and the internal energy found using the `Props` command as a function of the known density and an unknown variable, for instance the temperature. Then, the temperature and density value set can be used to find the remaining thermodynamic properties.

6.5 Control

As discussed in Section 5.8, it is necessary to implement two pressure controllers. That is, one controller for each process line. For the reduction valve, the controller will manipulate the mass flow by adjusting the valve coefficient (C_v) directly. In the compression line, the mass flow will be manipulated by changing the compressor speed (N_2). This can be summarized as:

$$\boldsymbol{u} = \begin{cases} [\, C_v \;\; 0 \,]^T, & p_{vt} < p_{st} - \Delta p_{switch} \\ [\, 0 \;\; N_2 \,]^T, & p_{vt} > p_{st} - \Delta p_{switch} \end{cases} \tag{6.20}$$

7 | Results and discussion: Model behavior

This chapter presents the general behavior of the model. All simulations will be run with an ambient temperature of 15°C. Both a refueling of a vehicle tank and a refilling of the storage tank are presented. A case where only the compressor in the refueling section is utilized in the refueling is also included. Additionally, the effect of an additional heat exchanger in the compression line has been examined (i.e. Case III). Finally, in order to ensure that the model is working for other conditions as well, the impact of different ambient temperatures and initial vehicle pressures is investigated. In each section, the model behavior for a specific case will be presented followed by a discussion.

7.1 Model parameters and controller settings

The controller settings for the two pressure controllers are given in Table 7.1. The process models used for tuning are obtained in Appendix D. In addition, the performance of controller settings achieved from different τ_cs is also presented in Appendix D.

Table 7.1: *Controller settings for the reduction valve and compressor controllers. τ_c is the desired closed-loop time constant, K_c the controller gain and τ_I the integral time constant.*

Parameter	Reduction valve	Compressor
τ_c	0.5	2
K_c	1.105×10^{-5}	6.494
τ_I	2	8

The model parameters are presented in Table 7.2. Note that the initial temperature in both tanks is assumed to be similar to the ambient temperature. In addition, all heat exchangers except for heat exchanger 3 cool down to the ambient temperature. Appendix B presents capacity calculations for the two compressors.

Table 7.2: *Model parameters used in the simulation. The first two parameters may vary from refueling to refueling.*

Parameter	Description	Value
T_{amb}	Ambient temperature [°C]	15
p^o_{VT}	Initial pressure in vehicle tank [MPa]	2
V_{VT}	Volume of vehicle tank [m^3]	0.172
T^o_{VT}	Initial temperature of vehicle tank [°C]	15
p_{EL}	Operating pressure in electrolyzer [MPa]	1.2
T_{EL}	Operating temperature in electrolyzer [°C]	90
η_{EL}	Electrolyzer efficiency	0.5
$V_{cyl,1}$	Compressor 1 cylinder volume [m^3]	2.3×10^{-3}
$V_{cyl,2}$	Compressor 2 cylinder volume [m^3]	3.1×10^{-4}
c	Compressor cylinder clearance [%]	10
T_{HX1}	Outlet temperature heat exchanger 1 [°C]	15
T_{HX2}	Outlet temperature heat exchanger 2 [°C]	15
T_{IC}	Outlet temperature of intercooler in compressor 1 [°C]	15
T_{HX3}	Outlet temperature heat exchanger 3 [°C]	-40
p^o_{ST}	Initial pressure in storage tank [MPa]	30
V_{ST}	Volume of station storage tank [m^3]	3
T^o_{ST}	Initial temperature of storage tank [°C]	15
Δp_{switch}	Pressure difference at which switch occurs [MPa]	0.5
C^o_v	Reduction valve controller bias [m^2]	2×10^{-6}
N^o_2	Initial compressor controller bias[1] [1/s]	0

1. Initially, the compressor is off. When the switch occurs, the controller bias for the compressor is calculated based on the current mass flow through the reduction valve.

7.2 Behavior during refueling

Based on the ambient temperature, the initial pressure and the vehicle tank capacity (1-7 kg) the APRR and the target pressure are found from the look-up tables in J2601 and are 0.47 MPa/s and 72.6 MPa, respectively [4]. The target pressure is reached within 150.1 seconds, and the state of charge (SOC) is then 89.63 %. The switch from the reduction valve to the compressor occurs after 56.1 seconds.

The pressure evolution in the storage tank and vehicle tank is presented in Figure 7.1a. Due to the assumption of no pressure loss in the station, the remaining pressures in the system are similar to the pressure either in the storage tank, the vehicle tank or the electrolyzer and are therefore not included. The operating pressure of the electrolyzer is fixed at 1.2 MPa during the whole refueling and is also not included. Figure 7.1b shows the pressure rise in the vehicle tank around the time of the switch from the reduction valve to the compressor.

The temperature evolution in the electrolyzer, storage tank, vehicle tank and at the outlet of the reduction valve/compressor 2 is given in Figure 7.2a. The outlet temperature of compressor 1 along with the temperature after the first compression stage in compressor 1 are included in a separate figure since these temperatures are significantly higher than the other temperatures at the station. This figure is referred to as Figure 7.2b.

The mass flows in the production section and the refueling section are presented in Figure 7.3. The cooling demands in heat exchanger 1, 2 and 3 and the intercooler are shown in Figure 7.4. The cooling demand of the internal heat exchanger in the electrolyzer is fixed throughout the refueling and is not included in the figure. The magnitude of the cooling demand is 2395 kW. Figure 7.5 shows the compressor work performed by compressor 1 and compressor 2 during a refueling. Similar to the cooling demand in the electrolyzer, the electrolyzer power input is fixed during the refueling as well. The power input is 4790 kW.

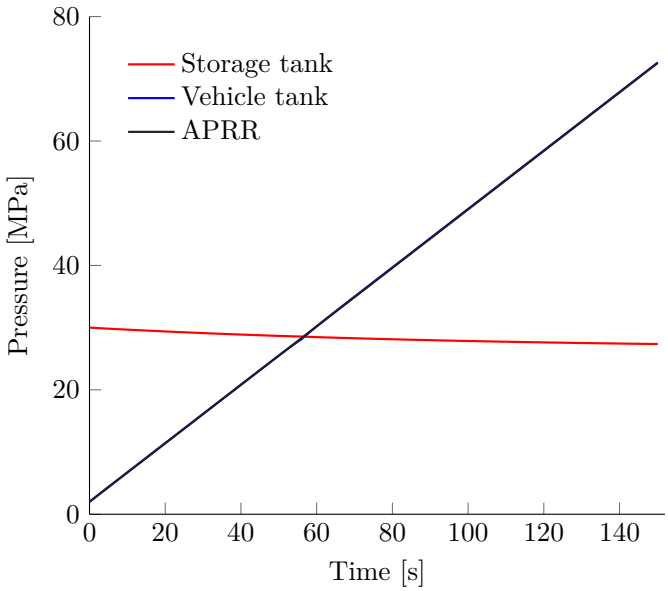

(a) *The pressure evolution during a refueling in the storage tank and vehicle tank along with the average pressure ramp rate.*

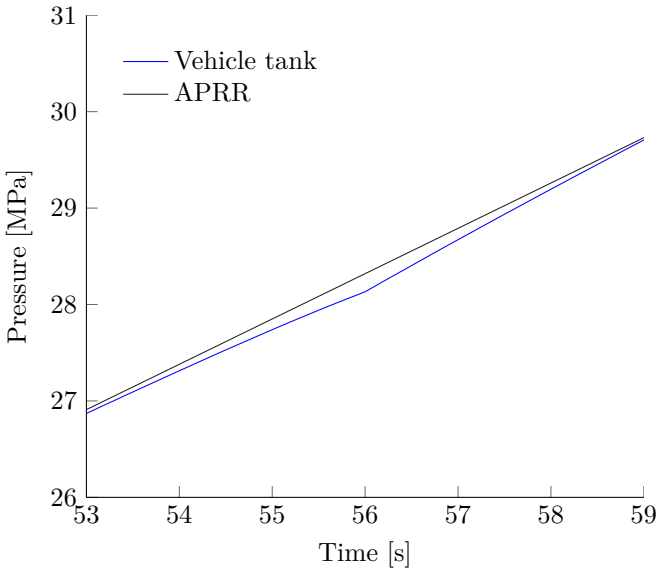

(b) *The pressure rise in the vehicle tank around the time of the switch from the reduction valve to the compressor.*

Figure 7.1: *Pressure evolution at the station during a refueling and at the time of the switch from the reduction valve to the compressor.*

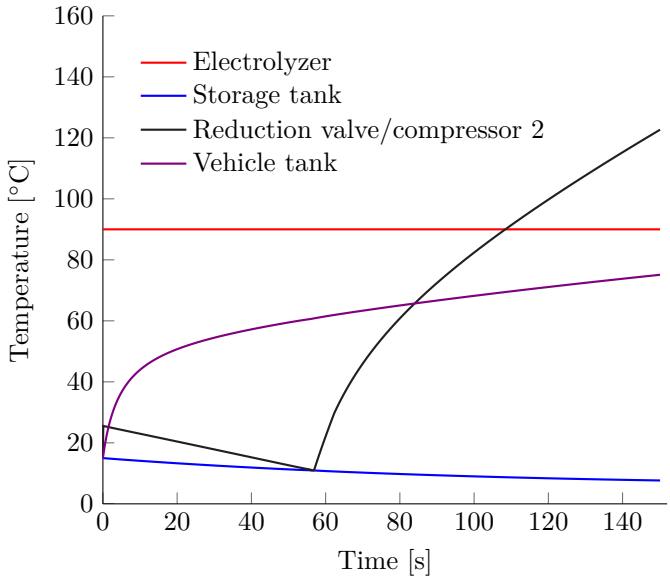

(a) *The temperatures in the electrolyzer and storage and vehicle tanks along with the outlet temperature of the reduction valve/-compressor 2.*

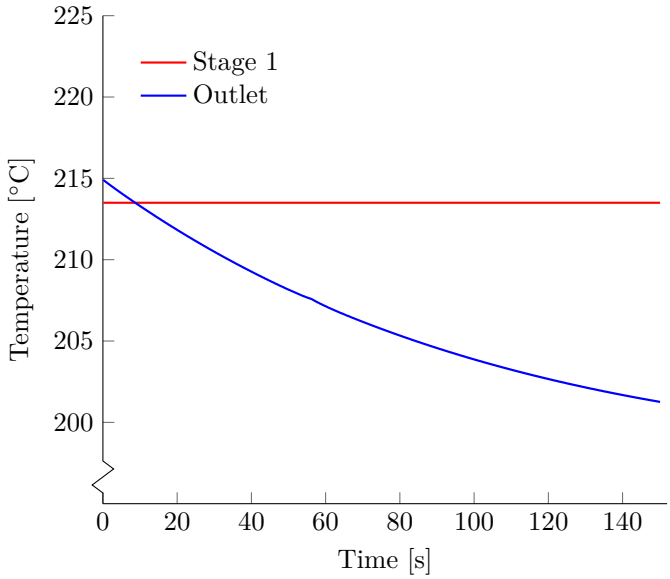

(b) *The temperature after the first and second (i.e. outlet) compression stage in compressor 1.*

Figure 7.2: *Temperature evolution in the station during a refueling.*

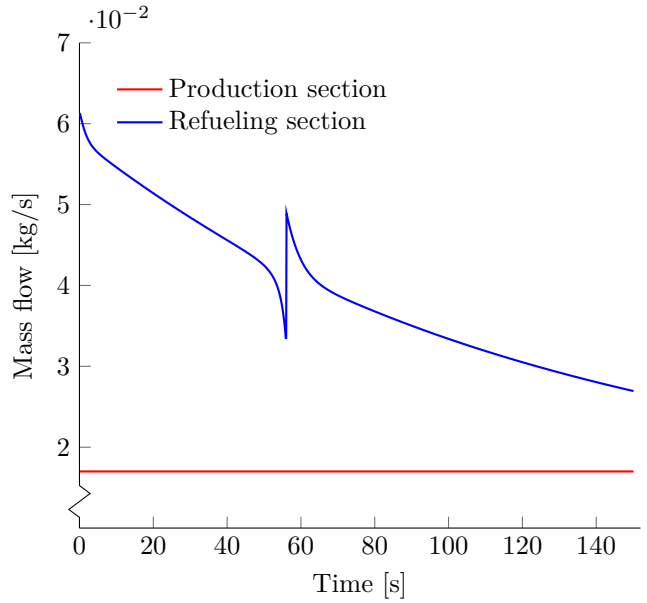

Figure 7.3: *The mass flows in the refueling and production section. The mass flow in the production section is induced by compressor 1 while the mass flow in the refueling section is induced by either the reduction valve or compressor 2.*

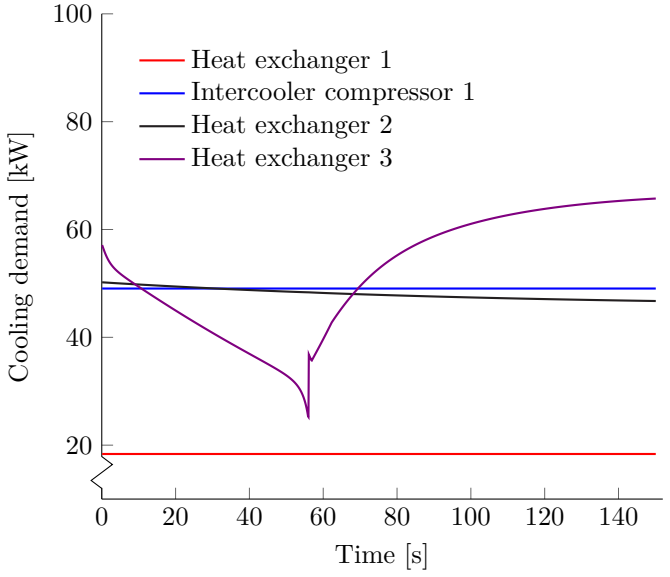

Figure 7.4: *The cooling demand in heat exchanger 1, 2, 3 and the intercooler in compressor 1.*

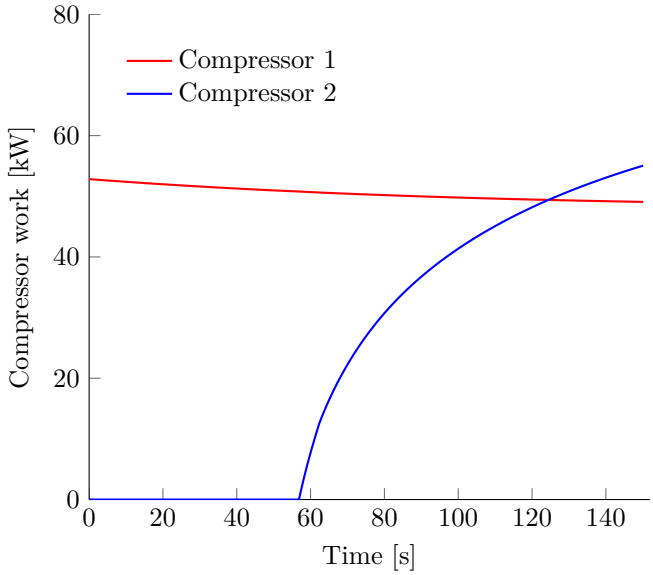

Figure 7.5: *The compressor work in compressor 1 and compressor 2 during a refueling.*

7.2.1 Discussion

Figure 7.1a presents the pressure evolution in the two tanks at the station. The pressure in the storage tank decreases during the refueling as mass is leaving the tank. However, the pressure decrease is very modest as mass is also added to the storage tank by compressor 1 in the production section. The pressure in the vehicle tank increases according to the APRR, and the target pressure is reached after 150.1 seconds. From Figure 7.1b, it can be seen that the deviation from the APRR increases as the switching limit approaches. This occurs because the pressure difference across the reduction valve is not sufficient to maintain the APRR anymore. However, the largest deviation is 0.7 % and hence within the deviation allowance set by the J2601 (10%). Except for this deviation, the pressure follows the APRR tightly.

In the model, the pressure losses in pipes and across components (except for the reduction valve) have not been considered. In order to see whether this assumption is reasonable, simple pressure loss calculations have been performed for the pipes in the refueling section. This section was selected as it has the largest mass flow and seemingly the highest pressure losses. The calculations are presented in Appendix E. Pressure losses during a refueling were found for the pipe segments between: 1) the storage tank and the reduction valve/compressor, and 2) the valve/-compressor and heat exchanger 3. Two different inner pipe diameters were used in the calculations (0.01 and 0.008 m). For the second pipe segment considered (i.e. between the valve/compressor and the heat exchanger), the pressure loss at the

start of the refueling is significantly high (0.6 MPa/m for a diameter of 0.01 m and 1.8 MPa/m for a diameter of 0.008 m). This is because of the large initial mass flow induced by the reduction valve. As the refueling proceeds and the mass flow decreases, the pressure loss in the pipe declines rapidly. The initial pressure loss in the first pipe segment is small compared to that of the second pipe segment. Similar in both pipe segments is that the pressure losses are quite low at the end of the refueling. Nevertheless, the high initial pressure losses in the second pipe segment indicate that the pressure losses at the station cannot be neglected. In addition, these calculations were only performed for pressure losses in a straight pipe. Typically, the pipes will have bends and also include several additional components such as mass flow meters and valves. These components will also contribute to the pressure losses occurring during a refueling. Furthermore, there will also be a pressure loss in the vehicle. This pressure loss depends on the vehicle type, and is not allowed to exceed 20 MPa [4] [5]. Such high pressure losses will have a great impact on the refueling in terms of mass flow and refueling time and should therefore be included in the model.

The temperature evolution in the station is given in Figure 7.2a and Figure 7.2b. In the electrolyzer, the temperature is kept fixed at 90°C during the refueling by the internal heat exchanger. From Figure 7.2b, it can be seen that the temperature after the first compression stage in compressor 1 is also fixed. This is because the compression ratio in the first stage is constant. The outlet temperature of compressor 1 (i.e. after the second compression stage), on the other hand, decreases as the refueling proceeds. As was discussed in the previous paragraph, the pressure in the storage tank decreases, and thereby, the compression ratio in the second stage will also decrease. A smaller compression ratio results in a lower outlet temperature.

Figure 7.2a shows that the temperature in the storage tank decreases during the refueling. As mass is leaving the tank, the remaining gas expands due to a reduction in pressure. This expansion is reversible and adiabatic (i.e. isentropic). Contrary to the Joule-Thomson effect where the enthalpy is fixed, the entropy is constant in this case, and the temperature will decrease. In addition to the hydrogen leaving the tank, there is also some hydrogen entering the tank. Since more hydrogen is leaving than entering, the hydrogen flowing into the tank will not have a big impact as there will be no compression of the hydrogen already in the tank. Additionally, the hydrogen holds a constant temperature upon entering (i.e. ambient temperature).

In the modeling phase it was assumed that the temperature in the storage tank would remain close to ambient temperature during a refueling. At the end of the refueling, the temperature in the storage tank is 8°C. The temperature difference between the surroundings and the contents of the tank is small (7°C). Hence, the assumption about no or very little heat transfer with the surroundings is a good assumption and will not have a big effect on the results when considering a single refueling. If a case where several vehicles refuel in a row is to be investigated,

however, it may be necessary to implement heat transfer between the storage tank and the surroundings. This is because, during several refuelings in a row, the temperature in the tank will continue to decrease and the temperature difference to the surroundings will increase.

When the gaseous hydrogen is expanded through the reduction valve, the temperature increases due to the reverse Joule-Thomson effect. As the refueling continues, however, the outlet temperature of the valve decreases. This is because the pressure difference across the valve is reduced as the pressure in the vehicle tank is increasing and pressure in the storage tank is decreasing. The station switches from the reduction valve to the compressor at 56.1 seconds. The pressure difference across the reduction valve is then 0.5 MPa. Figure 7.2a shows that the outlet temperature of the compressor is significantly higher than that of the reduction valve. This occurs because the heat of compression is more significant than the reverse Joule-Thomson effect. As the refueling proceeds, the outlet temperature increases greatly because of the increasing compression ratio between the storage tank and the vehicle tank. During the modeling process, it was assumed that the compression is adiabatic. In reality, there will be a heat transfer from the compressor to the surroundings due to the high temperatures achieved in the compression. Hence, the outlet temperature of the compressor will be lower, and thereby also the cooling demands in the heat exchangers associated to the compressors. According to [12], however, this heat loss is typically 5 % or less. Therefore, this assumption does not have a big impact on the obtained results.

The temperature in the vehicle tank increases rapidly the first 10 seconds of the refueling before it levels out and continues to increase with an almost fixed slope. The reason for this behavior is that the mass flow is considerably higher at the beginning of the refueling thus resulting in a larger heat of compression in the tank. In the modeling, it has been assumed that the filling is adiabatic. That is, it is assumed that no heat transfer to the surroundings will take place during the refueling time. However, the refueling lasts for 150.1 seconds and the final temperature in the tank is 75°C. Because of the long refueling time and the high final temperature, some heat will be dissipated to the tank walls and into the surroundings. Hence, the model will overestimate the final temperature during a refueling. This implies that the state of charge is underestimated as a higher temperature will result in a lower density. Therefore, heat exchange between the vehicle tank and the surroundings should be included in the model in order to make it more realistic.

Figure 7.3 shows the mass flows in the production and refueling sections. In the production section, the mass flow is induced by compressor 1 and is fixed. The mass flow in the refueling section, on the other hand, varies during the refueling. At the beginning of the refueling when the reduction valve is utilized, the mass flow declines almost constantly towards the time of the switch. The decline is due to the decreasing pressure difference across the reduction valve, resulting from discharging the storage tank and charging the vehicle tank. Right before the point of the

switch, the mass flow declines rapidly. This occurs because the pressure difference across the valve is no longer sufficient to keep up the necessary mass flow for maintaining the APRR. The deviation of the storage tank pressure from the APRR in Figure 7.1b is a result of this rapidly declining mass flow. At the switch, however, the mass flow increases as the compressor starts working. The large increase is to compensate for the low mass flow rate right before the switch. After the switch, the mass flow decreases rapidly for a couple of seconds before establishing a constant decline rate. This decline is a result of the reduced compressibility of the hydrogen gas in the vehicle tank as the pressure increases.

Figure 7.4 presents the cooling demands of the heat exchangers at the station (excluding the internal heat exchanger in the electrolyzer). The cooling demand in heat exchanger 1 is constant during the refueling because: 1) the operating temperature of the electrolyzer is fixed, 2) the heat exchanger cools the hydrogen down to the ambient temperature (which is also fixed during the refueling) and 3) the mass flow in the production section is constant. The heat exchanger following the first compression stage in compressor 1 (i.e. the intercooler), operates also with a constant cooling demand. This is due to the fixed mass flow and compression ratio of the first stage which result in a constant outlet temperature as shown in Figure 7.2b. Heat exchanger 2, however, does not have a constant cooling demand. The inlet temperature of heat exchanger 2 is the outlet temperature of compressor 1 which varies during the refueling as was discussed above. However, as can be seen from Figure 7.4, this variation is very small compared to the variation in the cooling demand of heat exchanger 3. When the reduction valve is utilized , the cooling demand curve in heat exchanger 3 is similar to the mass flow curve for the reduction valve. The cooling demand decreases towards the switch, and around the switch, the cooling demand is significantly lower than it was at the start of the refueling. This is because the outlet temperature of the reduction valve decreases due to the decreasing pressure difference across the valve.

When the compressor starts, the cooling demand increases considerably. As mentioned before, this occurs because the heat of compression is more significant than the reverse Joule-Thomson effect. The cooling demand curve for when the compressor is utilized is not similar to the compressor mass flow curve, but resembles the compressor's outlet temperature curve instead. Even though the cooling demand varies during the refueling, the magnitudes of the maximum cooling demand for the two process lines do not differ significantly (57 and 66 kW for the reduction valve and the compressor, respectively). These are found at the beginning and end of the refueling. In Figure 7.2a, it can be seen that the corresponding outlet temperatures of the two process lines differ greatly. The maximum outlet temperature of the compressor is 123°C while the maximum outlet temperature of the reduction valve is 26°C. An explanation is that the mass flow is considerably lower when using the compressor compared to when the valve is used. The lower mass flow compensates for the higher temperature. The cooling demand when the compressor is in use will therefore not be remarkably higher than when the reduction valve is in use.

The performed work in the two compressors are given in Figure 7.5. The work input to compressor 1 decreases as the refueling proceeds. This is because the compression ratio is reduced as the pressure in the storage tank decreases. Compressor 2 starts working at the time of the switch, and the work input increases because of the increased compression ratio between the two tanks.

7.3 Behavior during refilling of storage tank

After the refueling of the vehicle tank is aborted, the electrolyzer continues the production of hydrogen until the pressure in the storage tank reaches its nominal pressure. A refilling has been simulated with the same parameters as the refueling presented in the previous section. The time required for refilling the storage tank after a refueling at an ambient temperature of 15°C is 193.7 seconds. Note that this refilling time corresponds to the time from the refueling is complete to the storage tank is back at its nominal pressure. Refilling will also occur during the refueling, however, this was included in the previous section.

Figure 7.6 presents the pressure evolution in the storage tank along with the mass flow in the production section during the refilling. The cooling demand of heat exchanger 2, the performed work in compressor 1 and the temperature evolution in the storage tank during a refilling are given in Figure 7.7.

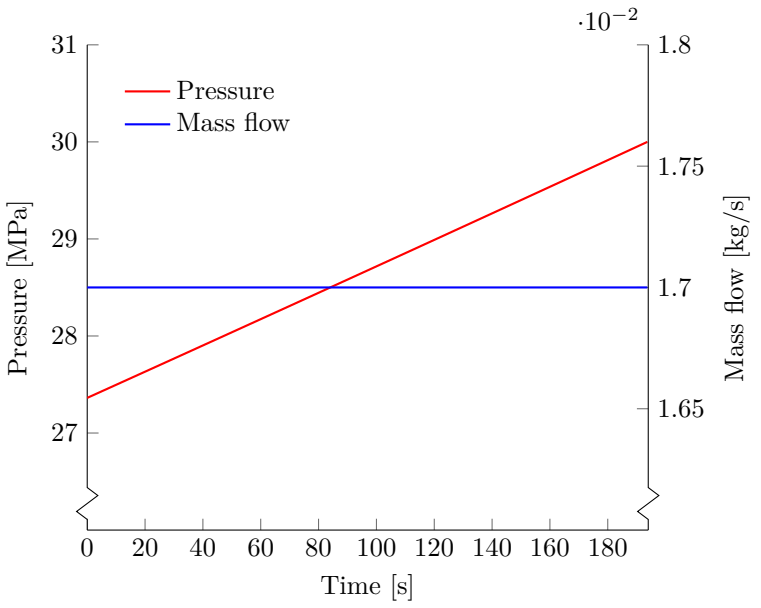

Figure 7.6: *The pressure evolution in the storage tank and the mass flow in the production section during a refilling.*

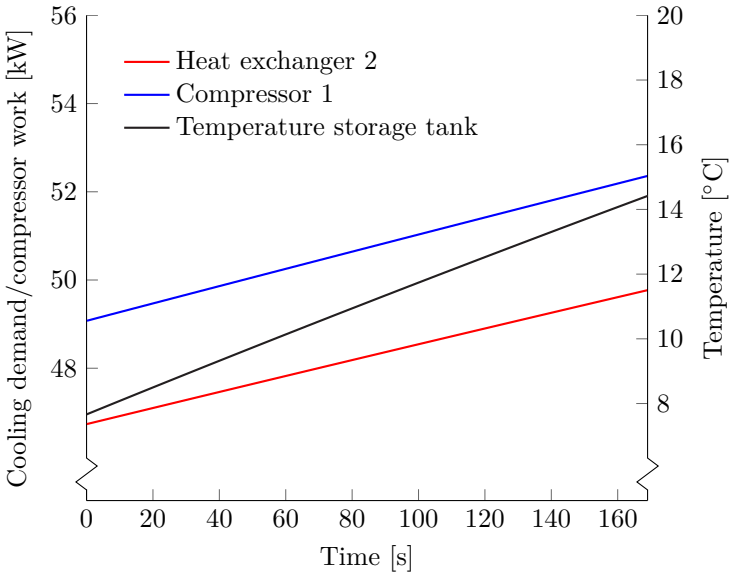

Figure 7.7: *The cooling demand in heat exchanger 2, the performed work in compressor 1 and the temperature evolution in the storage tank during a refilling. The ambient temperature is 15° C.*

The cooling demands in heat exchanger 1, the intercooler and the electrolyzer along with the power input to the electrolyzer remain the same as during the refueling and are therefore not included in the figure.

7.3.1 Discussion

Similar as during the refueling, the mass flow in the production section is fixed. Because of this, the refilling time depends on the refueling. That is, the refilling time depends on how much hydrogen is withdrawn from the storage tank during the refueling. This again, relies on the initial pressure in the vehicle tank and the ambient temperature. The effect these factors have on the refilling and on the refueling in general are discussed in Section 7.6. The pressure in the storage tank increases linearly until it reaches the nominal pressure after 193.7 seconds. The linear pressure increase is due to the fixed mass flow and that gaseous hydrogen behaves quite as an ideal gas in this pressure range.

As can be seen in Figure 7.7, the cooling demand in heat exchanger 2 increases slightly as the pressure in the storage tank, and thereby the compression ratio, increases. The increased compression ratio results in a higher outlet temperature, again resulting in a greater cooling demand. The work input in compressor 1 follows the same trend as the cooling demand in heat exchanger 2. During a refueling, the temperature in the storage tank decreases with time because of the pressure reduction. Conversely, during a refilling, the temperature increases. As explained

for the vehicle tank in the previous section, the hydrogen mass entering the tank compresses the hydrogen already in the tank. The temperature will then increase because of the heat of compression.

7.4 Behavior when only the compressor is used during refueling

A refueling where the initial pressure in the vehicle tank is higher than the storage tank pressure has been simulated. This implies that only the compressor is used during the refueling. Except for the different initial vehicle tank pressure, the simulation has been performed with the model parameters given in Table 7.2. The initial pressure is set to 30 MPa which gives a refueling time of 83.1 seconds. Figure 7.8 presents the pressure evolution in the storage tank and the vehicle tank along with the APRR during the refueling. The mass flow in the refueling section is also included in the figure. The temperatures in the two tanks and at the outlet of compressor 2 are presented along with the cooling demand of heat exchanger 3 in Figure 7.9. The production section is not affected by the change in initial pressure in the vehicle tank and its behavior remains similar as in the regular refueling presented in Section 7.2.

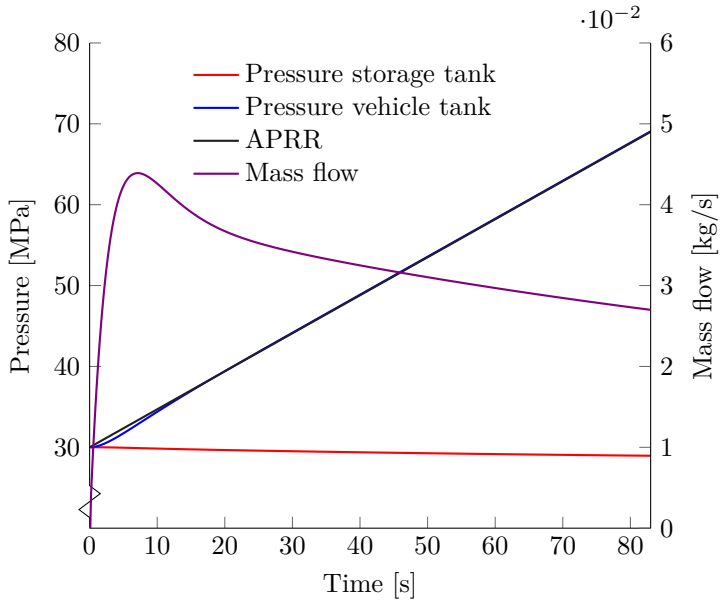

Figure 7.8: *The pressure evolution in the vehicle tank and storage tank along with the APRR for the given conditions. The mass flow in the refueling section is also included. In this refueling, only compressor 2 is utilized.*

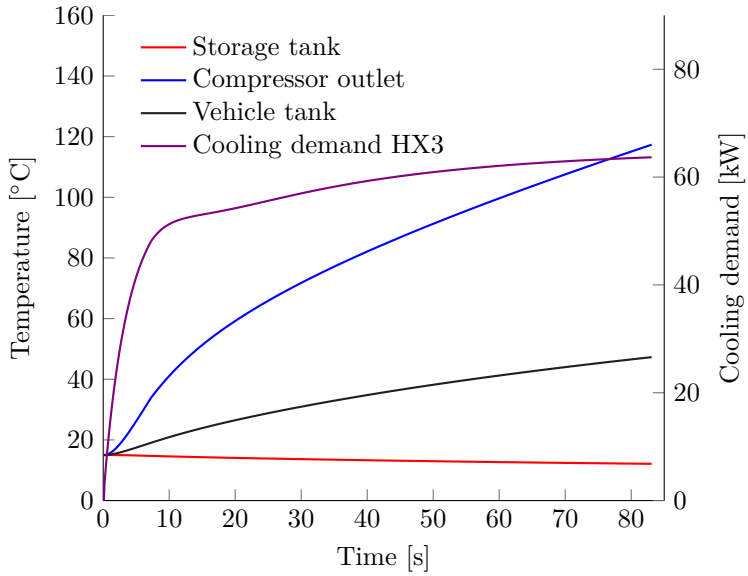

Figure 7.9: *The temperatures in the storage and vehicle tanks along with the outlet temperature of compressor 2 when only compressor 2 is applied in the refueling. The cooling demand in heat exchanger 3 is also included.*

7.4.1 Discussion

If the vehicle tank has an initial pressure of 29.5 MPa or higher, the refueling will be performed only by the compressor. This is because the pressure difference between the storage tank and vehicle tank is equal to or less than the defined switching pressure difference value[2]. From Figure 7.8 it can be seen that the pressure in the vehicle tank deviates slightly from the APRR the first 10 seconds of the refueling but follows the APRR tightly after. The deviation (2%), however, is within the allowed deviation. It occurs because the controller bias of the compressor controller is set by the mass flow in the reduction valve, which in this case is zero. Therefore, the controller bias is set to zero as well, resulting in a slower controller initially. The mass flow in the refueling section increases rapidly from zero mass flow and peaks after approximately 8 seconds before it starts declining. The value of the peak is approximately 0.045 kg/s and is lower than the peak value of the compressor flow in the regular refueling (0.05 kg/s). This is because less hydrogen is needed during the refueling because of the higher initial pressure in the vehicle tank.

The temperature in the storage tank decreases similar as in a regular refueling where both process lines are utilized. However, the final temperature in the storage tank is higher (12°C) because less mass is withdrawn. Compared to the regular refueling, the temperature in the vehicle tank increases more slowly. In the regular

2. 0.5 MPa in these simulations.

refueling, the vehicle tank temperature increases rapidly at the start before leveling out. This is because of the higher initial mass flow initiated by reduction valve. The final temperature in the vehicle tank during this refueling is lower (47°C) because less hydrogen is refueled compared to the regular refueling. The cooling demand in heat exchanger 3 increases rapidly at the start of the refueling, similar to the mass flow. Approximately at the time of the mass flow peak, the cooling demand levels out and increases slightly to the end of the refueling. This slight increase is a result of the rapidly increasing outlet temperature of the compressor and the decreasing mass flow.

7.5 Behavior when including heat exchanger 4

Section 4.4 introduced an alternative design in which a heat exchanger is included after the compressor in the refueling section (Case III). The new cooling demands in heat exchanger 3 and in the introduced heat exchanger (i.e. heat exchanger 4) are presented in Figure 7.10. The ordinary cooling demand of heat exchanger 3 is also included for comparison. Since the cooling demands in heat exchanger 1, heat exchanger 2 and the intercooler remain the same as presented in Figure 7.4, these are not included in the figure.

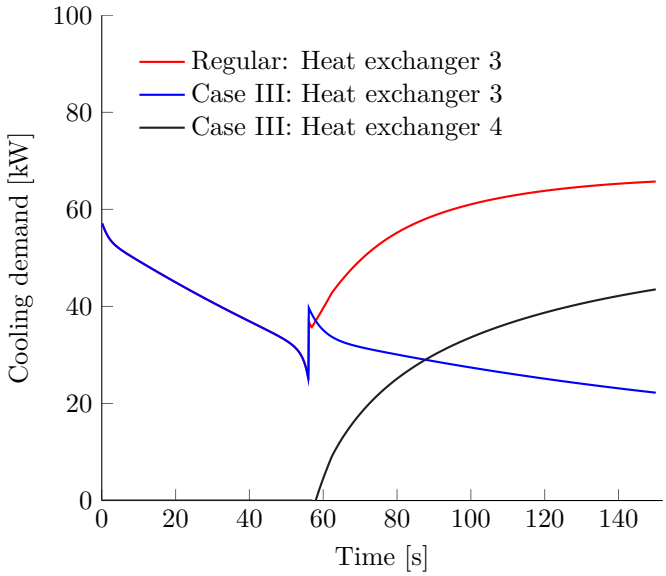

Figure 7.10: *The cooling demand in heat exchanger 3 and heat exchanger 4 together with the ordinary cooling demand in heat exhanger 3.*

7.5.1 Discussion

The inclusion of heat exchanger 4 does only affect the cooling demand in heat exchanger 3 when compressor 2 is utilized during the refueling. The behavior of the rest of the station is identical to its behavior in a regular refueling. The new cooling demand in heat exchanger 3 is therefore similar to the regular cooling demand when the reduction valve is used in the refueling. After the switch, however, the new cooling demand in heat exchanger 3 differs from the regular cooling demand because of the cooling occurring in heat exchanger 4. The new cooling demand curve is similar to the compressor 2 mass flow curve given in Figure 7.3. In the same manner, the cooling demand curve of heat exchanger 4 is comparable to the cooling demand curve of the regular heat exchanger 3 when the compressor is utilized.

As the refueling station already has the possibility of cooling the hydrogen down to the ambient temperature with cooling water, heat exchanger 4 should be included in the regular design. This will, as discussed in Section 4.4, contribute to a lower required heat input to the generator in an absorption refrigeration process. Even though the absorption refrigeration process is not achievable at the station, the inclusion of heat exchanger 4 would result in a lower work input to a conventional compression refrigeration process.

7.6 Effect of ambient temperature and initial vehicle tank pressure

Simulations with different ambient temperatures and initial vehicle tank pressures were performed to see what influence these factors have on the refueling. Additionally, the simulations were performed in order to examine whether the model and the controllers are behaving correctly for different conditions. All simulations are run in accordance with the SAE TIR J2601 look-up tables. The APRR is similar in all cases (0.47 MPa) except for when the ambient temperature is 30°C (0.46 MPa/s). The target pressures are provided in [4]. Table 7.3 presents the SOCs, the refueling and refilling times, and the final temperatures in the vehicle tank for the different ambient temperatures. The initial pressure in the vehicle tank during these simulations is 2 MPa. The same parameters are given in Table 7.4 for different initial vehicle tank pressures when the ambient temperature is 15°C. Note that these results are independent on whether heat exchanger 4 is included in the model or not.

Table 7.3: *The state of charge (SOC), the refueling and refilling times, and the final temperature in the vehicle tank for different ambient temperatures. The initial vehicle tank pressure is 2 MPa.*

Ambient temperature [°C]	State of charge [%]	Refueling time [s]	Vehicle tank temperature [°C]	Refilling time [s]
15	89.63	150.1	75.1	193.7
20	90.09	151.4	75.5	194.5
25	90.36	152.2	75.7	195.0
30	90.74	157.8	76.2	191.2

Table 7.4: *The state of charge (SOC), the refueling and refilling times, and the final temperature in the vehicle tank for different initial pressures in the tank. The ambient temperature is 15° C.*

Initial pressure [MPa]	State of charge [%]	Refueling time [s]	Vehicle tank temperature [°C]	Refilling time [s]
2	89.17	148.8	74.8	193.7
5	89.84	142.9	72.2	177.9
10	89.98	130.3	67.1	152.9
20	90.93	106.7	57.2	110.6
30	91.91	83.1	47.3	76.0

7.6.1 Discussion

As can be seen from Table 7.3, the results for the different ambient temperatures do not differ significantly. This is as expected since the simulations have been run in accordance with the SAE TIR J2601. The state of charge, the refueling time and the vehicle tank temperature all increase with increasing ambient temperature. The refilling time increases for the three first ambient temperatures, however, decreases when the ambient temperature is 30°C. This is because the APRR is smaller compared to the other ambient temperatures. Hence, less hydrogen is withdrawn from the storage tank during the refueling and less hydrogen has to be refilled. The reason for the smaller APRR is to increase the refueling time and hence decrease the mass flow rate in order to limit the heat of compression occurring in the vehicle tank. This is to ensure that the final temperature in the vehicle tank is below the maximum temperature limit.

Compared to the results for the different ambient temperatures, the results for the varying initial vehicle tank pressure differ more. The SOC increases slightly with increasing initial pressure, while the refueling and refilling times and the final

vehicle tank temperature all decrease. The latter trends are because less hydrogen is refueled when the initial vehicle pressure is higher. Hence, a shorter refueling time is required to reach the target pressure. The smaller amount of hydrogen entering the vehicle tank also results in a lower final temperature in the tank. This also implies less hydrogen must be refilled in the storage tank, thus the refilling time will also be lower. An initial pressure of 30 MPa is special since this results in a refueling utilizing only the compressor. This was discussed in Section 7.4.

7.7 Summary

Based on the behavior presented in this chapter, the model is working fine. Various conditions such as different initial vehicle tank pressures, ambient temperatures and APRRs have been tested. The implemented controllers are able to track the APRR both when the reduction valve and compressor are utilized in a refueling but also when only the compressor is utilized. However, in order to make the model more realistic, heat transfer in the vehicle tank and possibly also in the storage tank should be implemented. Additionally, pressure losses at the station and in the vehicle should also be considered.

8 | Results and discussion: Absorption refrigeration

This chapter presents the results from the four cases presented in Section 4.4. All simulations have been performed with an initial vehicle pressure of 2 MPa and an ambient temperature of 15°C corresponding to an APRR of 0.47 MPa/s [4]. According to Table 4.1 and Table 4.2, the required temperature of the input heat is 150°C and the coefficient of performance is 0.45, respectively. The required temperature corresponds to a pressure of 0.48 MPa. Note that the presented values are from a refueling only. That is, the heat generated during the corresponding refilling is not included. Appendix F presents the results from the four cases for ambient temperatures of 20, 25 and 30°C.

8.1 Case I: Use heat from only one heat source

The average and maximum cooling demand in heat exchanger 3 ($\dot{Q}_{HX3}$), the required heat input to the generator ($\dot{Q}_G$) and the corresponding heat removal in the electrolyzer ($\dot{Q}_{EL}$), heat exchanger 2 ($\dot{Q}_{HX2}$) and the intercooler in compressor 1 ($\dot{Q}_{IC}$) are presented in Table 8.1. The maximum cooling demand occurs at the end of the refueling. Note that the numbers in parenthesis correspond to the useful heat which can be utilized for heating at the required driving temperature. The temperatures at which the waste heat is generated are given in Table 8.2.

8.2 Case II: Increase the temperature of waste heat from electrolyzer with waste heat from heat exchanger 2 and intercooler

The required steam flow to the generator ($\dot{m}_{req}$), the available flow in the electrolyzer heat exchanger ($\dot{m}_{EL}$) and the actual and required steam flow coming from the intercooler and heat exchanger 2 ($\dot{m}_{HX,act}$, $\dot{m}_{HX,req}$) are summarized in Table 8.6. The temperature which the mixed steam flow obtains (T_{HX}) is also included. The values are given for both maximum and average cooling demand.

Similar to the previous case, the maximum cooling demand occurs at the end of the refueling. More detailed tables are given in Appendix F.

Table 8.1: *The maximum and average cooling demand for heat exchanger 3 ($\dot{Q}_{HX3}$) and the required heat input to the generator ($\dot{Q}_G$) with the corresponding heat removal in the electrolyzer ($\dot{Q}_{EL}$), heat exchanger 2 ($\dot{Q}_{HX2}$) and intercooler ($\dot{Q}_{IC}$) for an ambient temperature of 15° C. The numbers in parenthesis correspond to the heat which can be utilized for heating at the required temperature.*

	$\dot{Q}_{HX3}$ [kW]	$\dot{Q}_G$ [kW]	$\dot{Q}_{EL}$ [kW]	$\dot{Q}_{HX2}$ [kW]	$\dot{Q}_{IC}$ [kW]
Maximum	66	146	2395 (0)	47 (37)	49 (39)
Average	52	116		48 (38)	

Table 8.2: *The required temperature of the heat input (T_{req}) along with the temperatures of the available heat removed from the electrolyzer (T_{EL}), heat exchanger 2 (T_{HX2}) and the intercooler (T_{IC}) for an ambient temperature of 15° C.*

	T_{req} [°C]	T_{EL} [°C]	T_{HX2} [°C]	T_{IC} [°C]
Maximum	150	90	201	213
Average			206	

Table 8.3: *The required steam flow to the generator ($\dot{m}_{req}$) and the available flow of cooling water in the electrolyzer heat exchanger ($\dot{m}_{EL}$) along with the actual and required steam flow from the intercooler and heat exchanger 2 combined ($\dot{m}_{HX,act}$, $\dot{m}_{HX,req}$) for an ambient temperature of 15 ° C. The temperature of the mixed steam flow (T_{HX}) from the two latter heat exchangers is also included.*

	$\dot{m}_{req}$ [kg/s]	$\dot{m}_{EL}$ [kg/s]	T_{HX} [°C]	$\dot{m}_{HX,req}$ [kg/s]	$\dot{m}_{HX,act}$ [kg/s]
Maximum	0.069	7.63	207	0.066	0.034
Average	0.055		210	0.052	0.034

8.3 Case III: Include a heat exchanger in the compressor line

The new cooling demand in heat exchanger 3 along with the heat removed in heat exchanger 4 were presented in Figure 7.10. Table 8.4 presents the maximum and

average cooling demand ($\dot{Q}_{HX3}$) and the corresponding required heat input to the generator ($\dot{Q}_G$) for when heat exchanger 4 is included at the station. The equivalent heat removal in the electrolyzer, intercooler and heat exchanger 2 is also included in the table. Contrary to the two preceding cases, the maximum cooling demand in heat exchanger 3 occurs at the start of the refueling.

Table 8.4: *The maximum and average cooling demand for heat exchanger 3 ($\dot{Q}_{HX3}$) when heat exchanger 4 is included, the required heat input to the generator ($\dot{Q}_G$) and the corresponding heat generation in the electrolyzer ($\dot{Q}_{EL}$), heat exchanger 2 ($\dot{Q}_{HX2}$) and intercooler ($\dot{Q}_{IC}$) for an ambient temperature of 15° C. The numbers in parenthesis correspond to the heat which can be utilized for heating at the required temperature.*

	$\dot{Q}_{HX3}$ [kW]	$\dot{Q}_G$ [kW]	$\dot{Q}_{EL}$ [kW]	$\dot{Q}_{HX2}$ [kW]	$\dot{Q}_{IC}$ [kW]
Maximum	57	127	2395 (0)	50 (40)	49 (39)
Average	33	73		48 (38)	

Table 8.5: *The required temperature of the heat input (T_{req}) along with the temperatures of the available heat removed from the electrolyzer (T_{EL}), heat exchanger 2 (T_{HX2}) and intercooler in compressor 1 (T_{IC}) for an ambient temperature of 15° C.*

	T_{req} [°C]	T_{EL} [°C]	T_{HX2} [°C]	T_{IC} [°C]
Maximum	150	90	215	213
Average			206	

8.4 Case IV: Combination of Case II and III

The required steam flow to the generator ($\dot{m}_{req}$), the available flow in the electrolyzer heat exchanger ($\dot{m}_{EL}$) along with the actual and required steam flow from the intercooler and heat exchanger 2 ($\dot{m}_{HX,act}$, $\dot{m}_{HX,req}$) are summarized in Table 8.6. The temperature which the mixed steam flow obtains (T_{HX}) is also included. The values are given for both maximum and average cooling demand and for two ambient temperatures (15 and 20°C). For an ambient temperature of 20°C, the required driving temperature is 160°C. This corresponds to a pressure of 0.62 MPa. The coefficient of performance is then 0.40. More detailed tables are given in Appendix F.

Table 8.6: *The required steam flow to the generator ($\dot{m}_{req}$) and the available flow of cooling water in the electrolyzer heat exchanger ($\dot{m}_{EL}$) along with the actual and required flow from the intercooler and heat exchanger 2 ($\dot{m}_{HX,act}$, $\dot{m}_{HX,req}$) for the ambient temperatures of 15 and 20° C. The temperature of the mixed steam flow (T_{HX}) from the two heat exchangers is also included.*

T_{amb} [°C]		$\dot{m}_{req}$ [kg/s]	$\dot{m}_{EL}$ [kg/s]	T_{HX} [°C]	$\dot{m}_{HX,req}$ [kg/s]	$\dot{m}_{HX,act}$ [kg/s]
15	Maximum	0.060	7.63	214	0.057	0.035
	Average	0.035		210	0.033	0.034
20	Maximum	0.073	8.17	223	0.069	0.036
	Average	0.042		231	0.041	0.035

8.5 Discussion

8.5.1 Case I and II

For Case I and Case II, the required heat input to the generator is 146 kW at maximum cooling demand in heat exchanger 3 and 116 kW on average. The required temperature of this heat is 150°C. As can be seen in Table 8.1 and Table 8.2 the amount of heat generated in the electrolyzer (2395 kW) is sufficient to drive the cycle, but the temperature of the heat (90°C) is not high enough. Note that the maximum and average values are identical for the electrolyzer as the hydrogen production rate is constant. Conversely for heat exchanger 2 and the intercooler, the temperatures are high enough but the heat amount is not sufficient. The temperatures at the maximum cooling demand are 201 and 213°C, respectively, and 206 and 213°C on average. The useful generated waste heats are 37 kW (at maximum cooling demand) and 38 kW (average) in heat exchanger 2, and 39 kW for both situations in the intercooler. Thus, an absorption refrigeration process cannot be utilized by using only one of the waste heat sources when the ambient temperature is 15°C. Since a higher ambient temperature (i.e. a higher cooling water temperature) corresponds to a higher required temperature in the generator as well as a lower coefficient of performance, this approach will not work for higher ambient temperatures either.

Further, in Case II, it was evaluated whether the high-temperature heat from the intercooler and heat exchanger 2 can be used to increase the temperature of the heat generated in the electrolyzer. From Table 8.3 it can be seen that the temperature of the combined flow (207°C at maximum, 210°C on average) from these heat exchangers is sufficient to do so. Also, the amount of cooling water in the heat exchanger of the electrolyzer is more than sufficient to provide the required amount of hot water to be heated and vaporized. However, the actual mass flow coming from the intercooler and heat exchanger 2 is not sufficient compared to the required mass flow. The actual flow is 0.034 kg/s at maximum and on average

cooling demand while the required flow is 0.066 kg/s at maximum and 0.052 kg/s on average. Hence, in the case of an ambient temperature of 15°C, the combined mass flow of steam coming from heat exchanger 2 and the intercooler is not sufficient to heat up the water from the electrolyzer heat exchanger to the driving temperature and vaporize it. The same discussion on higher ambient temperature given for Case I also applies here.

8.5.2 Case III and IV

In Case III, a heat exchanger is included after the compressor in the refueling section. As can be seen in Table 8.4, the required heat input to the generator is considerably smaller compared to Case I and Case II. The maximum value is now 127 kW and the average is 73 kW. Despite the reduced required heat input, neither of the heat sources are able to drive the absorption refrigeration process alone. Likewise in Case I and Case II, the amount of heat from the electroyzer is sufficient, but the temperature of the heat is not high enough. The temperatures of the heat of the intercooler and heat exchanger 2 are high enough, however, the amount of heat is not sufficient.

Case IV constitutes a combination of the two preceding cases. From Table 8.6 it can be seen that, for an ambient temperature of 15°C, the average actual mass flow (0.034 kg/s) from the intercooler and heat exchanger 2 is sufficient to heat up the hot water flow (0.033 kg/s) from the electrolyzer to the required temperature. This is not the case at the maximum cooling demand. However, as introduced in Section 4.1, it is possible to store refrigerant in a reservoir between the condenser and evaporator. When the cooling demand in heat exchanger 3 is so low that not all of the generated refrigerant is needed in the cooling process, the excess refrigerant can be stored in this reservoir. The stored refrigerant can then be used when the cooling demand increases to a point where the generated refrigerant rate is not sufficient to meet the cooling demand. It is therefore acceptable to utilize the values obtained for the average cooling demand in heat exchanger 3. Thus, for an ambient temperature of 15°C, it is possible to utilize the combined flow from the intercooler and heat exchanger 2 to increase the temperature of the hot water flow coming from the electrolyzer. However, Table 8.6 also contains the results for when the ambient temperature is 20°C. The actual mass flow from the two heat exchangers is no longer sufficient. For the average cooling demand, the actual mass flow is 0.035 kg/s while the required mass flow is 0.041 kg/s. Hence, in this case, the absorption refrigeration process cannot be utilized for an ambient temperature higher than 15°C.

8.5.3 Assumptions

Several assumptions have been made in the estimation. First, it is assumed that the temperature of the cooling water is equal to the ambient temperature. This assumption will depend on the cooling water system design which is beyond the scope of this thesis. However, if the cooling water comes from a bigger storage tank

this is a good assumption. The water has then had time to heat exchange with the surroundings holding ambient temperature. Otherwise, the water may hold a slightly higher temperature than that of the surroundings. A higher cooling water temperature will result in a higher required temperature and also a lower coefficient of performance. The required heat input to the generator will thus be larger than found in this estimation. Either way, this assumption has no or very little impact on the result as the absorption refrigeration process will be unachievable in both situations.

In addition, it is assumed that the outlet temperature of the flow on the cold side is equal to the inlet temperature of the flow on the hot side. The assumption applies for the internal heat exchanger in the elecrolyzer, the intercooler and heat exchanger 2. Typically, this is the case when a large hot flow is being cooled by a small cold flow in a large heat exchanger. The flow on the hot side in this case, which is the mass flow in the production section (0.017 kg/s), is smaller than the cold flow in all of the considered heat exchangers. Hence, the outlet temperature of the cold flow will not obtain the same temperature as the inlet hot flow. Often, a pinch temperature of 5°C is applied. This implies that a larger mass flow on the cold side is required in order to cool the hydrogen down to the desired outlet temperature. Thus, the actual mass flow from the intercooler and heat exchanger 2 will be slightly bigger. However, the temperature of this flow will be lower. Additionally, the temperature of the hot water exiting the electrolyzer heat exchanger will also be lower. Hence, more heat is required to increase the temperature of this flow to the required temperature. This again, implies that a larger mass flow of the steam from the intercooler and heat exchanger 2 is required. The absorption refrigeration process will still be unattainable.

The additional assumptions made in the estimation (i.e. no heat loss in pipes and no resistance to heat transfer) both support that the absorption refrigeration process is not achievable. First, the distances at the station are small, and consequently, the pipes will be short too. Hence, the heat loss from the heated cooling medium (water/steam) to the pipes and the surroundings will be small. Second, if the heat loss is noticeable, it will result in a lower temperature of the heated cooling medium (i.e. hot water or steam). As discussed in the previous paragraph, this will neither result in the absorption refrigeration process becoming workable. Second, there will be resistance to heat transfer between the different parts at the station. This implies that the heat exchange between the different parts will be less than the heat transfer rate values given above. Since the absorption refrigeration process is not doable with the overestimated values, neither will it be with the actual ones.

8.5.4 Other alternatives

In the estimation, only heat generated during the refueling has been considered for the absorption refrigeration process. However, heat will also be generated during the refilling of the storage tank. Note that refilling also occurs during the refueling,

but in this case, a refilling refers to when no vehicle is connected to the station and when only the production section is operating. As discussed earlier, the refrigerant can be stored in a reservoir in the absorption refrigeration cycle. Hence, an additional alternative that may facilitate the absorption refrigeration process is to use the heat generated during the refilling to generate NH_3 that can be stored for use in the next refueling. The heat produced during the refueling will still generate NH_3, but now the additional amount of refrigerant needed can be supplied by the stored refrigerant generated by the refilling process. In all except for one of the cases investigated in Table 7.4, the refilling time is greater than the refueling time. Additionally, the amount of heat removed in heat exchanger 2 during a refilling is slightly larger than in a refueling. The other two heat exchangers considered (the intercooler and the internal electrolyzer heat exchanger) generate the same amount of heat as in the refueling. A more detailed discussion on this was given in Section 7.3. The heat generated during a refilling should therefore be sufficient to produce the additional amount of refrigerant needed, and especially if the heat exchanger from Case III is included.

There are, however, some factors that must be considered in this approach. The station does not have the need for recovery time between refueling vehicles. Thus, several vehicles may refuel in a row. If this is the case, there will be no or very little refilling between the refuelings. Since the generated heat during a refueling is not sufficient to drive the absorption refrigeration process alone, the cooling process will depend on the refrigerant produced during the refilling. It is therefore necessary to estimate the amount of refrigerant generated during a refilling and how many refuelings this amount can support. The latter is, however, difficult as each refueling will differ in terms of initial vehicle tank pressure and also vehicle tank capacity. That is, it will differ in the amount of hydrogen needed in the refueling in order to reach the target pressure. In addition, it is necessary to be able to predict how many vehicles will refuel in a day and the time between them in order to see whether the refillings are able to generate enough refrigerant for providing sufficient cooling during the refuelings.

8.5.5 Summary

Four different cases have been considered for making the absorption refrigeration process workable. Only in the last case, Case IV, does the absorption refrigeration process become so. However, this is only for an ambient temperature of 15°C and, therefore, from a general point of view, the absorption refrigeration process is not achievable at a hydrogen refueling station operated at the conditions presented in this thesis. Further, several of the assumptions made during the estimation were discussed. These support the conclusion that the absorption refrigeration process is not workable at this station. Then, an additional alternative for making the refrigeration cycle feasible was discussed. However, several factors including prediction of refueling patterns and initial conditions in the vehicle have to be known in order to do this estimation.

9 | Conclusion and further work

A simple dynamic model of a hydrogen refueling station with a direct compression refueling design has been developed and implemented in MATLAB. An on-site production section where hydrogen is produced from electrolysis of water has also been included in the model. Various conditions such as different initial vehicle tank pressures, ambient temperatures and APRRs have been tested. All the tested conditions are handled well by the model. Additionally, the implemented controllers are able to track the APRR tightly in different refueling situations.

Further, four cases for making an absorption refrigeration process workable at the refueling station were investigated. The process is workable when an additional heat exchanger is included after the compressor in the refueling section and when waste heat from several of the heat sources is utilized. However, this applies only for a cooling water temperature of 15°C and presumably below. Based on this and the assumptions made in the estimation, an absorption refrigeration process is not achievable at a hydrogen refueling station operated at the conditions given in this thesis.

9.1 Further work

In order to make the model more realistic, heat transfer in the vehicle tank and possibly also in the storage tank should be implemented. Additionally, pressure losses at the station and in the vehicle should also be included in the model.

Further work regarding the absorption refrigeration process may be to investigate whether the waste heat generated during the refilling of the storage tank can be utilized in the absorption refrigeration process. The generated heat may be used to generate the additional refrigerant needed during a refueling in order to make the absorption refrigeration process feasible.

Bibliography

[1] M. Ball and M. Wietschel. The future of hydrogen - opportunities and challenges. *International Journal of Hydrogen Energy*, 34(2):615 – 627, 2009.

[2] I. H. Bell, J. Wronski, S. Quoilin, and V. Lemort. Pure and Pseudo-pure Fluid Thermophysical Property Evaluation and the Open-Source Thermophysical Property Library CoolProp. *Industrial & Engineering Chemistry Research*, 53(6):2498–2508, 2014.

[3] L. Schlapbach. Technology: Hydrogen-fuelled vehicles. *Nature*, 460(7257):809–811, 2009.

[4] Society of Automotive Engineers. Fueling Protocols for Light Duty Gaseous Hydrogen Surface Vehicles. *Tehcnical Information Report J2601*, 2010.

[5] E. Rothuizen, W. Merida, M. Rokni, and M. Wistoft-Ibsen. Optimization of hydrogen vehicle refueling via dynamic simulation. *International Journal of Hydrogen Energy*, 38(11):4221 – 4231, 2013.

[6] S. Maus, J. Hapke, C. N. Ranong, E. Wüchner, G. Friedlmeier, and D. Wenger. Filling procedure for vehicles with compressed hydrogen tanks. *International Journal of Hydrogen Energy*, 33(17):4612 – 4621, 2008.

[7] M. Carmo, D.L. Fritz, J. Mergel, and D. Stolten. A comprehensive review on PEM water electrolysis. *International Journal of Hydrogen Energy*, 38(12):4901–4934, 2013.

[8] A. Ursua, L. M. Gandìa, and P. Sanchis. Hydrogen Production From Water Electrolysis: Current Status and Future Trends. *Proceedings of the IEEE*, 100(2):410–426, 2012.

[9] Ø. Ulleberg. Modeling of advanced alkaline electrolyzers: a system simulation approach. *International Journal of Hydrogen Energy*, 28(1):21 – 33, 2003.

[10] E. Rothuizen and M. Rokni. Optimization of the overall energy consumption in cascade fueling stations for hydrogen vehicles. *International Journal of Hydrogen Energy*, 39(1):582 – 592, 2014.

[11] P. C. Hanlon. *Compressor Handbook*. McGraw-Hill, 2001.

[12] E. Rothuizen. *Hydrogen Fuelling Stations. A Thermodynamic Analysis of Fuelling Hydrogen Vehicles for Personal Transportation.* PhD thesis, Danmarks Tekniske Universitet, 2013.

[13] C. J. B. Dicken and W. Merida. Measured effects on filling time and initial mass on the temperature distribution within a hydrogen cylinder during refuelling. *Journal of Power Sources*, 165(1):324 – 336, 2007.

[14] P. Srikhitin, S. Aphornratane, and S. Chungpaibulpatana. A review of absorption refrigeration technologies. *Renewable and Sustainable Energy Reviews*, 5(4):343 – 372, 2001.

[15] colibri b. v. Ammonia Absorption Technology. `http://colibris.home.xs4all.nl/pages/documentation.html`, accessed May 12 2014.

[16] M. J. Moran and H. N. Shapiro. *Fundamentals of Engineering Thermodynamics.* John Wiley & Sons, 6th edition, 2010.

[17] D. Kong, J. Liu, L. Zhang, H. He, and Z. Fang. Thermodynamic and Experimental Analysis of an Ammonia-Water Absorption Chiller. *Energy and Power Engineering*, (2):298–305, 2010.

[18] T. Smolinka. Water electrolysis. In *Encyclopedia of Electrochemical Power Sources*, pages 394 – 413. Elsevier, Amsterdam, 2009.

[19] R. Smith. *Chemical Process Design and Integration.* John Wiley & Sons, 1st edition, 2005.

[20] Ingersoll-Rand. *Gas Properties and Compressor Data.* Ingersoll-Rand, 1981.

[21] *Engineering Data Book.* Gas Processors Suppliers Association, 13th edition, 2012.

[22] A. Shavit and C. Gutfinger. *Thermodynamics. From concepts to applications.* Prentice Hall International, 1st edition, 1995.

[23] S. Skogestad. Probably the best simple PID tuning rules in the world. *submitted to Journal of Process Control*, July 3 2001.

[24] D. E. Seborg, T. F. Edgar, and D. A. Mellichamp. *Process Dynamics and Control.* John Wiley & Sons, 2nd edition, 2005.

[25] S. Skogestad and C. Grimholt. The SIMC method for Smooth PID Control. In *PID Control in the Third Millennium.* Springer.

[26] B. W Bequette. *Process dynamics: modeling, analysis, and simulation.* Prentice Hall PTR, 1st edition, 1998.

[27] H. A. Preisig. The ABC of Process Modelling, 2013. Lecture notes.

[28] J. W. Leachman, R. T. Jacbsen, S. G. Penoncello, and E. W. Lemmon. Equations of State for Parahydrogen, Normal Hydrogen, and Orthohydrogen. *J. Phys. Chem. Ref. Data*, (38):721–748, 2009.

[29] Engineering Toolbox. Properties of Saturated Steam. `http://www.engineeringtoolbox.com/saturated-steam-properties-d_101.html`, accessed June 2, 2014.

[30] C. J. Geankoplis. *Transport Processes and Separation Process Principles*. Pearson Education, 4th edition, 2003.

[31] P. Swamee and A. Jain. Explicit equations for pipe-flow problems. *Journal of the Hydraulics Division*, 102(5):657–664, 1976.

Appendices

A | Derivations

This appendix contains a derivation of the energy balance for an open system with one species from the first law of thermodynamics along with the derivation of the total differential of enthalpy expressed in temperature and pressure terms.

A.1 Derivation of energy balance

The first law of thermodynamics for a closed system is

$$dE = \delta Q - \delta W \tag{A.1}$$

where dE is the change in total energy of the system, δQ the heat flow to the system and δW the work performed by the system on the surroundings. In an open system, there is some energy exchange caused by the mass flow across the system boundary. The energy balance for an open system and only one species can be written as

$$\frac{dE_{sys}}{dt} = \dot{Q} - \dot{W} + \dot{E}_{in} - \dot{E}_{out} \tag{A.2}$$

where dE_{sys}/dt is the rate of accumulation of energy in the system, $\dot{Q}$ is the rate of heat flow into the system, $\dot{W}$ is the rate of work performed by the system and $\dot{E}_{in}$ and $\dot{E}_{out}$ are the rates of energy added to or leaving the system by mass flows crossing the system boundaries.

The work term can be divided into flow work ($p\dot{V}$) and other work ($\dot{W}_s$) usually denoted shaft work. For one species, the work term can be expressed as

$$\dot{W} = -(p\dot{V})_{in} + (p\dot{V})_{out} + \dot{W}_s \tag{A.3}$$

where p is the pressure and $\dot{V}$ is the volumetric flow. Substituting this equation into A.2 and rearranging give:

$$\frac{dE_{sys}}{dt} = \dot{Q} - \dot{W}_s + (\dot{E} + p\dot{V})_{in} - (\dot{E} + p\dot{V})_{out} \tag{A.4}$$

The total energy is the sum of internal energy, U, kinetic energy, E_k, potential energy, E_p and other energies (e.g. electric or magnetic energy).

$$E = U + E_k + E_p + other \tag{A.5}$$

Neglecting the "other" energy term, the energy balance is reduced to:

$$\frac{dE_{sys}}{dt} = \dot{Q} - \dot{W}_s + (\dot{U} + p\dot{V} + \dot{E}_k + \dot{E}_p)_{in} - (\dot{U} + p\dot{V} + \dot{E}_k + \dot{E}_p)_{out} \tag{A.6}$$

Enthalpy, H, is defined as

$$H \hat{=} U + pV \tag{A.7}$$

and stagnation enthalpy, H^0, is defined as

$$H^0 \hat{=} H + E_k + E_p \tag{A.8}$$

Substituting this into A.6 gives

$$\frac{dE_{sys}}{dt} = \dot{Q} - \dot{W}_s + \dot{H}^0_{in} - \dot{H}^0_{out} \tag{A.9}$$

The kinetic, potential and other energy terms are usually negligible compared to the enthalpy, work and heat terms. The energy balance is then reduced to

$$\frac{dU_{sys}}{dt} = \dot{Q} - \dot{W}_s + \dot{H}_{in} - \dot{H}_{out} \tag{A.10}$$

and on specific form

$$\frac{dU_{sys}}{dt} = \dot{Q} - \dot{W}_s + (\dot{m}h)_{in} - (\dot{m}h)_{out} \tag{A.11}$$

where $\dot{m}$ is the mass flow in or out of the system.

A.2 Total differential of enthalpy

The total differential of internal energy (U) can be written as

$$dU(S,V)_n = T\mathrm{d}S - p\mathrm{d}V \tag{A.12}$$

where S is entropy, V is volume, T is temperature and p is pressure. From Legendre transformations the relationship between enthalpy (H) and internal energy is known

$$H = U + pV \tag{A.13}$$
$$dH = \mathrm{d}U + \mathrm{d}(pV) \tag{A.14}$$
$$dH = T\mathrm{d}S - p\mathrm{d}V + (V\mathrm{d}p + p\mathrm{d}V) \tag{A.15}$$
$$dH = T\mathrm{d}S + V\mathrm{d}p \tag{A.16}$$

Enthalpy is canonical in entropy (S) and pressure (p), but by substituting in for the entropy differential, the enthalpy differential can be converted to be a function of temperature and pressure. The differential of entropy as a function of temperature and pressure is as follows:

$$dS(T,p) = \Big(\frac{\partial S}{\partial T}\Big)_p \mathrm{d}T + \Big(\frac{\partial S}{\partial p}\Big)_T \mathrm{d}p \tag{A.17}$$

The two partial derivative terms can be expressed as

$$\Big(\frac{\partial S}{\partial T}\Big)_p \hat{=} \frac{C_p}{T} \tag{A.18}$$
$$\Big(\frac{\partial S}{\partial p}\Big)_T = \Big(\frac{\partial V}{\partial T}\Big)_p \tag{A.19}$$

where the former is a definition of the constant pressure capacity and the latter is a Maxwell relation. The differential of enthalpy as a function of temperature and pressure is thus:

$$\begin{aligned} dH(T,p) &= T\Big[\frac{C_p}{T}\mathrm{d}T - \Big(\frac{\partial V}{\partial T}\Big)_p \mathrm{d}p\Big] + V\mathrm{d}p \\ &= C_p\mathrm{d}T + \Big[V - T\Big(\frac{\partial V}{\partial T}\Big)_p\Big]\mathrm{d}p \end{aligned} \tag{A.20}$$

For an ideal gas, the volume can be expressed as

$$V = \frac{nRT}{p} \tag{A.21}$$

where n is number of moles and R is the ideal gas constant. The partial derivative of volume with respect to temperature is:

$$\Big(\frac{\partial V}{\partial T}\Big)_p = \frac{nR}{p} \tag{A.22}$$

Inserting these two equations into A.20 yields:

$$\begin{aligned} dH(T,p) &= C_p \mathrm{d}T + \Big[\frac{nRT}{p} - T\frac{nR}{p}\Big]\mathrm{d}p \\ &= C_p \mathrm{d}T \end{aligned} \tag{A.23}$$

The enthalpy of an ideal gas is thus independent of pressure.

B | Compressor capacity

The cylinder volume (V_{cyl}) for the two compressors are found from

$$V_{cyl} = \frac{\dot{m}}{\rho \eta_v N} \tag{B.1}$$

where $\dot{m}$ is the mass flow, ρ is the inlet density, η_v is the volumetric efficiency and N is the compressor speed.

The cylinder volume of compressor 1 ($V_{cyl,1}$) is estimated based on a specified compressor speed, maximum refilling time (t_{refill}) of the storage tank and a constant mass flow. It is assumed that each vehicle refuels on average 5 kg (m_{avg}) of hydrogen in one refueling cycle. The refilling time of the storage tank has been set to 5 minutes. The required mass flow in compressor 1 is then given by:

$$\dot{m} = \frac{m_{avg}}{t_{refill}} \tag{B.2}$$

The inlet density is calculated based on the constant inlet conditions ($p = 1.2$ MPa, $T = 15°$C) and the volumetric efficiency is the same as the one used in the simulations. The numerical values along with the estimated cylinder volume are presented in Table B.1.

The cylinder volume of compressor 2 ($V_{cyl,2}$) is estimated based on a maximum mass flow (0.06 kg/s) set by the SAE TIR J2601 and a fixed compressor speed (N_2) for this mass flow. The volumetric efficiency are calculated for the largest compression ratio as this will give the lowest volumetric efficiency, thus yielding the largest cylinder volume. The numeric values along with the estimated cylinder volume are presented in Table B.1.

Table B.1: *The calculated compressor cylinder volumes along with the numerical values applied in the calculations.*

Parameter	Unit	Compressor 1	Compressor 2
m_{avg}	[kg]	5	-
t_{refill}	[s]	300	-
$\dot{m}$	[kg/s]	0.017	0.06
p_{in}	[MPa]	1.2	30
p_{out}	[MPa]	6	70
T_{in}	[°C]	15	15
ρ	kg/m^3	0.99	20.85
η_v	-	0.75	0.93
N	[1/s]	10	10
$\boldsymbol{V_{cyl}}$	[m^3]	2.3e-3	3.1e-4

C | Saturated steam properties

Table C.1 presents specific enthalpies for water and steam at saturated conditions. The data is found from [29].

Table C.1: *Specific enthalpies for water and steam at different temperatures and the corresponding saturating pressures.*

Pressure [MPa]	Temperature [°C]	Specific enthalpy water [kJ/kg]	Specific enthalpy steam [kJ/kg]
0.48	150	633.5	2746
0.62	160	670.4	2756
0.90	175	742.6	2772
1.19	186	790	2781

D | Controller tuning

The process models for the two different refueling cases (reduction valve and compressor) are found graphically. The controllers are then tuned using the Simple (or Skogestad) Internal Model Control (SIMC) tuning rules [25]. For the reduction valve controller, it is the valve coefficient (C_v) that is the manipulated variable. The compressor controller uses the compressor speed (N_2) as the manipulated variable. Note that, in this appendix, the notation compressor refers to compressor 2.

The SIMC tuning rules for an integrating process are given as:

$$K_c = \frac{1}{k'}\frac{1}{\tau_c} \tag{D.1}$$

$$\tau_I = 4(\tau_c + \theta) \tag{D.2}$$

The process model and tuning parameters are summarized in Table D.1.

Table D.1: *Description of process model and tuning parameters.*

Symbol	Description
k'	Slope of integrating response
K_c	Controller gain
τ_I	Integral time constant
τ_c	Desired closed-loop time constant
θ	Time delay

The pressure rise in the vehicle tank when the reduction valve is applied for refueling is shown in Figure D.1a. The figure is obtained from a refueling with a fixed valve coefficient (C_v) (i.e. open-loop). The pressure rise in the vehicle tank when the compressor is utilized with fixed speed (N_2) can be seen in Figure D.1b. The pressure rise in the vehicle tank is approximated as integrating processes in both cases. An integrating model can be expressed as:

$$G(s) = \frac{k'e^{-\theta s}}{s} \tag{D.3}$$

Figure D.2 illustrates how to find a process model for an integrating process.

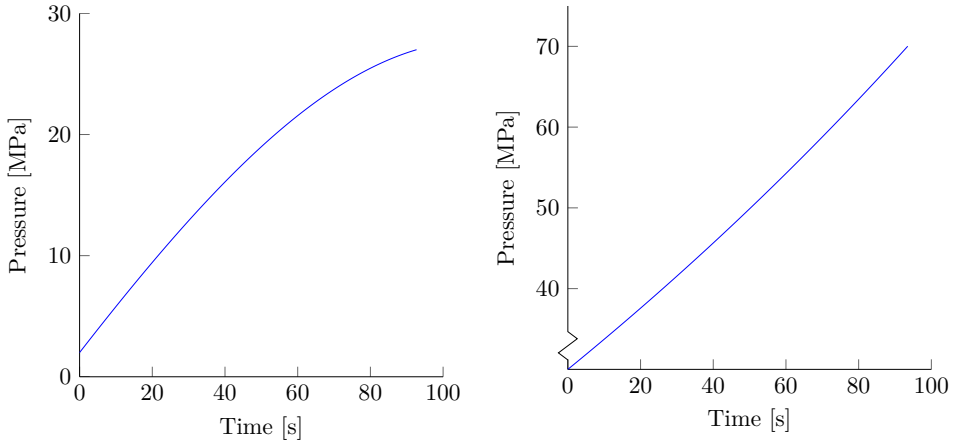

(a) *Reduction valve.*

(b) *Compressor.*

Figure D.1: *The open-loop response for when the reduction valve (a) and the compressor (b) are utilized for refueling.*

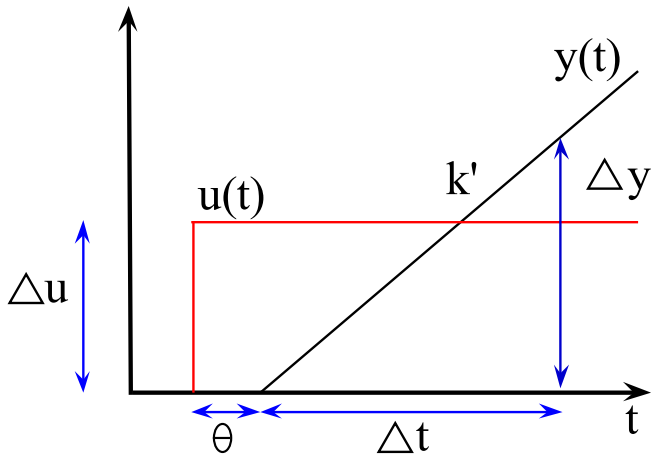

Figure D.2: *Illustration on how to obtain a process model for an integrating process. y(t) is process output, u(t) is process input, θ is process time delay and k' is the slope of the integrating response (i.e. process gain).*

The process model gain (k') can then be obtained from the following equation

$$k' = \frac{\Delta y}{\Delta u \Delta t} \tag{D.4}$$

where Δy is the change in the output variable (pressure), Δu the magnitude of the step (C_v/N_2) and Δt the time period. The obtained process models for the two cases are presented in Table D.2.

Table D.2: *Process model parameters for the pressure rise when utilizing the reduction valve and when utilizing the compressor for refueling.*

Parameter	Reduction valve	Compressor
Δu	2.00×10^{-6}	5.00
Δy	10.88	11.55
Δt	30.00	30.00
k'	1.81×10^{5}	7.70×10^{-2}
θ	0.00	0.00

Obtained tuning settings for the two controllers with different τ_cs are presented in Table D.3a and Table D.3b. The controller bias is set to zero during the tuning.

Table D.3: *Process model and tuning settings for the reduction valve and compressor controllers.*

(a) *Reduction valve controller.*

τ_c	$K_c \times 10^{-5}$	τ_I
0.5	1.10	2
1	0.55	4
2	0.28	20
4	0.14	40

(b) *Compressor controller.*

τ_c	K_c	τ_I
0.5	25.98	2
1	12.99	4
2	6.50	20
4	3.25	40

D.1 Controller performance

Figures D.3 and D.4 show the performance of the different controller settings for the reduction valve and compressor controllers, respectively. The different cases are simulated at the operating conditions of the two units. That is, in the corresponding pressure range at which the unit is used during a refueling. The highest value of τ_c having an acceptable tracking of the APRR has been chosen for tuning settings. Therefore, $\tau_c = 0.5$ and $\tau_c = 2$ are chosen for the reduction valve and the compressor controllers, respectively.

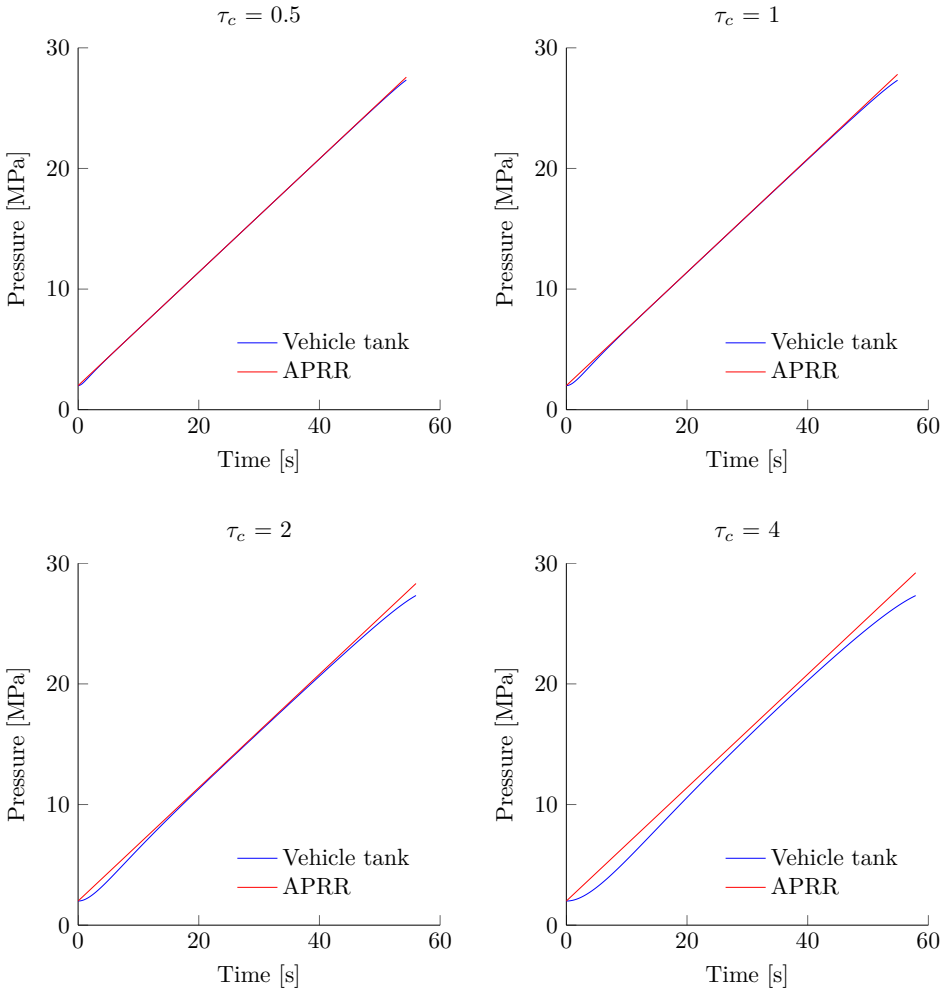

Figure D.3: *The performance of the reduction valve controller with different values of the desired closed-loop time constant, τ_c.*

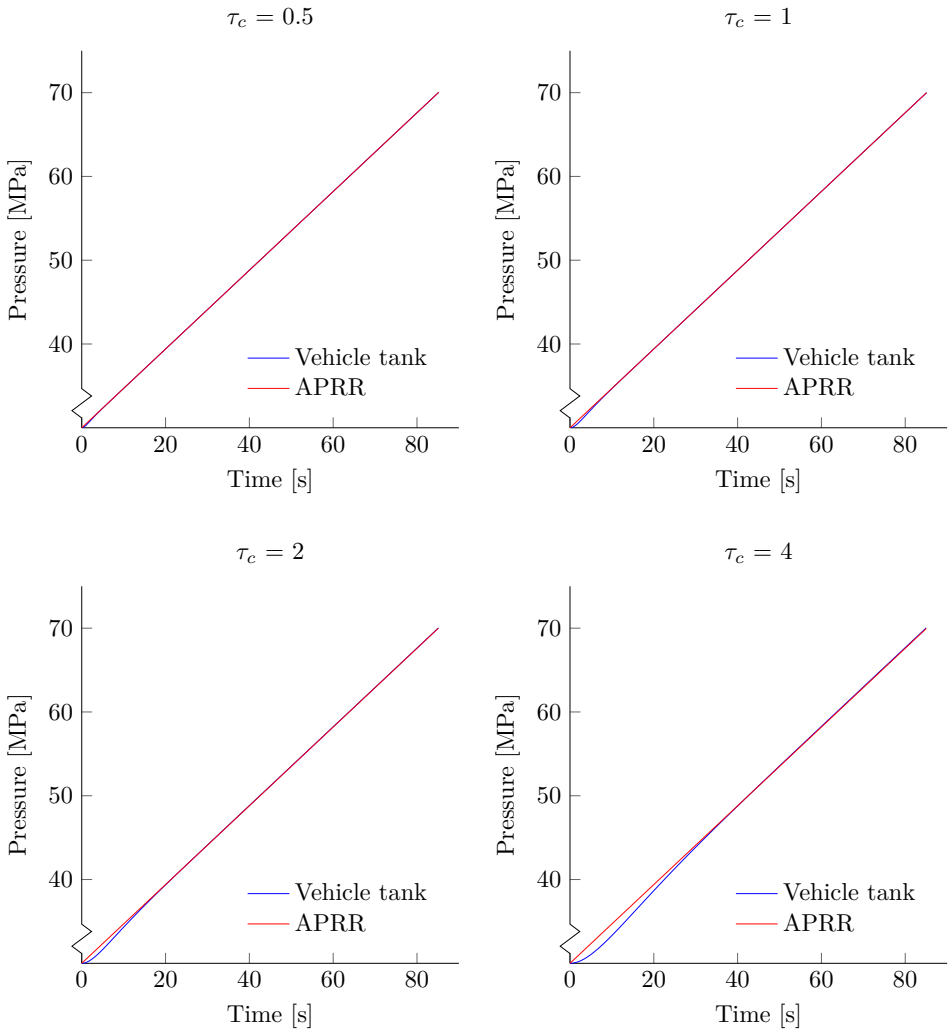

Figure D.4: *The performance of the compressor controller with different values of the desired closed-loop time constant, τ_c.*

E | Pressure loss calculations

This appendix presents pressure loss calculations performed in order to see whether the assumption saying that the pressure losses at the station are negligible is reasonable.

E.1 Pressure losses in pipes

The pressure drop in a pipe (Δp) is calculated from the Darcy-Weisbach equation

$$\Delta p = f\rho\frac{\Delta L}{D}\frac{v^2}{2} \tag{E.1}$$

where f is the Darcy friction factor, ρ the density of the flow, ΔL the length of the pipe, D the inner diameter of the pipe and v the average velocity in the pipe [30]. The velocity can be found from

$$v = \frac{\dot{m}}{\rho A} \tag{E.2}$$

where A is the cross-sectional area of the pipe. The friction factor, f, depends on whether the flow is laminar or turbulent. The Reynolds number, N_{Re}, is used to describe the flow type. For a straight, circular pipe, the flow is always laminar when the value of the Reynolds number is less than 2100. When the Reynolds number is over 4000, the flow will be turbulent. In between these numbers, the flow can be viscous or turbulent. The Reynolds number is as follows

$$N_{Re} = \frac{Dv\rho}{\mu} \tag{E.3}$$

where μ is the dynamic viscosity. The friction factor for a laminar flow depends only on the Reynolds number:

$$f = \frac{16}{N_{Re}} \tag{E.4}$$

For a turbulent flow, the friction factor does not only depend on the Reynolds number, but also on the pipe roughness (ϵ). The friction factor for a turbulent

flow must therefore be determined empirically. However, several equations have been developed for estimating this friction factor. One of these is the Swamee-Jain equation where the friction factor is found explicitly [31].

$$f = 0.25\Big[\log\Big(\frac{\epsilon/D}{3.7} + \frac{5.74}{N_{Re}^{0.9}}\Big)\Big]^{-2} \tag{E.5}$$

E.2 Pressure loss: Refueling section

The pressure loss in the pipe between the storage tank and the reduction valve/-compressor along with the pressure loss in the pipe between reduction valve/heat exchanger and heat exchanger 3 have been calculated during a refueling. The refueling occurs with an ambient temperature of 15°C and an initial vehicle tank pressure of 2 MPa. First, the Reynolds number was calculated in order to determine whether the flow is laminar or turbulent. It was found that the flow is turbulent during the whole refueling. The pressure losses per pipe length for both cases are presented in Figure E.1. Two different inner diameters have been applied in the calculations: 0.01 and 0.008 m. The roughness of the pipe is set to 4.6×10^{-5} (commercial steel) [30].

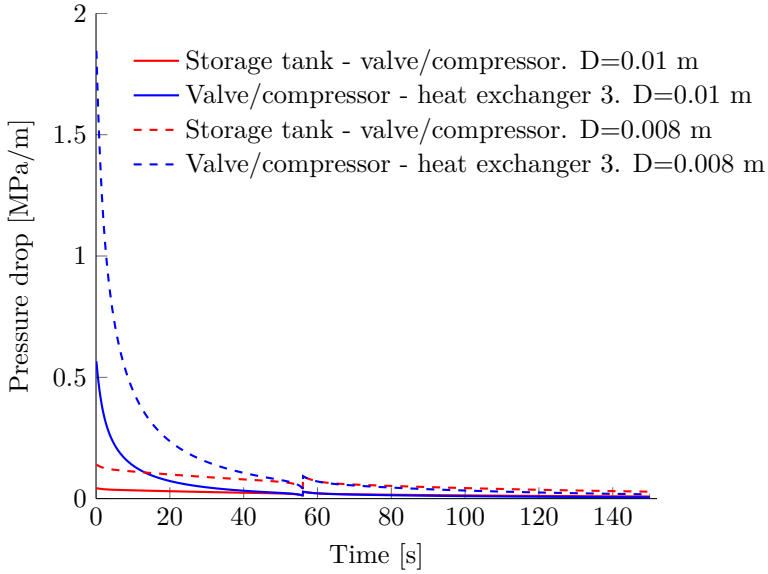

Figure E.1: *Pressure losses in the pipes between the storage tank and the reduction valve/compressor and between the reduction valve/compressor and heat exchanger 3. The pressure losses are given per pipe length and for a whole refueling.*

F | Absorption refrigeration

This appendix presents similar calculations and results as those presented in Chapter 8 for additional ambient temperatures (20, 25 and 30°C). The results for 15°C is also included. Note that the values presented are from a refueling only. That is, the heat generated during the corresponding refilling is not considered.

F.1 Case I: Use heat from only one heat source

In the following calculations, the maximum and average cooling demand of heat exchanger 3 ($\dot{Q}_{HX3}$) have been applied. Table F.1 shows the cooling demand in heat exchanger 3, the required heat input to the generator ($\dot{Q}_G$) and the heat removal in the heat exchangers for different ambient temperatures during a refueling. The heat exchangers included are the internal heat exchanger in the electrolyzer, the heat exchanger following the first compressor (i.e. heat exchanger 2) and the intercooler between the two compression stages in compressor 1. Note that the numbers in parenthesis correspond to the useful heat which can be utilized for heating at the required driving temperature and above. The temperatures at which the heat is removed in the heat exchangers along with the required temperature (T_{req}) are presented in Table F.2.

F.2 Case II: Increase temperature of waste heat from electrolyzer with waste heat from heat exchanger 2 and intercooler

This section presents more detailed tables for the Case II results.

F.2.1 Generator

Table F.3 presents the necessary mass flow of saturated steam ($\dot{m}_{req}$) to transfer the required heat input to the generator ($\dot{Q}_G$) for different ambient temperatures. The conditions of the steam (temperature, pressure) are also included. Note that the given pressure is the pressure of the rest of the cooling system as well.

Table F.1: *Case I: The cooling demand in heat exchanger 3 ($\dot{Q}_{HX3}$), the required generator heat input ($\dot{Q}_G$) and available heat from the electrolyzer ($\dot{Q}_{EL}$), heat exchanger 2 ($\dot{Q}_{HX2}$) and the intercooler ($\dot{Q}_{IC}$) for different ambient temperatures. The coefficients of performance for the different ambient temperatures are also included. The numbers in parenthesis correspond to the heat which can be utilized for heating at the required temperature.*

T_{amb} [°C]		COP	$\dot{Q}_{HX3}$ [kW]	$\dot{Q}_G$ [kW]	$\dot{Q}_{EL}$ [kW]	$\dot{Q}_{HX2}$ [kW]	$\dot{Q}_{IC}$ [kJ/kg]
15	Maximum	0.45	66	146	2395 (0)	47 (37)	49 (39)
	Average		52	116		48 (38)	
20	Maximum	0.40	69	171	2395 (0)	48 (37)	50 (40)
	Average		56	139		49 (39)	
25	Maximum	0.40	71	178	2395 (0)	48 (38)	51 (41)
	Average		59	147		50 (41)	
30	Maximum	0.30	72	240	2395 (0)	49 (39)	52 (42)
	Average		60	202		50 (41)	

Table F.2: *Case I: The required temperature of the heat input (T_{req}) along with the temperatures of the available heat removed from the electrolyzer (T_{EL}), heat exchanger 2 (T_{HX2}) and intercooler in compressor 1 (T_{IC}).*

T_{amb} [°C]		T_{req} [°C]	T_{EL} [°C]	T_{HX2} [°C]	T_{IC} [°C]
15	Maximum	150	90	201	213
	Average			207	
20	Maximum	160	90	209	222
	Average			214	
25	Maximum	175	90	217	230
	Average			222	
30	Maximum	186	90	225	238
	Average			231	

Table F.3: *Case II: The mass flow of steam required ($\dot{m}_{req}$) to transfer the heat amount that is necessary to drive the cycle ($\dot{Q}_G$) and meet the cooling demand. The desired temperature (T_{req}) and pressure (p) of the saturated steam are also included. Values for both maximum and average cooling demand are presented.*

T_{amb} [°C]		T_{req} [°C]	p [bar]	$\dot{Q}_G$ [kW]	$\dot{m}_{req}$ [kg/s]
15	Maximum	150	4.8	146	0.069
	Average			116	0.055
20	Maximum	160	6.2	171	0.082
	Average			139	0.067
25	Maximum	175	9	178	0.085
	Average			147	0.071
30	Maximum	186	11.9	240	0.11
	Average			202	0.097

F.2.2 Electrolyzer

The temperature of the hot water leaving the electrolyzer heat exchanger (T_{EL}), the outlet temperature after heating which corresponds to the required driving temperature (T_{req}) and the required steam flow ($\dot{m}_{req}$) are shown in Table F.4. Additionally, the available mass flow of the water coming from the electrolyzer ($\dot{m}_{EL}$) and the heat amount necessary to heat up and vaporize the hot water at the required temperature ($\dot{Q}_{HX2|EL}$) are given. Values for both maximum and average cooling demand in heat exchanger 3 are included.

F.2.3 Heat exchanger 2 and intercooler

Table F.5 presents the temperature of the combined steam flow from heat exchanger 2 and the intercooler (T_{HX}), the temperature after the heat exchange ($T_{HX,out}$), the required mass flow in order to vaporize the electrolyzer cooling water ($\dot{m}_{HX,req}$) and the actual mass flow available ($\dot{m}_{HX,act}$).

F.3 Case III: Include an heat exchanger in the compressor line

By including a heat exchanger after compressor 2, the cooling demand in heat exchanger 3, and accordingly the required heat input to the generator, will be reduced. The new cooling demand in heat exchanger 3 and required heat input to the generator are presented along with the available waste heats in Table F.6. The temperatures at which the waste heat are generated are presented in Table F.7

Table F.4: *Case II: The heat required to heat up and vaporize the hot cooling water leaving the electrolyzer to and at the driving temperature ($\dot{Q}_{HX2|EL}$). The available cooling water mass flow in the electrolyzer ($\dot{m}_{EL}$) and its corresponding temperature (T_{EL}) along with the required steam flow ($\dot{m}_{req}$) and its corresponding temperature (T_{req}) are also included.*

T_{amb} [°C]		T_{EL} [°C]	T_{req} [°C]	$\dot{m}_{req}$ [kg/s]	$\dot{m}_{EL}$ [kg/s]	$\dot{Q}_{HX2\|EL}$ [kW]
15	Maximum	90	150	0.069	7.63	164
	Average			0.055		130
20	Maximum	90	160	0.082	8.17	195
	Average			0.067		159
25	Maximum	90	175	0.085	8.80	203
	Average			0.071		168
30	Maximum	90	186	0.11	9.53	273
	Average			0.097		230

Table F.5: *Case II: The required ($\dot{m}_{HX,req}$) and actual ($\dot{m}_{HX,act}$) mass flow from the heat exchanger and intercooler along with the conditions at which the heat exchange to the hot water leaving the electrolyzer occurs.*

T_{amb} [°C]		T_{HX} [°C]	$T_{HX,out}$ [°C]	$\dot{m}_{HX,req}$ [kg/s]	$\dot{m}_{HX,act}$ [kg/s]
15	Maximum	207	150	0.066	0.034
	Average	210		0.052	0.034
20	Maximum	216	160	0.078	0.035
	Average	218		0.063	0.035
25	Maximum	224	175	0.081	0.035
	Average	226		0.066	0.036
30	Maximum	232	186	0.11	0.036
	Average	234		0.090	0.036

Table F.6: *Case III: The cooling demand in heat exchanger 3 ($\dot{Q}_{HX3}$), the required generator heat input ($\dot{Q}_G$) and available heat from the electrolyzer ($\dot{Q}_{EL}$), heat exchanger 2 ($\dot{Q}_{HX2}$) and the intercooler in compressor 1 ($\dot{Q}_{IC}$) for different ambient temperatures. The coefficients of performance for the different ambient temperatures are also included. The numbers in parenthesis correspond to the heat which can be utilized for heating at the required temperature and above.*

T_{amb} [°C]		COP	$\dot{Q}_{HX3}$ [kW]	$\dot{Q}_G$ [kW]	$\dot{Q}_{EL}$ [kW]	$\dot{Q}_{HX2}$ [kW]	$\dot{Q}_{IC}$ [kJ/kg]
15	Maximum	0.45	57	127	2395 (0)	50 (40)	49 (39)
	Average		33	73		48 (38)	
20	Maximum	0.40	61	153	2395 (0)	51 (40)	50 (40)
	Average		36	89		49 (39)	
25	Maximum	0.40	65	163	2395 (0)	52 (41)	51 (41)
	Average		39	96		50 (40)	
30	Maximum	0.30	69	229	2395 (0)	53 (40)	52 (42)
	Average		40	202		50 (41)	

Table F.7: *Case III: The required temperature of the heat input (T_{req}) along with the temperatures of the available heat removed from the electrolyzer (T_{EL}), heat exchanger 2 (T_{HX2}) and intercooler in compressor 1 (T_{IC}).*

T_{amb} [°C]		T_{req} [°C]	T_{EL} [°C]	T_{HX2} [°C]	T_{IC} [°C]
15	Maximum	150	90	215	213
	Average			207	
20	Maximum	160	90	223	222
	Average			214	
25	Maximum	175	90	231	230
	Average			222	
30	Maximum	186	90	240	238
	Average			231	

F.4 Case IV: Combination of Case II and III

This section presents more detailed tables for the Case IV results.

F.4.1 Generator

Table F.8 presents the necessary mass flow of steam ($\dot{m}_{req}$) to transfer the required heat input to the generator ($\dot{Q}_G$) for different ambient temperatures. The conditions of the steam (temperature, pressure) are also included. Note that the given pressure is the pressure of the rest of the cooling system as well.

Table F.8: *Case IV: The mass flow of steam required ($\dot{m}_{req}$) to transfer the heat amount that is necessary to drive the cycle ($\dot{Q}_G$) and meet the cooling demand. The desired temperature (T_{req}) and pressure (p) of the saturated steam are also included. Values for both maximum and average cooling demand are presented..*

T_{amb} [°C]		T_{req} [°C]	p [bar]	$\dot{Q}_G$ [kW]	$\dot{m}_{req}$ [kg/s]
15	Maximum	150	4.8	127	0.060
	Average			73	0.035
20	Maximum	160	6.2	153	0.073
	Average			89	0.043
25	Maximum	175	9	163	0.078
	Average			96	0.046
30	Maximum	186	11.9	229	0.11
	Average			134	0.064

F.4.2 Electrolyzer

The temperature of the hot water coming from the electrolyzer heat exchanger (T_{EL}), the outlet temperature after heating which corresponds to the required driving temperature (T_{req}) and the required saturated steam flow ($\dot{m}_{req}$) are shown in Table F.4. Additionally, the available mass flow of the water coming from the electrolyzer ($\dot{m}_{EL}$) and the heat amount necessary to heat up and vaporize the water at the required temperature ($\dot{Q}_{HX2|EL}$) are given. Values for both maximum and average cooling demand in heat exchanger 3 are presented.

F.4.3 Heat exchanger 2 and intercooler

Table F.5 presents the temperature of the combined steam flow from heat exchanger 2 and the intercooler (T_{HX}), the temperature after the heat exchange ($T_{HX,out}$), the required mass flow in order to vaporize the electrolyzer cooling water ($\dot{m}_{HX,req}$) and the actual mass flow available ($\dot{m}_{HX,act}$)

Table F.9: *Case IV: The heat required to heat up and vaporize the hot cooling water leaving the electrolyzer to and at the driving temperature ($\dot{Q}_{HX2|EL}$). The available cooling water mass flow in the electrolyzer ($\dot{m}_{EL}$) and its corresponding temperature (T_{EL}) along with the required steam flow ($\dot{m}_{req}$) and its corresponding temperature (T_{req}) are also included.*

T_{amb} [°C]		T_{EL} [°C]	T_{req} [°C]	$\dot{m}_{req}$ [kg/s]	$\dot{m}_{EL}$ [kg/s]	$\dot{Q}_{HX2\|EL}$ [kW]
15	Maximum	90	150	0.060	7.63	142
	Average			0.035		82
20	Maximum	90	160	0.073	8.17	175
	Average			0.043		102
25	Maximum	90	175	0.078	8.80	186
	Average			0.046		110
30	Maximum	90	186	0.11	9.53	262
	Average			0.064		153

Table F.10: *Case IV: The required ($\dot{m}_{HX,req}$) and actual ($\dot{m}_{HX,act}$) mass flow from the heat exchanger and intercooler along with the conditions at which the heat exchange to the electrolyzer cooling water occurs.*

T_{amb} [°C]		T_{HX} [°C]	$T_{HX,out}$ [°C]	$\dot{m}_{HX,req}$ [kg/s]	$\dot{m}_{HX,act}$ [kg/s]
15	Maximum	214	150	0.057	0.035
	Average	210		0.033	0.034
20	Maximum	223	160	0.069	0.036
	Average	218		0.041	0.035
25	Maximum	231	175	0.073	0.036
	Average	226		0.043	0.036
30	Maximum	239	186	0.10	0.037
	Average	234		0.060	0.036

G | MATLAB script

This appendix contains the MATLAB script of the model along with its sub functions. Only the script for the case without heat exchanger 4 is included. The script used for the absorption refrigeration process is also presented in this appendix. Documentation is provided in the scripts.

G.1 Main script: refueling_station.m

```
% DESCRIPTION
% Dynamic model of a hydrogen refueling station with direct compression of
% hydrogen gas into the vehicle tank.
% The station consists of an electrolyzer that produces hydrogen from
% water, three heat exchangers whose job is to remove heat that is added in
% compression and expansion processes, two compressors, a storage tank and
% a reduction valve.
% The vehicle that connects to the station consists of one hydrogen storage
% tank.
% The mass flows in the station are induced by compressor 1 (mflow2) and
% the reduction valve/compressor 2 (mflow5A/B).
% The rest of the mass flows are given by steady state mass balances:
%           mflow1 = mflow2 and mflow4 = mflow3 = mflow2
%           mflow7 = mflow6A/B = mfow5A/B
%
% COMPONENTS in station
%%%%%%%%%%%%%%%%%%%%%%%%%%%%%%%%%%%%%%%%%%%%%%%%%%%%%%%%%%%%%%%%%%%%%%%%%%%%
% Flows:  1        2       3        4      5A/B       6A/B      7        %
%     EL ---> HX1 ---> C1 ---> HX2 ---> ST ---> RV/C2 ---> HX3 ---> VT   %
%                                                                         %
%%%%%%%%%%%%%%%%%%%%%%%%%%%%%%%%%%%%%%%%%%%%%%%%%%%%%%%%%%%%%%%%%%%%%%%%%%%%
% EL: Electrolyzer
% HX: Heat exchanger
% C:  Compressor
% ST: Storage tank
% RV: Reduction valve
% VT: Vehicle tank
%
% ASSUMPTIONS
% No pressure drop in pipelines or in heat exchangers.
% Steady-state operation of heat exchangers.
% Adiabatic compression and expansion in compressors and reduction valve.
% Adiabatic filling of vehicle tank. No heat exchange with environment from
% storage tank.
%
% INTEGRATOR
% Explicit Euler method.
%
% PARAMETERS/VARIABLES
```

```
% aprr         Average pressure ramp rate, [MPa/s]
% Cv           Valve coefficient
% h            Specific enthalpy, [kJ/kg]
% i            Loop counter
% Kc           Controller gain
% m            Mass in tank, [kg]
% mflow        Mass flow, [kg/s]
% N            Compressor speed, [1/s]
% rho          Density, [kg/m3]
% t            Time, [s]
% tau_C        Desired closed-loop time constant, [s]
% tau_D        Derivative time constant, [s]
% tau_I        Integral time constant, [s]
% T            Temperature, [K]
% u            Specific internal energy, [kJ/kg]
% U            Internal energy, [kJ]
% V            Tank volume, [m3]
% W            Work flow, [kW]
% Q            Heat flow, [kW]


clear all
close all

global T_amb V_vt del_t aprr

refill          = true;

%%%%%%%%%%%%%%%%%%%% INPUT VARIABLES %%%%%%%%%%%%%%%%%%%%%%%%%%%%%%%%
% The ambient temperature, vehicle tank pressure and volume will be
% different for different vehicles. APRR is decided based on these
% variables. The pressure in storage tank can be optimized to save
% compressor work.
T_amb           = 273 + 15;          %Ambient temperature, [K]
p_vehicle_tank  = 2;                 %Initial pressure in vehicle tank, [MPa]
V_vehicle_tank  = 0.172;             %Volume of vehicle tank, [m3]
p_storage_tank  = 30;                %Initial pressure in storage tank, [MPa]


%%%%%%%%%%%%%%%%%%%% HYDROGEN VEHICLE %%%%%%%%%%%%%%%%%%%%%%%%%%%%%%%%
% The primary (u and m) and secondary (p, T, rho, h) states of the vehicle
% tank before refueling.
p_vt            = p_vehicle_tank;
T_vt            = T_amb;
V_vt            = V_vehicle_tank;
rho_vt          = Props('D', 'P', p_vt*1e3, 'T', T_amb, 'H2');
m_vt            = rho_vt*V_vt;
u_vt            = Props('U', 'P', p_vt*1e3, 'T', T_amb, 'H2');
h_vt            = Props('H', 'P', p_vt*1e3, 'T', T_amb, 'H2');

% Filling targets: Target density [kg/m3] and target pressure [MPa] based on
% target density and ambient temperature.
% Switching limit [MPa] between the red. valve and compressor
rho_target      = 40.2;
dp_switch       = 0.5;

if T_amb == 273 + 10
    p_target    = 72;
    aprr        = 28.2/60;  %Tabulated average pressure ramp rate, [MPa/s].
elseif T_amb == 273 + 15    %REF: SAE TIR J2601
    p_target    = 72.6;
    aprr        = 28.2/60;
elseif T_amb == 273 + 20
    p_target    = 73.2;
    aprr        = 28.2/60;
elseif T_amb == 273 + 25
    p_target    = 73.6;
    aprr        = 28.2/60;
```

```
elseif T_amb == 273 + 30
    p_target    = 74.1;
    aprr        = 27.4/60;
else
    disp('Not valid ambient temperature input.The valid options are 10, 15, 20, 25 and 30 Celsius')
    return
end

if p_vt > p_storage_tank - dp_switch
    p_target        =   69.1;          % When initial pressure is 30 MPa
end
disp(['Target pressure in vehicle tank is ', num2str(p_target), ' MPa'])

%%%%%%%%%%%%%%%%%%%% REFUELING STATION %%%%%%%%%%%%%%%%%%%%%%%%%%%%%

%Electrolyzer
p_electrolyzer  = 1.2;                    %Operating pressure, [MPa]
T_electrolyzer  = 273 + 90;               %Operating temperature, [K]

%Heat exchangers. Outlet temperatures are specified.
Thx1_out        = T_amb;
Thx2_out        = T_amb;
Thx3_out        = 273 - 40;

%Storage tank: Primary (u and m) and secondary states (p, T, rho, h).
p_st            = p_storage_tank;
T_st            = T_amb;
V_st            = 3;
rho_st          = Props('D', 'P', p_st*1e3, 'T', T_st, 'H2');
m_st            = rho_st*V_st;
u_st            = Props('U', 'P', p_st*1e3, 'T', T_st, 'H2');
h_st            = Props('H', 'P', p_st*1e3, 'T', T_st, 'H2');

%Initiation of flows: Secondary states.
T_1             = T_electrolyzer;
p_1             = p_electrolyzer;
T_2             = Thx1_out;
p_2             = p_1;
T_3             = T_amb;
p_3             = p_st;
T_4             = Thx2_out;
p_4             = p_st;
T_5             = T_st;
p_5             = p_st;
T_6             = T_amb;
p_6             = p_vt;
T_7             = Thx3_out;
p_7             = p_vt;

mflow6          = 0;        %For when compressor 2 starts directly

%Initial conditions for integrator
x0              = [ m_st , m_st*u_st , ...
                    m_vt   , m_vt*u_vt ]';

%%%%%%%%%%%%%%%%%%%% TIME DEFINITIONS %%%%%%%%%%%%%%%%%%%%%%%%%%%%%
t               = 0;                            %Start at t = 0, [s]
del_t           = 0.1;                          %Time steps, [s]
i               = 1;                            %Counter

%%%%%%%%%%%%%%%%%%%% CONTROLLERS %%%%%%%%%%%%%%%%%%%%%%%%%%%%%%%%%%

%Reduction valve controller settings
tauC_rv         = 0.5;

%Integrating
k_rv            = 1.81e5;
Kc_rv           = 1/(k_rv*tauC_rv);
```

```
tauI_rv          = 4*tauC_rv;

%PID-controller for reduction valve.
controller1      = @(cv, error, int_error)  ...
                     cv + Kc_rv*(error + 1/tauI_rv*int_error*del_t);

%Compressor controller settings
tauC_c2          = 2;
k_c2             = 0.077;
Kc_c2            = 1/(k_c2*tauC_c2);
tauI_c2          = 4*tauC_c2;

%PID-controller for compressor 2.
controller2      = @(N, error, int_error)  ...
                     N + Kc_c2*(error + 1/tauI_c2*int_error*del_t);

%Initiation of controllers
p_SP             = p_vt + aprr*del_t; %Set point for pressure in vehicle tank
error            = p_SP - p_vt;       %Error between set point and msrd variable
int_error        = 0;                 %Integrator error
flag             = 0;                 %Decides initiation of N2

Cv0              = 2e-6;      %Bias value for valve coefficient
N2               = 0;         %Compressor 2 is off

%%%%%%%%%%%%%%%%%%% ALLOCATION OF PROFILES %%%%%%%%%%%%%%%%%%%%%%%%%
t_aprr           = round(p_target/aprr)-70;        %Approximate filling time
len              = t_aprr/del_t;
tspan            = zeros(len, 1);
aprr_prof        = zeros(len, 1);

pst_prof         = zeros(len, 1);
mst_prof         = zeros(len, 1);
ust_prof         = zeros(len, 1);
hst_prof         = zeros(len, 1);
Tst_prof         = zeros(len, 1);

pvt_prof         = zeros(len, 1);
mvt_prof         = zeros(len, 1);
uvt_prof         = zeros(len, 1);
hvt_prof         = zeros(len, 1);
Tvt_prof         = zeros(len, 1);

mf_2_prof        = zeros(len, 1);
mf_5_prof        = zeros(len, 1);

Pel_prof         = zeros(len, 1);
Qel_prof         = zeros(len, 1);
T3_prof          = zeros(len, 1);
Tc1_int_prof     = zeros(len, 1);
Qc1_prof         = zeros(len, 1);
Wc1_prof         = zeros(len, 1);
T6_prof          = zeros(len, 1);
Wc2_prof         = zeros(len, 1);
Qhx1_prof        = zeros(len, 1);
Qhx2_prof        = zeros(len, 1);
Qhx3_prof        = zeros(len, 1);

Cv_prof          = zeros(len, 1);
N2_prof          = zeros(len, 1);

Re_prof          = zeros(len, 1);
dp_prof          = zeros(len, 1);

%Initial profiles at t = 0 (NOTE: Must have i = 1)
tspan(1)         = t;
aprr_prof(1)     = p_vt;

```

```
244 pst_prof(1)      = p_st;
245 mst_prof(1)      = m_st;
246 ust_prof(1)      = u_st;
247 hst_prof(1)      = h_st;
248 Tst_prof(1)      = T_st;
249
250 pvt_prof(1)      = p_vt;
251 mvt_prof(1)      = m_vt;
252 uvt_prof(1)      = u_vt;
253 hvt_prof(1)      = h_vt;
254 Tvt_prof(1)      = T_vt;
255
256 T3_prof(1)       = T_3;
257 Tc1_int_prof(1)  = T_2;
258 T6_prof(1)       = T_6;
259
260
261 while p_vt < p_target
262
263     %Mass flow and work in compressor 1. Sets mass flow in production line.
264     [ W_compressor1, mflow2, T_3, Tc1_int, Qc1_int ]    ...
265                     = compressor1( p_2, p_3, T_2, T_3 );
266     mflow3          = mflow2;
267
268     %Electrolyzer
269     mflow1          = mflow2;
270     [ P_electrolyzer, Q_electrolyzer ] ...
271                     = electrolysis( mflow1, T_electrolyzer );
272
273     %Heat exchanger 1
274     [ Q_hx1, h_2 ] ...
275                     = heatexchanger( mflow1, T_1, p_1, Thx1_out );
276
277     %Heat exchanger 2
278     [ Q_hx2, h_4 ] ...
279                     = heatexchanger( mflow3, T_3, p_3, Thx2_out );
280     mflow4          = mflow3;
281
282
283     %Switching between reduction valve and compressor
284     if p_st - p_vt >= dp_switch
285
286         %Calculating new valve coefficient from controller
287         Cv          = controller1( Cv0, error, int_error );
288
289         %Mass flow in reduction valve
290         [ mflow5, T_6 ]  ...
291                     = red_valve( p_5, T_5, rho_st, p_6, Cv );
292         mflow6      = mflow5;
293
294         W_compressor2 = 0;
295
296     elseif p_st - p_vt < 0
297
298         %Controller
299         N2          = controller2( N20, error, int_error );
300
301         %Work, mass flow and outlet temp. in compressor 2
302         [ W_compressor2, mflow5, T_compressor2 ]    ...
303                     = compressor2( p_5, p_6, T_5, T_6, N2 );
304         T_6         = T_compressor2;
305         mflow6      = mflow5;
306
307     else
308     %At the switch, the pressure in the vehicle tank is lower than the
309     %pressure in the storage tank. Therefore, the outlet pressure of the
310     %compressor is set equal to the inlet pressure
311
```

```
312         if flag == 0
313             %Initiation of N2 the first time the compressor runs. N2 is
314             %initiated based on the mass flow in the reduction valve when
315             %the switch occurs.
316 
317             Cv      = 0;                            %Closing valve
318             N2      = init_n2(mflow6, p_st, T_st, rho_st);
319             N20     = N2;
320             flag    = 1;                           %Turns off N2 initiation
321 
322             time    = tspan(i);
323             disp(['Change from reduction valve to compressor at ', ...
324                                                     num2str(time), ' s'])
325             disp(['Initial N2 is ', num2str(N2), ' strokes per second'])
326 
327         else
328 
329             %Controller calculating compressor speed
330             N2      = controller2( N20, error, int_error );
331 
332         end
333 
334         %Work, mass flow and outlet temp. in compressor 2
335         %Assume outlet pressure is equal to inlet pressure
336         [ W_compressor2, mflow5, T_compressor2 ]    ...
337                     = compressor2( p_5, p_5, T_5, T_6, N2 );
338         T_6   = T_compressor2;
339         mflow6      = mflow5;
340 
341     end
342 
343     %Heat exchanger 3
344     [ Q_hx3, h_7 ]  = heatexchanger( mflow6, T_6, p_6, Thx3_out );
345     mflow7          = mflow6;
346 
347     %Integration - Explicit Euler
348     [ x, x0 ]       = euler_integrator( mflow4, h_4, ...
349                                         h_st, mflow7, h_7, x0 );
350 
351     %Calculating new primary and secondary states in tanks
352     m_st            = x(1);
353     u_st            = x(2)/m_st;
354     rho_st          = m_st/V_st;
355     T_st            = T_solver(u_st, rho_st, T_st);
356     p_st            = Props('P', 'D', rho_st, 'T', T_st, 'H2')/(1e3);
357     h_st            = Props('H', 'P', p_st*1e3, 'T', T_st, 'H2');
358 
359     m_vt            = x(3);
360     u_vt            = x(4)/m_vt;
361     rho_vt          = m_vt/V_vt;
362     T_vt            = T_solver(u_vt, rho_vt, T_vt);
363     p_vt            = Props('P', 'D', rho_vt, 'T', T_vt, 'H2')/(1e3);
364     h_vt            = Props('H', 'P', p_vt*1e3, 'T', T_vt, 'H2');
365 
366     %Updating flows
367     p_4             = p_st;
368     p_3             = p_st;
369     T_5             = T_st;
370     p_5             = p_st;
371     p_6             = p_vt;
372     p_7             = p_vt;
373 
374 
375     %Updating profiles
376     tspan(i + 1)    = tspan(i) + del_t;
377     aprr_prof(i + 1)= p_SP;
378 
379     pst_prof(i + 1) = p_st;
```

```
    mst_prof(i + 1) = m_st;
    ust_prof(i + 1) = u_st;
    hst_prof(i + 1) = h_st;
    Tst_prof(i + 1) = T_st;

    pvt_prof(i + 1) = p_vt;
    mvt_prof(i + 1) = m_vt;
    uvt_prof(i + 1) = u_vt;
    hvt_prof(i + 1) = h_vt;
    Tvt_prof(i + 1) = T_vt;

    mf_2_prof(i + 1) = mflow2;
    mf_5_prof(i + 1) = mflow7;

    Pel_prof(i + 1) = P_electrolyzer;
    Qel_prof(i + 1) = Q_electrolyzer;
    T3_prof(i + 1)  = T_3;
    Tc1_int_prof(i + 1) = Tc1_int;
    T6_prof(i + 1)  = T_6;
    Qhx1_prof(i + 1)= Q_hx1;
    Qc1_prof(i + 1) = Qc1_int;
    Qhx2_prof(i + 1)= Q_hx2;
    Qhx3_prof(i + 1)= Q_hx3;
    Wc1_prof(i + 1) = W_compressor1;
    Wc2_prof(i + 1) = W_compressor2;

    Cv_prof(i + 1)  = Cv;
    N2_prof(i + 1)  = N2;

    Re_prof(i + 1)  = Re;
    dp_prof(i + 1)  = dp;

    %Updating error for controller action
    p_SP            = p_SP + aprr*del_t;
    error           = p_SP - p_vt;
    int_error       = int_error + error;

    i               = i + 1;

end

%%%%%%%%%%%%%%%%%%% STATE OF CHARGE %%%%%%%%%%%%%%%%%%%%%%%%
soc                 = rho_vt/rho_target*100;

disp(['Final pressure in vehicle tank ', num2str(p_vt), ' MPa'])
disp(['Final mass in vehicle tank ', num2str(m_vt), ' kg'])
disp(['The state of charge is ', num2str(soc), '%'])
disp(['The refueling lasts ', num2str(tspan(end)), ' s'])

%%%%%%%%%%%%%%%%%%%%% REFILLING STORAGE TANK %%%%%%%%%%%%%%%%%%%%

%New system matrix for Euler integration. Only charging of tank.
F                   = [ 1 , h_4 ]';
y0                  = [ m_st, m_st*u_st]';

%Time
t                   = 0;
j                   = 1;

%Allocation of profiles
t_refill_guess      = 2*70;
len_refill          = t_refill_guess/del_t;

t_refill            = zeros(len, 1);
pst_refill          = zeros(len, 1);
mst_refill          = zeros(len, 1);
Tst_refill          = zeros(len, 1);
mf_2_refill         = zeros(len, 1);
```

```
448
449 T3_refill           = zeros(len, 1);
450 Tc1_refill          = zeros(len, 1);
451
452 Wc1_refill          = zeros(len, 1);
453 Pel_refill          = zeros(len, 1);
454
455 Qel_refill          = zeros(len, 1);
456 Qhx1_refill         = zeros(len, 1);
457 Qhx2_refill         = zeros(len, 1);
458 Qc1_refill          = zeros(len, 1);
459
460 %Refill profiles (NOTE: Must have j=1)
461 %t_refill(j)         = t_start_refill;
462 t_refill(j)         = 0;
463
464 pst_refill(j)       = p_st;
465 mst_refill(j)       = m_st;
466 Tst_refill(j)       = T_st;
467 mf_2_refill(j)      = mflow2;
468
469 T3_refill(j)        = T_3;
470 Tc1_refill(j)       = Tc1_int;
471
472 Wc1_refill(j)       = W_compressor1;
473 Pel_refill(j)       = P_electrolyzer;
474 Qel_refill(j)       = Q_electrolyzer;
475 Qhx1_refill(j)      = Q_hx1;
476 Qhx2_refill(j)      = Q_hx2;
477 Qc1_refil(j)        = Qc1_int;
478
479
480 if refill == true
481 %Fill up to maximum pressure of storage tank
482 while p_st < p_storage_tank
483
484     %Mass flow and work in compressor 1. Sets mass flow in production line.
485     [ W_compressor1, mflow2, T_3, Tc1_int, Qc1_int ]    ...
486                     = compressor1( p_2, p_3, T_2, T_3 );
487     mflow3          = mflow2;
488
489     %Electrolyzer
490     mflow1          = mflow2;
491     [ P_electrolyzer, Q_electrolyzer ] ...
492                     = electrolysis( mflow1, T_electrolyzer );
493
494     %Heat exchanger 1
495     [ Q_hx1, h_2 ] ...
496                     = heatexchanger( mflow1, T_1, p_1, Thx1_out );
497
498     %Heat exchanger 2
499     [ Q_hx2, h_4 ] ...
500                     = heatexchanger( mflow3, T_3, p_3, Thx2_out );
501     mflow4          = mflow3;
502
503     %Integration
504     y               = y0 + del_t*mflow4.*F;
505     y0              = y;
506
507     %Calculating new primary and secondary states in storage tank
508     m_st            = y(1);
509     u_st            = y(2)/m_st;
510     rho_st          = m_st/V_st;
511     T_st            = T_solver(u_st, rho_st, T_st);
512     p_st            = Props('P', 'D', rho_st, 'T', T_st, 'H2')/(1e3);
513     h_st            = Props('H', 'P', p_st*1e3, 'T', T_st, 'H2');
514
515     %Flows
```

```
    p_3             = p_st;

    %Profiles
    t_refill(j + 1)     = t_refill(j) + del_t;

    mst_refill(j + 1)   = m_st;
    pst_refill(j + 1)   = p_st;
    Tst_refill(j + 1)   = T_st;

    mf_2_refill(j + 1)  = mflow2;

    T3_refill(j + 1)    = T_3;
    Tc1_refill(j + 1)   = Tc1_int;

    Wc1_refill(j + 1)   = W_compressor1;
    Pel_refill(j + 1)   = P_electrolyzer;
    Qel_refill(j + 1)   = Q_electrolyzer;
    Qhx1_refill(j + 1)  = Q_hx1;
    Qhx2_refill(j + 1)  = Q_hx2;
    Qc1_refill(j + 1)   = Qc1_int;

    j               = j + 1;

end

t_refill_total      = t_refill(end);
disp(['Duration of refilling of storage tank was ', num2str(t_refill_total), ' s'])

end
```

G.2 Electrolyzer: electrolysis.m

```
function [ P_el, Q_gen ] = electrolysis( mflow, T )
% ELECTROLYSIS  Calculates the power input and heat generated based on
%               the given mass flow.
%               It is assumed that the pressure and temperature in the
%               stack remain constant, also during off-time.
%               It is assumed that oxygen and hydrogen are ideal gases
%               under these conditions and that the heat capacities are
%               constant.
%
% INPUT
% mflow       Mass flow demand, [kg/s]
% T           Operating temperature, [K]
%
% OUTPUT
% P_el    Electical power input, [kW]
% Q_gen   Heat generated, [W]

%Reference temperature [K] and pressure [MPa] (standard conditions)
T_ref       = 273.15 + 25;
p_ref       = 0.1;

%Molar masses, [kg/mol]
Mm_h2       = Props('H2','molemass')*1e-3;
Mm_o2       = Props('O2','molemass')*1e-3;
Mm_h2o      = Props('H2O','molemass')*1e-3;

%Molar heat capacities, [kJ/K mol]
Cp_h2       = Props('C', 'P', p_ref*1e3, 'T', T_ref, 'H2')*Mm_h2;
Cp_o2       = Props('C', 'P', p_ref*1e3, 'T', T_ref, 'O2')*Mm_o2;
Cp_h2o      = Props('C', 'P', p_ref*1e3, 'T', T_ref, 'H2O')*Mm_h2o;

%Formation enthalpy at standard conditions, [kJ/mol]
```

```
H0_h2        = 0;
H0_o2        = 0;
H0_h2o       = -286;

%Overall electrolyzer efficiency
eta          = 0.5;

%Enthalpies at new temperature, [kJ/mol]
H_h2         = H0_h2 + Cp_h2*(T - T_ref);
H_o2         = H0_o2 + Cp_o2*(T - T_ref);
H_h2o        = H0_h2o + Cp_h2o*(T - T_ref);

%Enthalpy of reaction, [kJ/mol]
del_H_rx     = 0.5*H_o2 + H_h2 - H_h2o;

%Power input needed, [kW]
P_el         = mflow*del_H_rx/(Mm_h2*eta);

%Heat generated, [kW]
Q_gen        = (1-eta)*P_el;


end
```

G.3 Heat exchangers: heatexchanger.m

```
function [ Q , h_out ] = heatexchanger( mflow, T_in,  p_in, T_out)
% HEATEXCHANGER Calculates the heat exchanger duty from the steady-state
%               energy balance:
%                                   Q = mflow*(h_in - h_out)
%               It is assumed that the pressure drop is zero across the
%               heat exchanger, that is p_out = p_in.
%               The outlet temperature is predefined by the SAE TIR J2601.
%
% INPUT
% mflow         Mass flow rate, [kg/s]
% T_in          Inlet temperature, [K]
% p_in          Inlet pressure, [MPa]
% T_out         Specified outlet temp., [K]
%
% OUTPUT
% Q             Heat removed, [kW]
% h_out         Outlet enthalpy, [kJ/kg]

%Inlet conditions
h_in    = Props('H', 'P', p_in*1e3, 'T', T_in, 'H2');

%Outlet conditions
p_out   = p_in;               % No pressure drop
h_out   = Props('H', 'P', p_out*1e3, 'T', T_out, 'H2');

%Heat removed, [kW]
Q       = mflow*(h_in - h_out);

end
```

G.4 Compressor 1: compressor1.m

```
function [ W, mflow, T_out, T_int1, Q_int ] = ...
                                compressor1( p_in, p_out, T_in, T_out_last )
% COMPRESSOR1   Calculates the shaft work for compressor 1. The
%               compression is considered adiabatic, and the work
%               is calculated from the energy balance:
%                       W   =   m*( h_out(T,p) - h_in(T,p) )
%               The outlet enthalpy, h_out is calculated from the
%               isentropic efficiency and the outlet isentropic enthalpy:
%                       h_out   = ( h_out,is - h_in )/eta_is + h_in
%               The isentropic enthalpy is then calculated from the
%               outlet entropy and pressure.
%               The compression is performed in two stages with
%               intercooling.
%               The compression ratio in the first stage is 5.
%
% INPUT
% p_in          Inlet pressure, [MPa]
% p_out         Outlet pressure, [MPa]
% T_in          Inlet temperature, [K]
% T_out_last    Outlet temperature, [K]
%
% OUTPUT
% W             Compressor work, [kW]
% mflow         Mass flow, [kg/s]
% T_out         Outlet temperature, [K]
% T_int1        Intermediate temperature, [K]
% Q_int         Heat removed in intercooling, [Q]

global T_amb

%Parameters
Vcyl        = 2.3e-3;           %Cylinder volume for both compressors, [m3]
c           = 10;               %Cylinder clearance, [%]
mflow       = 0.017;            %Constant mass flow, [kg/s]

%Heat capacities
Cp          = Props('C', 'P', p_in*1e3, 'T', T_in, 'H2');
Cv          = Props('O', 'P', p_in*1e3, 'T', T_in, 'H2');
gamma       = Cp/Cv;

%Compressibility factors
Zin         = Props('Z', 'T', T_in, 'P', p_in*1e3, 'H2');
Zout        = Props('Z', 'T', T_out_last, 'P', p_out*1e3, 'H2');

%%%%%%%%%% EFFICIENCIES AND TRANSPORT %%%%%%%%%%%%%%%%%

eta_v       = @(p1, p2)     (100 - p2/p1 - c*((p2/p1)^(1/gamma)...
                            *Zin^2/Zout^2 - 1))*1e-2;
eta_is      = @(p1, p2)     0.1091*(log(p2/p1))^3 - ...
                            0.5247*(log(p2/p1))^2 + 0.8577*log(p2/p1)+ ...
                            0.3727;
speed       = @(eta, rho)   mflow/(Vcyl*rho*eta);

%%%%%%%%% TWO STAGE COMPRESSION %%%%%%%%%%%%%%%%%%%%%
r           = 5;                %Compression ratio
p_int       = r*p_in;           %Intermediate pressure

%%%%%%%%% INLET CONDITIONS %%%%%%%%%%%%%%%%%

% Calculate inlet enthalpy and entropy from known T and p.
h_in        = Props('H', 'T', T_in, 'P', p_in*1e3, 'H2');
s_in        = Props('S', 'T', T_in, 'P', p_in*1e3, 'H2');
rho_in      = Props('D', 'T', T_in, 'P', p_in*1e3, 'H2');

%%%%%%%% MASS FLOW %%%%%%%%%%%%%%%%%%%%%%%%

N           = speed(eta_v(p_in, p_int), rho_in);    %Compressor speed, [1/s]
```

```
68
69  %%%%%%% STAGE 1 %%%%%%%%%%%%%%%
70  s_int1      = s_in;             %Isentropic compression
71
72  %Solving for outlet temperature instead of outlet enthalpy. Without this
73  %fix, it is not possible to compress to a pressure higher than 22 MPa when
74  %inlet pressure is 1.2 MPa.
75  options     = optimset('Display', 'off', 'TolX', 1e-4);
76  F_int       = @(x) Props('S', 'T', x, 'P', p_int*1e3, 'H2') - s_int1;
77  T_guess     = T_out_last;
78  T_int1_is   = fsolve(F_int, T_guess, options);
79  h_int1_is   = Props('H', 'T', T_int1_is, 'P', p_int*1e3, 'H2');
80
81  %Calculate real outlet enthalpy by using isentropic efficiency, [kJ/kg]
82  h_int1      = h_in + (h_int1_is - h_in)/eta_is(p_in, p_int);
83
84  %Real intermediate temperature, [K]
85  T_int1      = Props('T', 'H', h_int1, 'P', p_int*1e3, 'H2');
86
87  %%%%%%%% INTERCOOLING %%%%%%%%%%%%
88  % Cooling down to ambient temperature
89  h_int2      = Props('H', 'T', T_amb, 'P', p_int*1e3, 'H2');
90  Q_int       = mflow*(h_int1 - h_int2);
91
92  %%%%%%%% STAGE 2 %%%%%%%%%%
93  s_int2      = Props('S', 'T', T_amb, 'P', p_int*1e3, 'H2');
94  s_out       = s_int2;
95
96  F_out       = @(x) Props('S', 'T', x, 'P', p_out*1e3, 'H2') - s_out;
97  T_out_is    = fsolve(F_out, T_guess, options);
98  h_out_is    = Props('H', 'T', T_out_is, 'P', p_out*1e3, 'H2');
99
100 %Using isentropic efficiency to calculate real enthalpy
101 h_out       = h_in + (h_out_is - h_in)/eta_is(p_int, p_out);
102
103 %Real outlet temperature, [K]
104 T_out       = Props('T', 'H', h_out, 'P', p_out*1e3, 'H2');
105
106 %%%%%%%% COMPRESSOR WORK %%%%%%%%%%%%%%
107 W1          = mflow*(h_int1 - h_in);
108 W2          = mflow*(h_out - h_int1);
109 W           = W1 + W2;                  %Total compressor work, [kW]
110
111 end
```

G.5 Reduction valve: red_valve.m

```
1  function [ mflow, T_out  ] = red_valve( p_in, T_in, rho_in, p_out, Cv )
2  % RED_VALVE     Calculates the expansion of the hydrogen gas through the
3  %               reduction valve. It is assumed that the expansion
4  %               is adiabatic. That is; the flow is isenthalpic (dh = 0).
5  %               The massflow induced by the pressure difference and the
6  %               given valve coefficient (Cv) is also calculated.
7  %
8  % INPUT
9  % p_in          Inlet pressure, [MPa]
10 % T_in          Inlet temperature, [K]
11 % rho_in        Inlet density, [kg/m3]
12 % p_out         Outlet pressure, [MPa]
13 % Cv            Valve coefficient
14 %
15 % OUTPUT
16 % mflow         Mass flow through valve, [kg/s]
17 % T_out         Outlet temperature, [K]
```

```
18
19 %Inlet conditions
20 h_in         = Props('H', 'P', p_in*1e3, 'T', T_in, 'H2');
21
22 %Outlet conditions
23 h_out        = h_in;
24 T_out        = Props('T', 'H', h_out, 'P', p_out*1e3, 'H2');
25
26 %Mass flow
27 mflow        = Cv*sqrt(((p_in - p_out)*1e6)/rho_in)*rho_in;
28
29
30 end
```

G.6 Compressor 2: compressor2.m

```
1  function [ W, mflow, T_out ] = compressor2( p_in, p_out, T_in, T_out_last, N )
2  % COMPRESSOR2   Calculates the shaft work for compressor 2. The
3  %               compression is considered adiabatic, and the work
4  %               is calculated from the energy balance:
5  %                       W   =   m*( h_out(T,p) - h_in(T,p) )
6  %               The outlet enthalpy, h_out is calculated from the
7  %               isentropic efficiency and the outlet isentropic enthalpy:
8  %                       h_out   = ( h_out,is - h_in )/eta_is + h_in
9  %               The isentropic enthalpy is then calculated from the
10 %               outlet entropy and pressure.
11 %
12 % INPUT
13 % p_in          Inlet pressure, [MPa]
14 % p_out         Outlet pressure, [MPa]
15 % T_in          Inlet temperature, [K]
16 % T_out_last    Outlet temperature, last time step, [K]
17 % N             Strokes per minute, [1/s]
18 %
19 % OUTPUT
20 % W             Compressor work, [kW]
21 % mflow         Mass flow, [kg/s]
22 % T_out         Outlet temperature, [K]
23 %
24 % PARAMETERS
25 % eta_is        Isentropic efficiency
26 % eta_v         Volumetric efficiency
27
28 %Parameters
29 Vcyl         = 3.1e-4;               %Cylinder volume, [m3].
30 c            = 10;                   %Cylinder clearance, [%]
31
32 %Heat capacities
33 Cp           = Props('C', 'P', p_in*1e3, 'T', T_in, 'H2');
34 Cv           = Props('O', 'P', p_in*1e3, 'T', T_in, 'H2');
35 gamma        = Cp/Cv;
36
37 %Compressibility factors
38 Zin          = Props('Z', 'T', T_in, 'P', p_in*1e3, 'H2');
39 Zout         = Props('Z', 'T', T_out_last, 'P', p_out*1e3, 'H2');
40
41 %%%%%%%%%% EFFICIENCIES AND TRANSPORT %%%%%%%%%%%%%%%%%
42
43 eta_v        = @(p1, p2)     (100 - p2/p1 - c*((p2/p1)^(1/gamma)...
44                              *Zin^2/Zout^2 - 1))*1e-2;
45 eta_is       = @(p1, p2)     0.1091*(log(p2/p1))^3 - ...
46                              0.5247*(log(p2/p1))^2 + 0.8577*log(p2/p1)+ ...
47                              0.3727;
48 m_flow       = @(eta, rho)   Vcyl*N*rho*eta;
```

```
49
50 %Isentropic and volumetric efficiency when out of bound
51 eta_is_0    = eta_is(1, 1.1);       %Efficiency when p2/p1 = 1.1
52
53 %%%%%%%%%% INLET AND OUTLET CONDITIONS %%%%%%%%%%%%%%
54
55 % Calculate inlet enthalpy and entropy from known T and p.
56 h_in        = Props('H', 'T', T_in, 'P', p_in*1e3, 'H2');
57 s_in        = Props('S', 'T', T_in, 'P', p_in*1e3, 'H2');
58 rho_in      = Props('D', 'T', T_in, 'P', p_in*1e3, 'H2');
59
60 % Outlet conditions. Isentropic compression.
61 s_out       = s_in;
62 h_out_is    = Props('H', 'S', s_out, 'P', p_out*1e3, 'H2');
63
64
65 %Calculate real outlet enthalpy by using isentropic efficiency
66 if p_out/p_in >= 1.1 && p_out/p_in <= 5
67     h_out    = h_in + (h_out_is - h_in)/eta_is(p_in, p_out);
68     %Mass flow
69     mflow        = m_flow(rho_in, eta_v(p_in, p_out));
70 else
71     h_out    = h_in + (h_out_is - h_in)/eta_is_0;
72     mflow        = m_flow(rho_in, eta_v(p_in, p_out));
73 end
74
75 %Real temperature out of compressor
76 T_out       =    Props('T', 'H', h_out, 'P', p_out*1e3, 'H2');
77
78 %Calculate compressor work
79 W           = mflow*(h_out - h_in);
80
81 end
```

G.7 Compressor speed initiation: init_n2.m

```
1  function [ N2 ] = init_n2( m_flow, p_in, T_in, rho_in )
2  % INIT_N2       Calcuates an initial N2 that gives the same mass flow
3  %               as flowing through the reduction valve.
4  %               At this point, the pressure in the vehicle tank is lower
5  %               than the pressure in the storage tank. Therefore, the
6  %               compression ratio (r) is set to 1.
7  %
8  % INPUT
9  % m_flow       Mass flow in reduction valve at switch, [kg/s]
10 % p_in         Inlet pressure, [MPa]
11 % T_in         Inlet temperature, [K]
12 % rho_in       Inlet density, [kg/m3]
13 %
14 % OUPUT
15 % N2           Compressor speed, [1/s]
16
17 global T_amb
18
19 %Parameters
20 Vcyl        = 3.1e-4;   %Cylinder volume, [m3]
21 c           = 10;       %Clearance, [%]
22 T_out_last  = T_amb;
23
24 %Heat capacities
25 Cp          = Props('C', 'P', p_in*1e3, 'D', rho_in, 'H2');
26 Cv          = Props('O', 'P', p_in*1e3, 'D', rho_in, 'H2');
27 gamma       = Cp/Cv;
28
```

```
%Compression ratio
r            = 1;        %Set outlet pressure equal to inlet pressure

%Compressibility factors
p_out        = p_in*r;
Zin          = Props('Z', 'T', T_in, 'P', p_in*1e3, 'H2');
Zout         = Props('Z', 'T', T_out_last, 'P', p_out*1e3, 'H2');

%Volumetric efficiency
eta_v        = @(r)     (100 - r - c*((r)^(1/gamma)...
                             *Zin^2/Zout^2 - 1))*1e-2;

%Initial compressor speed
N2           = m_flow/(Vcyl*rho_in*eta_v(r));

end
```

G.8 Integrator: euler_integrator.m

```
function [ y, y0 ] = euler_integrator( mflow4, h_4, ...
                                       h_st, mflow7, h_7, y0 )
% EULER_INTEGRATOR  Explicit euler is used as integrator
%                       y(k + 1)    = y(k)    + del_t*y(k)
%                   where y(k)  = F*v.
%                   y is a vector containing the conserved
%                   quanitites, y = [U , m]', F is the incidence matrix
%                   providing the directionality of the mass flows and v is
%                   a transport vector, v = [m4 , m7]'.
%                   Because of conservation, the outlet flow of the storage
%                   tank is equal to the inlet flow of the vehicle tank.
%
% INPUT
% mflow4            Inlet flow of the storage tank, [kg/s]
% h_4               Inlet specific enthalpy of the storage tank, [kJ/kg]
% h_st              Specific enthalpy in the storage tank, [kJ/kg]
% mflow7            Inlet flow of vehicle tank, [kg/s]
% h_7               Inlet specific enthalpy of vehicle tank, [kJ/kg]
% y0                Values from last time step, y(k).
%
% OUTPUT
% y                 Updated primary states
% y0                New "initial" values for next round.

global del_t

%Incidence matrix
F            = [ 1           -1      ; ...
                 h_4         -h_st   ; ...
                 0           1       ; ...
                 0           h_7     ];

%Transport matrix
v            = [ mflow4  mflow7]';

%Euler integration
f_vector     = F*v;
y            = y0    + del_t*f_vector;
y0           = y;

end
```

G.9 Solving for new temperature: T_solver.m

```
function [ T ] = T_solver( u, rho, x0 )
% T_SOLVER  Calculates the temperature based on the updated states in the
%           storage tank and the vehicle tank.
%           The specific internal energy along with the density in the
%           tanks are known.
%           fsolve is used to find what temperature corresponds to the two
%           known states.
%
% INPUTS
% u         Specific internal energy, [kJ/kg]
% rho       Density in tank, [kg/m3]
% x0        Initial guess of temperature. The temperature found in the
%           previous step is used.
%
% OUTPUTS
% T         New temperature in tank, [K]

%fsolve settings
options     = optimset('Display', 'off', 'TolX', 1e-4);

%Equation to be solved
F           = @(x)  u  - ...
                    Props('U', 'T', x, 'D', rho, 'H2');

%Solver
T           = fsolve(F, x0, options);




end
```

G.10 Absorption refrigeration: abs_ref.m

```
function [ mf_nh3, Q_generator ] = abs_ref( T_amb, Q_e, Q_el, T_el, ...
                                                Q_hx2, T_hx2, Q_IC, T_IC )
% ABS_REF   Calculating the required mass flow of NH3 to comply the
%           cooling demand.
%           Calculating the heat input required for the generator.
%           The heat from heat exchanger 2 and the intercooler in
%           compressor 1 is used to heat up the cooling
%           media applied in the internal electrolyzer heat exchanger
%           to the required input temperature, T_input.
%           The cooling medium is water. The heating medium is steam.
%           The steam is assumed to be saturated at T_input.
%           The temperature in the evaporator is assumed to be -45 degrees.
%
% INPUT
% T_amb     Ambient temperature, [K]
% Q_e       Heat that needs to be removed by the evaporator, [kW]
% Q_el      Heat removed in eletrolysis, [kW]
% T_el      Operating temperature of electrolyzer, [K]
% Q_hx2     Heat removed in heat exchanger 2, [kW]
% T_hx2     Outlet temperatureof cooling water in HX2, [K]
% Q_IC      Heat removed in intercooling in compressor 1, [kW]
% T_IC      Intermediate temperature in compressor 1, [K]
%
% OUTPUT
% mf_nh3        Required mass flow of refrigerant NH3, [kg/s]
% Q_generator   Required heat input to the generator, [kW]
```

```
27
28 %%%%%%%%%%%%%%%%%%% PARAMETERS %%%%%%%%%%%%%%%%%%%%
29 T_cw              = T_amb;            %Cooling water temperature
30
31 %Coefficient of performance based on cooling water temepratures
32 if T_cw < 273 + 20
33     COP           = 0.45;
34 elseif 273 + 20 <= T_cw && T_cw < 273 + 30
35     COP           = 0.4;
36 else
37     COP           = 0.3;
38 end
39
40 %Required input temperature and corresponding enthalpies based on
41 %cooling temperatures.
42 if T_cw <= 273 + 15
43     %T_input      = 273 + 150;
44     p_cw          = 0.48;             %Saturation pressure, [MPa]
45
46     %Enthalpies of water at 4.8 bar and 150 degrees C, [kJ/kg]
47     %(Saturated state)
48     h_l_cw        = 633.5;
49     h_v_cw        = 2746;
50
51 elseif 273 + 15 < T_cw <= 273 + 20
52     %T_input      = 273 + 160;
53     p_cw          = 0.62;
54
55     %Enthalpies of water at 6.2 bar and 160 degrees, [kJ/kg]
56     h_l_cw        = 670.4;
57     h_v_cw        = 2756;
58
59 elseif 273 + 21 <= T_cw <= 273 + 25
60     %T_input      = 273 + 175;
61     p_cw          = 0.9;
62
63     %Enthalpies of water at 9 bar and 175 degrees, [kJ/kg]
64     h_l_cw        = 742.6;
65     h_v_cw        = 2772;
66
67 else
68     %T_input      = 273 + 186;
69     p_cw          = 1.19;
70
71     %Enthalpies of water at 11.9 bar and 186 degrees, [kJ/kg]
72     h_l_cw        = 790;
73     h_v_cw        = 2781;
74 end
75
76 %Cooling water
77 h_cw_0            = Props('H', 'P', p_cw*1e3, 'T', T_cw, 'H2O');
78
79 %%%%%%%%%%%%%%%%%%% EVAPORATOR %%%%%%%%%%%%%%%%%%%%%%%%%%
80
81 %Specific enthalpy for liquid and vapor ammonia, [kJ/kg]. Ref: NIST
82 h_l_nh3           = -965.06;      % T = -45degC, p = 0.545 bar
83 h_v_nh3           = 437.67;
84
85 %Energy balance evaporator where Q_e is the cooling demand.
86 %The required ammonia mass flow in the refrigeration cycle is calculated.
87 mf_nh3            = Q_e/(h_v_nh3 - h_l_nh3);
88
89 %%%%%%%%%%%%%%%%%%% GENERATOR %%%%%%%%%%%%%%%%%%%%%%%%%%%%
90
91 %Required heat input in generator
92 Q_generator       = Q_e/COP;
93
94 %Required steam mass flow
```

```
mf_gen          = Q_generator/(h_v_cw - h_l_cw);

disp(['Required mass flow of steam is ', num2str(mf_gen), ' kg/s'])

%%%%%%%%%%%%%%%%% ELECTROLYZER %%%%%%%%%%%%%%%%%%%%%%%%%%
%Need to heat the cooling water coming from the electrolyzer to T_input.
%Therefore, it is necessary to calculate how much heat is needed
%to produce the required steam flow, mf_gen.

%Enthalpies
h_l_el          = Props('H', 'P', p_cw*1e3, ...     %Hot water from elect.
                                            'T', T_el, 'H2O');
h_v_el          = h_v_cw;       %After heating up to T_input

%Available mass flow from electrolyzer
mf_el           = Q_el/(h_l_el - h_cw_0);

if mf_el < mf_gen
    disp('Mass flow from electrolyzer cooling is not sufficient')
    return      %Break if mass flow is not sufficient
else
    disp(['Available mass flow from electrolyzer cooling is ', ...
                                        num2str(mf_el), ' kg/s']);
end

%Required heat from hx2 to heat up to necessary temperature
Q_req_hx2       = mf_gen*(h_v_el - h_l_el);

%%%%%%%%%%%%%%%%% HEAT EXCHANGER 2 %%%%%%%%%%%%%%%%%%%%%%

%Enthalpies
h_l_hx2         = h_cw_0;                   %Cooling water at ambient temp.
h_v_hx2         = Props('H', 'P', p_cw*1e3, ...
                        'T', T_hx2, 'H2O'); %Outlet cooling water conditions

%Mass flow of available water for heating the electrolyzer flow
mf_hx2          = Q_hx2/(h_v_hx2 - h_l_hx2);

%Heat that can be used for heating at the required temperature
Q_hx2_avail     = -mf_hx2*(h_l_cw - h_v_hx2);

%Mass flow of water required from heat exchanger 2
mf_req_hx2      = -Q_req_hx2/(h_l_el - h_v_hx2);

disp(['The required mass flow from heat exchanger 2 is ', ...
                                num2str(mf_req_hx2), ' kg/s'])
disp(['The available mass flow from heat exchanger 2 is ', ...
                                num2str(mf_hx2), ' kg/s'])

%%%%%%%%%%%%%%%% HEAT EXCHANGER 2 + INTERCOOLER %%%%%%%%%%
h_l_ic          = h_cw_0;                       %Inlet conditions intercooler
h_v_ic          = Props('H', 'T', T_IC, ...     %Outlet conditions intercooler
                                        'P', p_cw*1e3, 'H2O');

%Mass flow in intercooler
mf_ic           = Q_IC/(h_v_ic - h_l_ic);

%Heat that can be used for heating at the required temperature
Q_ic_avail      = -mf_ic*(h_l_cw - h_v_ic);

%Mixing these two flows together
mf_hx2_ic       = mf_ic + mf_hx2;
h_hx2_ic        = (mf_ic*h_v_ic + mf_hx2*h_v_hx2)/mf_hx2_ic;
T_hx2_ic        = Props('T', 'P', p_cw*1e3, ...     %Combined flow temperature
                                            'H', h_hx2_ic, 'H2O');

%Required mass flow from heat exchanger 2 + intercooler
mf_req_hx2_ic   = -Q_req_hx2/(h_l_el - h_hx2_ic);
```

```
163
164 disp(['The required mass flow from heat exchanger 2 plus the intercooler is '...
165                                         , num2str(mf_req_hx2_ic), ' kg/s'])
166 disp(['The available mass flow from heat exchanger 2 plus the intercooler is ' ...
167                                         , num2str(mf_hx2_ic), ' kg/s'])
168
169
170
171 end
```